Tissue-specific versus pleiotropic enhancers within the *bric-a-brac* tandem gene duplicates display differential regulatory activity and evolutionary conservation

Henri-Marc G. Bourbon[1#], Mikhail H. Benetah[1#], Emmanuelle Guillou[1], Luis Humberto Mojica-Vazquez[1, 3], Aissette Baanannou[1, 4], Sandra Bernat-Fabre[1], Vincent Loubiere[2, 5], Frédéric Bantignies[2], Giacomo Cavalli[2], and Muriel Boube[1]*

[1]Center for Integrative Biology, Molecular Cellular and Developmental (MCD) Biology Unit, Federal University of Toulouse, 118 Route de Narbonne, F-31062 Toulouse, France; [2]Institute of Human Genetics, UMR9002 CNRS/University of Montpellier, 141 Rue de la Cardonille, F-34396 Montpellier, France; [3]Genotoxicología Ambiental, Departamento de Ciencias Ambientales, Centro de Ciencias de la Atmósfera, Universidad Nacional Autónoma de México, Circuito Exterior s/n, Ciudad Universitaria Coyoacán, 04510, México, México; [4]Laboratory of Molecular and Cellular Screening Processes, Center of Biotechnology of Sfax, Sfax, Tunisia; [5]Research Institute of Molecular Pathology (IMP), Vienna BioCenter (VBC), Vienna, Austria; Medical University of Vienna, Vienna BioCenter (VBC), Vienna, Austria.

[#] Authors having contributed equally to this work.

*Corresponding author: muriel.boube-trey@univ-tlse3.fr

Running title: Differential enhancer conservation and activity within the *bric-a-brac* locus

Abstract

During animal evolution, de novo emergence and modifications of pre-existing transcriptional enhancers have contributed to biological innovations, by implementing gene regulatory networks. The *Drosophila melanogaster bric-a-brac* (*bab*) complex, comprising the tandem paralogous genes *bab1-2*, provides a paradigm to address how enhancers contribute and co-evolve to regulate jointly or differentially duplicated genes. We previously characterized an intergenic enhancer (named LAE) governing *bab2* expression in leg and antennal tissues. We show here that LAE activity also regulates *bab1*. CRISPR/Cas9-mediated LAE excision reveals its critical role for *bab2*-specific expression along the proximo-distal leg axis, likely through paralog-specific interaction with the *bab2* gene promoter. Furthermore, LAE appears involved but not strictly required for *bab1-2* co-expression in leg tissues. Phenotypic rescue experiments, chromatin features and a gene reporter assay reveal a large "pleiotropic" *bab1* enhancer (termed BER) including a series of *cis*-regulatory elements active in the leg, antennal, wing, haltere and gonadal tissues. Phylogenomics analyses indicate that (i) *bab2* originates from *bab1* duplication within the Muscomorpha sublineage, (ii) LAE and *bab1* promoter sequences have been evolutionarily-fixed early on within the Brachycera lineage, while (iii) BER elements have been conserved more recently among muscomorphans. Lastly, we identified conserved binding sites for transcription factors known or prone to regulate directly the paralogous *bab* genes in diverse developmental contexts. This work provides new insights on enhancers, particularly about their emergence, maintenance and functional diversification during evolution.

Author summary

Gene duplications and transcriptional enhancer emergence/modifications are thought having greatly contributed to phenotypic innovations during animal evolution. However, how enhancers regulate distinctly gene duplicates and are evolutionary-fixed remain largely unknown. The *Drosophila bric-a-brac* locus, comprising the tandemly-duplicated genes *bab1-2*, provides a good paradigm to address these issues. The twin *bab* genes are co-expressed in many tissues. In this study, genetic analyses show a partial co-regulation of both genes in the developing legs depending on tissue-specific transcription factors known to bind a single enhancer. Genome editing and gene reporter assays further show that this shared enhancer is also required for *bab2*-specific expression. Our results also reveal the existence of partly-redundant regulatory functions of a large pleiotropic enhancer which contributes to co-regulate the *bab* genes in distal leg tissues. Phylogenomics analyses indicate that the *Drosophila bab* locus originates from duplication of a dipteran *bab1*-related gene, which occurred within the Brachycera (true flies) lineage. *bab* enhancer and promoter sequences have been differentially-conserved among Diptera suborders. This work illuminates how transcriptional enhancers from tandem gene duplicates (i) differentially interact with distinct cognate promoters and (ii) undergo distinct evolutionary changes to diversifying their respective tissue-specific gene expression pattern.

Introduction

Gene duplications have largely contributed to create genetic novelties during evolution (1, 2). Intra-species gene duplicates are referred to as "paralogs", which eventually diverged functionally during evolution in a phylogenetic manner. Gene family expansion has facilitated phenotypic innovation through (i) acquisition of new molecular functions or (ii) the subdivision of the parental gene function between the duplicate copies (3-5). Phenotypic novelties are thought having originated mainly from evolutionary emergence or modifications of genomic *Cis*-Regulatory Elements (CREs) or modules, most often dubbed as "enhancer" regions, which regulate gene transcription in a stage-, tissue- and/or cell-type-specific manner (6-10). How CRE (enhancers) within gene complexes (i) are distinctly interacting with their cognate promoters and (ii) are differentially (co-)evolving remain largely unknown.

The *Drosophila melanogaster bric-a-brac* (*bab*) locus comprises two tandemly-duplicated genes (Fig 1A), *bab1-2*, which encode paralogous transcription factors sharing two conserved domains: (i) a Bric-a-brac/Tramtrack/Broad-complex (BTB) domain involved in protein-protein interactions, and (ii) a specific DNA-binding domain (referred to as BabCD, for Bab Conserved Domain), in their amino(N)- and carboxyl(C)-terminal moieties, respectively (11). Bab1-2 proteins are co-expressed in many tissues (11, 12). In the developing abdominal epidermal cells, within so-called histoblast nests, they jointly regulate directly *yellow* expression in a sexually-dimorphic manner, thus controlling adult male versus female body pigmentation traits (13-16). *bab1-2* co-expression in the developing epidermal histoblast nests is partially governed by two CREs which drive reporter gene expression (i) in a monomorphic pattern in the abdominal segments A2-A5 of both sexes (termed AE, for "Anterior Element"), and (ii) in a female-specific pattern in the A5-A7 segments (DE, for "Dimorphic Element") (Fig 1A) (14, 17). In addition to controlling male-specific abdominal pigmentation traits, *bab1-2* are required, singly, jointly or in a partially-redundant manner, for embryonic cardiac development,

sexually-dimorphic larval somatic gonad formation, salivary glue gene repression, female oogenesis, wing development as well as distal leg (tarsal) and antennal segmentation (11, 13, 17-24). In addition to abdominal AE and DE, two other *bab* enhancers, termed CE and LAE (see Fig 1A), have been characterized, which recapitulate *bab2* expression in embryonic cardiac cells and developing tarsal as well as distal antennal cells, respectively (17, 21, 25).

Adult T1-3 legs, on the pro-, meso- and meta-thoraces, respectively, are derived from distinct mono-layered epithelial cell sheets, organized as sac-like structures, called leg imaginal discs (hereafter simply referred to as leg discs) (26-28). Upon completion of the third-instar larval stage (L3), each leg disc is already patterned along the proximo-distal (P-D) axis through regionalized expression of the Distal-less (Dll), Dachshund (Dac) and Homothorax (Hth) transcriptional regulators in the distal (center of the disc), medial and proximal (peripheral) regions, respectively (26). The five (ts1-5) tarsal and the single pretarsal (distalmost) segments are patterned through genetic cascades mobilizing transcription factors, notably the distal selector protein Dll and the tarsal Rotund protein as well as nuclear effectors of Notch and Epidermal Growth Factor Receptor (EGFR) signaling, i.e., Bowl and C15, respectively (26, 27).

While both *bab* genes are required for dimorphic abdominal pigmentation traits and somatic gonad specification (13, 22), only *bab2* is critical for tarsal segmentation (11). While *bab1* loss-of-function legs are apparently wild-type, a null allele (bab^{AR07}) removing *bab2* (and *bab1*) activities causes segmental transformation along the P-D leg axis, notably sex comb teeth in tarsal segments ts2-3 of male forelegs, normally only found in ts1, as well as ts2-5 tarsal fusions in both genders (11). While the two *bab* genes are co-expressed within ts1-4 cells, *bab2* is expressed more proximally than *bab1* in ts1, and in a graded manner along the P-D leg axis in ts5 (11, 29). We previously showed that *bab2* expression in distal leg (and antennal) tissues is governed by a 567-bp-long CRE/enhancer (termed LAE for "Leg and Antennal Enhancer")

which is situated between the *bab1-2* transcription units (Fig 1A) (17, 25). However, LAE enhancer contribution to *bab1-2* co-regulation in the developing distal legs remains to be investigated in tarsal segments ts3-4 where expression levels of both paralogous BTB-BabCD proteins are the highest (see Fig 1B) (11).

Here, we show that *bab1* expression in the developing distal leg also depends on the Rotund, Bowl and C15 proteins, three transcription factors known to regulate directly *bab2* expression, by binding to dedicated LAE sequences (17, 25). LAE excision by CRISPR/Cas9-mediated genome editing indicates that this enhancer is partly involved in *bab1-2* co-regulation and, more unexpectedly, is also required for their differential expression along the P-D leg axis. Additionally, we show that LAE acts redundantly with a large enhancer signature region (termed BER), located within the *bab1* transcription unit, which is bound by dedicated transcription factors involved in diverse developmental processes and thus BER is prone to act as a "pleiotropic" enhancer region. Our phylogenomics analyses indicate that LAE and *bab1* promoter sequences have been fixed early on during dipteran evolution, well before *bab1* duplication. Conversely, BER and *bab2* promoter sequences have been fixed much later. Lastly, within *D. melanogaster* BER, we identified conserved binding sites for many transcriptional regulators known or prone to regulate *bab1* and/or *bab2* expression in the developing leg and antenna, but also in wing, haltere, mesodermal and gonadal tissues. This work illuminates how transcriptional enhancers from tandem gene duplicates (i) differentially interact with distinct cognate promoters and (ii) undergo distinct evolutionary changes to diversifying their respective tissue-specific gene expression pattern.

Results

The tandem *bab1-2* gene paralogs are co-regulated in the developing distal leg

In addition to the distal selector homeodomain (HD) protein Distal-less, we and others have previously shown that the C15 HD protein (homeoprotein) as well as Rotund and Bowl Zinc-Finger (ZF) transcription factors (TFs) bind dedicated sequences within LAE to ensure precise *bab2* expression in four concentric tarsal rings within the leg discs (Fig 1B) (17, 25). *bab1-2* are co-expressed in ts2-4 tarsal segments, while *bab2* is specifically expressed in ts5 and more proximally than *bab1* in ts1, both in a graded manner along the P-D leg axis (Fig 1C and S1A Fig) (11). Given *bab1-2* co-expression in ts1-4, we first asked whether *C15*, *rotund* and *bowl* activities are also controlling *bab1* expression in the developing distal leg. To this end, we compared Bab1 expression with that of a X-linked *LAE-GFP* (or *LAE-RFP*) reporter gene faithfully reproducing the *bab2* expression pattern there (17, 25), in homozygous mutant leg discs for a null *C15* allele or in genetically-mosaic leg discs harboring *rotund* or *bowl* loss-of-function mutant cells (Fig 1D-F).

C15 is specifically activated in the distalmost (center) part of the leg disc giving rise to the pretarsal (pt) segment (see Fig 1B) (30, 31). We have previously shown that the C15 homeoprotein down-regulates directly *bab2* to restrict its initially broad distal expression to the tarsal segments (25). Bab1 expression analysis in a homozygous *C15* mutant leg disc revealed that both *bab1* and *LAE-RFP* (*bab2*) are similarly de-repressed in the pretarsus (Fig 1, compare panels C-D).

In contrast to *C15*, *rotund* expression is restricted to the developing tarsal segments (32) and the transiently-expressed Rotund ZF protein contributes directly to *bab2* up-regulation in proximal (ts1-2) but has no functional implication in distal (ts3-5) tarsal cells (17). Immunostaining of genetically-mosaic leg discs at the L3 stage revealed that *bab1* is cell-autonomously down-regulated in large *rotund* mutant clones in ts1-2, but not in ts3-4 segments (Fig 1E), as it is the case for *LAE-GFP* reflecting *bab2* expression. Lastly, we examined whether the Bowl ZF protein, a repressive TF active in pretarsal but not in most tarsal cells, is down-

regulating *bab1* expression there (33), like *bab2* (25). Both *bab1* and *LAE-RFP* (*bab2*) appeared cell-autonomously de-repressed in *bowl* loss-of-function pretarsal clones (Fig 1F).

In addition to loss-of-function, we also conducted gain-of-function experiments for *bowl* and *rotund*. Bowl TF gain-of-function was achieved by down-regulating *lines* which encodes a related but antagonistic ZF protein (i) destabilizing nuclear Bowl and is specifically expressed in the tarsal territory (33). As previously shown for *LAE-GFP* (and *bab2*) expression, nuclear Bowl stabilization in the developing tarsal region appears sufficient to down-regulate cell-autonomously *bab1* (S1C Fig). Prolonged expression of the Rotund protein in the entire distal part of the developing leg disc, i.e., tarsal in addition to pretarsal primordia, induces ectopic *bab1* expression in the presumptive pretarsal territory, albeit with some differences with *bab2* expression (S1B Fig, differentially-expressing cells are indicated with arrows), thus suggesting differential sensitivity of the two gene duplicates to Rotund TF levels (see discussion).

Taken together, these data indicate that the C15, Bowl and Rotund transcription factors, previously shown to interact physically with specific LAE sequences and thus to regulate directly *bab2* expression in the developing distal leg, are also regulating *bab1* expression there. These results suggest that the limb-specific intergenic LAE enhancer activity regulates directly both *bab* genes.

LAE activity regulates both *bab1* and *bab2* gene paralogs along the proximo-distal leg axis

To test the role of LAE in regulating *bab1-2*, we deleted precisely the LAE sequence through CRISPR/Cas9 genome editing (see Materials and Methods) (Fig 2A). Two independent deletion events (termed *ΔLAE-M1* and *-M2*; see S2 Fig for deleted DNA sequences) were selected for phenotypic analysis. Both are homozygous viable and give rise to fertile adults with identical fully-penetrant distal leg phenotypes, namely ectopic sex-comb teeth on ts2 (normally

only found on ts1) tarsal segment in the male prothoracic (T1) legs (Fig 2B), which are typical of *bab2* hypomorphic alleles (11). The *ΔLAE-M1* allele was selected for detailed phenotypic analyses and is below referred to as $bab^{\Delta LAE}$.

First, we quantified *bab1* and *bab2* mRNAs prepared from dissected wild-type and homozygous $bab^{\Delta LAE}$ mutant leg discs. As shown in Fig 2C, both mRNAs were detected in mutant discs, although *bab1* levels were two times lower than wild-type. Second, Bab1-2 expression patterns were analyzed in homozygous $bab^{\Delta LAE}$ leg discs (Fig 3). To identify leg cells that should normally express *bab2*, we used the X-linked *LAE-GFP* reporter. In homozygous $bab^{\Delta LAE}$ mutant leg discs, *bab2* specific expression (see Fig. 1B) is no longer observed (Fig 3B-C), while Bab1-2 shared expression is very low in ts3-4 to undetectable in ts1-2. Nevertheless, residual *bab1-2* co-expression in homozygous $bab^{\Delta LAE}$ mutant discs indicates that additional *cis*-regulatory region(s) within the *bab* locus act(s), at least partly, redundantly with the LAE enhancer.

Taken together, our data indicate that LAE enhancer activity is (i) required for *bab1-2* co-expression in the two proximal-most tarsal segments, particularly ts1, (ii) dispensable for their co-expression in ts3-4, suggesting the presence of redundant *cis*-regulatory information and (iii) critically required for *bab2*-specific tarsal expression both proximally and distally. Thus, LAE activity governs both shared and paralog-specific expression of the *bab1-2* gene duplicates.

LAE paralog-specific activity requires the *bab2* core promoter

Whereas enhancer emergence has been proposed to account for acquisition of novel tissue- or paralog-specific functions for gene duplicates (34-36), LAE regulatory function provides an example of a single enhancer responsible both for shared and differential expression of two tandemly-repeated gene paralogs. Previously tested LAE reporter constructs fused *bab2* core

promoter sequences to the minimal *Hsp70* promoter region (*pHsp70*) (17, 25). To examine the contribution of the *bab2* promoter to LAE activity we compared the expression of two LAE reporters containing (*LAE-RFP*) or not (*LAE-pHsp70only-GFP*) the *bab2* promoter sequence (Fig 3D). Strikingly, the *LAE-pHsp70only-GFP* reporter was no longer activated in *RFP+* (*bab2*-expressing) ts1 and ts5 cells (Fig 3E; see white brackets and arrows). These data indicate that *bab2*-specific regulation by LAE activity requires the *bab2* core promoter sequences.

In addition to the intergenic LAE, other leg-specific enhancer elements are present within the *bab1* first intron

Since LAE appeared dispensable for *bab1-2* co-expression in ts3-4 cells, our data suggested the existence of other redundant *cis*-regulatory elements, presumably located also within the *bab* locus. On one side, a X-linked Bacterial Artificial Chromosome (BAC) construct, $BAC26B15^{ZH2A}$, encompassing the *bab2* gene and downstream intergenic sequence including LAE (see Fig 4A), could rescue (i) Bab2 expression in the tarsal primordium and (ii), distal leg phenotypes detected in homozygous animals for the null allele bab^{AR07} (17). On the other side, a *BAC26B15* construct ($BAC26B15\Delta LAE^{ZH2A}$) inserted at the same genomic landing site and specifically lacking LAE sequence did not (Fig 4B-D). These results confirmed that (i) in absence of redundant *cis*-regulatory information, LAE is essential for *bab1-2* expression in the tarsal segments and (ii) the *cis*-information redundant with LAE is located outside the genomic region covered by *BAC26B15*.

To identify limb-specific redundant *cis*-regulatory information within the *bab* complex, we first tested the capacity of another BAC, *BAC69B22*, which overlaps *bab1* and lacks LAE (see Fig 4A), to restore Bab1 expression in bab^{AR07} mutant leg discs. As shown in Fig 4E-F, the X-linked $BAC69B22^{ZH2A}$ could restore *bab1* expression in ts2-4, indicating that it contains *cis*-regulatory

information redundant with LAE activity in these segments. To test the capacity of *BAC69B22* sequences to also regulate *bab2* expression in ts2-4, we placed *BAC69B22*^{ZH2A} across *BAC26B15ΔLAE*^{ZH2A}, to allow pairing-dependent *trans*-interactions (i.e., transvection) between the two X chromosomes in females. This configuration partially restored Bab2 expression in ts2-4 cells from *bab*^{AR07} mutant L3 leg discs, albeit in salt and pepper patterns (Fig 4G), diagnostic of transvection effects (37).

From these data, we predicted the existence of *cis*-regulatory information within the *69B22* chromosomal interval capable to drive some *bab1-2* expression in distal leg tissues and acting redundantly with the LAE enhancer.

Chromatin features predict limb-specific *cis*-regulatory elements within *bab1*

Next, we sought to identify *cis*-regulatory information acting redundantly with LAE by taking advantage of available genome-wide chromatin features and High-throughput chromosome conformation Capture (Hi-C) experiments performed from L3 eye-antennal and/or leg discs (Fig 5). *bab1-2* are indeed co-expressed in distal antennal cells within the composite eye-antennal imaginal disc (11). A topologically-associating domain covering the entire *bab* locus was detected in Hi-C data from eye-antennal discs (Fig 5A and S3A Fig) (38), revealing particularly strong interactions between *bab1-2* promoter regions.

We then used published genome-wide data from Chromatin Immuno-Precipitation (ChIP-Seq), Formaldehyde-Assisted Isolation of Regulatory Elements (FAIRE-Seq) and Assay for Transposase-Accessible Chromatin (ATAC-Seq) experiments (38-41), looking for active enhancer marks (H3K4me1 and H3K27Ac) and nucleosome-depleted chromatin regions (thus accessible to transcription factors). Active enhancer signatures are mainly associated with a ~15-kb-long genomic region that we termed BER, for "*bab1* Enhancer Region", encompassing

the *bab1* promoter, first exon and part of its first intron (Fig 5B, lanes 1-2 and 5-6, respectively; see also S3B Fig for peak calling data). Note that LAE is also accessible to transcription factors and carries H3K4me1 marks, consistently with enhancer activity in distal antennal cells (17).

To more precisely locate putative enhancer element(s) within BER, we analyzed previously-published ChIP-Seq data from L3 leg discs (42) for binding sites for Dll, Sp1 and Hth proteins, known to regulate *bab1* and/or *bab2* expression in the developing legs (17, 42-44). Strong Dll binding is detected throughout BER, including over the *bab1* promoter (Fig 5B, lane 10; see also S3B Fig). In leg discs, Dll binding is detected over 8 out of 10 Open Chromatin Subregions (OCS) within BER (Fig 6C and S3B Fig) and six of those eight are also bound by Sp1 ZF protein. Of note, all nucleosome-depleted (i.e., OCS) BER subregions in the leg are also accessible in the eye-antennal discs (40) (Fig 5B, compare lanes 2 and 9, and Fig 6C, two upper lanes). Lastly, of six OCS sequences co-bound by Dll and Sp1, four are also bound by Hth protein (Fig 5B, lane 8, and Fig 6C, bottom lane). FAIRE-Seq data indicate that, in addition to LAE, only OCS7 is nucleosome-depleted in the leg and eye-antennal discs but not the wing and/or haltere discs (Fig 5B, lanes 13, 16, 18, and Fig 6C, four upper lines; see also S3B Fig). Importantly, ventral limb-specific OCS7 is co-bound by Dll, Sp1 and Hth transcription factors (Fig 6C). Thus, within the entire *bab* locus, only LAE and BER OCS7 are specifically bound by transcriptional regulators in the developing leg and antenna.

In summary, data mining indicates that BER includes a cluster of enhancer elements bound by Dll and Sp1 in leg discs and thus are good candidates for acting redundantly with LAE in regulating *bab* genes in a ventral limb-specific manner.

BER includes multiple *cis*-regulatory elements active in diverse developmental contexts

To further ascribe regulatory roles to BER subregions, we took advantage of a systematic analysis of Gal4 reporter lines (45). Out of six lines containing BER fragments (Fig 6B), only two, *73C11* and *73C05*, overlapping OCS1-3, are active in the leg and eye-antennal discs (FlyLight database; (http://flweb.janelia.org/cgi-bin/flew.cgi; S4B Fig). Nevertheless, none reproduce the *bab1/2* leg or antennal expression patterns in four or two concentric distal rings, respectively. These and other published data from reporter constructs including *bab*1 first intron sequences (14) indicate that OCS1-7 (see Fig 6B) are not sufficient to properly drive *bab1/2* expression in the developing legs and suggest the requirement of additional BER elements, particularly the *bab1* promoter region (i.e., OCS9). This hypothesis is consistent with binding of the known *bab1-2* leg regulators Dll and Sp1 throughout BER, in addition to LAE (Fig 5, lane 10; and S3B Fig).

The *73C05* BER fragment also drives reporter gene expression in the wing, haltere and genital discs (S4 Fig, panels E and H-J) in patterns strikingly similar to those described for *bab2* (11, 44). Consistently, FAIRE- and ChIP-Seq data from haltere discs indicate respectively that OCS1-3 are nucleosome-free and bind the Ultrabithorax (Ubx) Hox-type homeoprotein known to activate directly *bab2* expression in haltere tissues (Fig 5B, lanes 16-17, and Fig 6C) (46, 47). Furthermore, ChIP-Seq data from whole L3 larvae (modENCODE), showed binding over the entire BER region of the Hox Abd-B genital selector (Fig5B, lane 20) (48). Lastly, BER includes (i) nucleosome-depleted sequences governing expression in adult muscles and bound by the mesodermal transcription factors Mef2, Slp1 and Tinman in late embryos (14, 49) as well as (ii) a sequence element (overlapping OCS5) which confers enhancer activity in ovarian somatic cells (50) (see Fig 6D).

Taken together, our data indicate that BER sequences drive *bab1-2* expression in developing limbs but also in other tissues such as wing, haltere, genitalia and mesoderm. Moreover, owing to the presence of binding sites for transcription factors known to regulate *bab* gene expression

in these respective tissues, spread out over the whole BER sequence, the latter is thus proposed to act as a pleiotropic enhancer region.

Cross- and auto-regulations among the *bab* genes

Bab proteins interact with A/T-rich DNA sequences through their BabCD DNA-binding domain, including binding sites within their own locus (51). We therefore tested whether the Bab1-2 proteins autoregulate and/or cross-regulate their own expression. Previous data indicated that Bab2 protein expression is unaffected in *bab1* loss-of-function mutants (11). Given that protein null *bab2* alleles are not available, we used RNA interference coupled to flip-out (FO) Gal4 expression to down-regulate clonally *bab2* expression within developing legs, and examine *LAE-RFP* and *bab1* expression in mosaic L3 leg discs (Fig 7). Strikingly, both *LAE-RFP* and *bab1* were up-regulated cell-autonomously in most tarsal mitotic clones (n=17/20) (Fig 7, panels A-A"). Moreover, *bab2* down-regulation in proximal-most RFP+ ts1 cells (expressing only *bab2*) activated cell-autonomously *bab1*, in addition to up-regulating *LAE-RFP* expression (Fig 7, white arrows in panels B-B"). These results suggested to us that the *bab2* paralog specifically down-regulates its own expression through partial repression of LAE enhancer activity. To confirm these observations, we generated mutant clones for the bab^{AR07} null allele, lacking both *bab2* and *bab1* activities. A slight cell-autonomous *LAE-GFP* reporter up-regulation could be observed in all examined bab^{AR07} clones (detected with anti-Bab2 antibodies; n>20) (Fig 7, panels C-C"), independently of their size and position within *bab2*-expressing tarsal cells (see white arrows and arrowheads).

Altogether, we conclude that *bab2* down-regulates its own expression, likely via partial repression of LAE activity, thus ensuring appropriate levels of both paralogous BTB-BabCD transcription factors in distal leg tissues, and most likely in other appendages as well.

The *bab* gene complex arose from *bab1* duplication in the Muscomorpha infraorder

The different levels of *cis*-regulatory element redundancy within the *bab* locus led us to trace back the evolutionary origin of the *bab* duplication found in *D. melanogaster* (*Dmel*). To start, we identified proteins orthologous to *Dmel* Bab1 or Bab2, i.e., displaying an N-terminal BTB associated to a C-terminal BabCD domain (collectively referred to as BTB-BabCD proteins) (11) within highly diverse dipteran species (see Fig 8A). Two distinct BTB-BabCD proteins strongly related to *Dmel* Bab1 and Bab2, respectively, were identified in the Muscomorpha (higher flies, also known as Cyclorrhapha) superfamily, both within the Schizophora (in Calyptratae, such as *Musca domestica* and *Glossina morsitans*, and in Acalyptratae, particularly among Drosophilidae) and Aschiza subsections (Fig 8A-B and Supplementary data). In contrast, a single BTB-BabCD protein could be identified in evolutionarily-distant dipteran species within (i) the brachyceran Asilomorpha and Stratiomyomorpha superfamilies (such as *Proctacanthus coquilletti* and *Hermetia illucens*, respectively), collectively referred to as Orthorrhapha; (ii) the Nematocera suborder families (with rare exceptions, in Psychodomorpha and Bibionomorpha, see below); (iii) other Insecta orders (e.g., Coleoptera, Hymenoptera and Lepidoptera), and in crustaceans (e.g., *Daphnia pulex*) (see Supplementary data).

To analyze the phylogenetic relationships between these different Bab-related proteins, their primary sequences were aligned and their degree of structural relatedness examined through a maximum likelihood analysis. As expected from an ancient duplication, muscomorphan Bab1-2 paralogs cluster separately, while singleton asilomorphan BTB-BabCD proteins are more related to muscomorphan Bab1 than Bab2 (Fig 8B and S5 Fig), indicating that muscomorphan *bab2* originated from *bab1* duplication.

Interestingly, contrary to most nematocerans, two or even three *bab1* paralogs are present in the fungus gnat *Coboldia fuscipes* (Psychodomorpha) and the gall midge *Mayetiola destructor* (Bibionomorpha), respectively. Significantly, *M. destructor* and *C. fuscipes bab1* paralogs (i) cluster separately in our phylogenetic analysis (Fig 8B and S5 Fig) and (ii) two are arrayed in the same chromosomal contexts for both species (S6 Fig), indicating that they have likely been generated through independent gene duplication processes in the Bibionomorpha and Psychodomorpha, respectively.

Taken together, and updating a previous work (13), our phylogenomics analysis (summarized in Fig 9B-C) indicates that a single ancestral *bab* gene related to *bab1* has been duplicated to give rise to *bab2* within the Muscomorpha (Cyclorrhapha) infraorder.

LAE sequences have been fixed in the Brachycera, thus predating *bab1* duplication

Having traced back the *bab* gene duplication raised the question of the evolutionary origin of the LAE enhancer, which regulates both *bab1* and *bab2* expression (17) (this work). We have previously shown that LAE includes three subsequences highly-conserved among twelve reference Drosophilidae genomes (52), termed CR1-3 (for Conserved Regions 1 to 3; see S7A Fig and Supplementary data), of which only two, CR1 and 2, are critical for tissue-specificity (17, 25). The 68 bp CR1 includes contiguous binding sites for Dll and C15 homeoproteins, while the 41 bp CR2 comprises contiguous binding sites for Dll as well as the ZF protein Bowl (S7 Fig, panels B and C, respectively) (17, 25).

To trace back the LAE evolutionary origin, we then systematically searched for homologous CR1-3 sequences (>50% identity) in dipteran genomes. Importantly, conserved LAE sequences have not been yet reported outside drosophilids. Small genomic regions with partial or extensive homologies to the CR1 (encompassing the C15 and Dll binding sites) and CR2 (particularly the

Dll and Bowl binding sites) could be detected in all examined Brachycera families but not in any nematoceran (Fig 9B and S7B-C Fig). Contrary to closely-associated CR1-2 homologous sequences, no CR3-related sequence could be identified nearby, in any non-Drosophilidae species. Significantly, homologous LAE sequences are situated (i) in between the tandemly-duplicated paralogs in muscomorphan species for which the entire *bab* locus sequence was available to us, suggesting an evolutionarily-conserved enhancer role, or (ii) 20 kb upstream of the *bab1*-related singleton in the asilomorphan *P. coquilletti* (see Fig 9C).

Taken together, as summarized in Fig 9A-C, these data suggest that a LAE-like enhancer with CR1- and CR2-related elements emerged early on in the Brachycera suborder, 180-200 million years ago, and has been since fixed within or upstream the *bab* locus in the Muscomorpha and Asilomorpha infraorders, respectively.

Like LAE elements, *bab1* promoter sequences have been fixed early on in the Brachycera

Given their differential interplay with the long-lasting LAE enhancer, we next analyzed the evolutionary conservation of *Dmel bab1-2* promoter core sequences (Fig 9B and S8 Fig). Both *bab* promoters are TATA-less. Whereas *bab1* has a single transcriptional initiator (Inr) element (TTCAGTC), its *bab2* paralog displays tandemly-duplicated Inr sequences (ATTCAGTTCGT) (53, 54) (S8 Fig). Both promoters display 64% sequence identity over 28 base pairs, including Inr (TTCAGT) and downstream putative Pause Button (PB; consensus CGNNCG) sequences (55) (see S8A Fig). These data suggested that (i) the duplication process having yielded *bab2* included the ancestral *bab1* promoter and (ii) PolII pausing ability previously shown for *bab2* promoter (56-58) probably also occurs for *bab1* promoter.

Homology searches revealed that *bab1* promoter sequences have been strongly conserved in the three extant Muscomorpha families and even partially in some asilomorphans (e.g., *P.*

coquellitti), for which a *bab1*-related singleton gene is present (Fig 9B and S8B Fig). In striking contrast to *bab1*, sequence conservation of the *bab2* promoter could only be detected among some Acalyptratae drosophilids (Fig 9B and S8C Fig). In agreement with a fast-evolutionary drift for *bab2* promoter sequences, the duplicated Inr is even only detected in Drosophila group species.

Taken together, these evolutionary data (summarized in Fig 9B) indicate that, likewise for the LAE enhancer, *bab1* promoter sequences have been under strong selective pressure among the Brachycera, both in the Muscomorpha and Asilomorpha infraorders, while paralogous *bab2* promoter sequences diverged rapidly among muscomorphans.

Unlike LAE, other *bab* CRE sequences have not been conserved beyond the Muscomorpha

The broad LAE sequence conservation led us to also trace back the evolutionary origins of the pleiotropic BER enhancer region as well as the cardiac CE, abdominal anterior AE and sexually-dimorphic DE *cis*-regulatory elements (see Fig 9). Sequences homologous to half of the BER OCS subregions could be detected among the 12 reference Drosophilidae genomes (52), in Calyptratae schizophorans and even in the Muscomorpha Aschiza subsection (e.g., OCS3) (S10-18 Fig). Unlike the LAE enhancer, homologous BER sequence elements (except the *bab1* promoter) could not be detected in non-muscomorphan families. Cardiac CE and abdominal DE are even less conserved given that related sequences could be only detected within schizophoran (excepted in Calyptratae) (Fig 9B and S9 Fig, panels B and C, respectively), whereas abdominal AE sequences could be only identified among drosophilids (Supplementary data) but not in aschizan, asilomorphan and nematoceran *bab* loci.

In conclusion, contrary to the LAE enhancer which among the Diptera emerged early on in the Brachycera suborder, other so-far identified *bab* *cis*-regulatory sequences have not been conserved beyond the Muscomorpha infraorder. Thus, as summarized in Fig 9B, and unlike the long-lasting brachyceran LAE (CR1-2) sequences, these data suggest that other enhancer sequences have been fixed within the Muscomorpha concomitantly (BER) or even after (CE, DE and AE) the *bab2* paralog emergence. Moreover, as expected for a pleiotropic enhancer region, BER sequence conservation allowed us to predict binding sites for transcription factors known, or so far unsuspected, prone to regulate directly the two *bab* genes in many distinct developmental contexts, and which are presented hereafter.

Predictive TF combinatorial code governing *bab* gene expression in diverse tissues

We gathered our data from TF binding site evolutive conservation (described in Supplementary data and S10-19 Fig) with ChIP-Seq experiments from the literature (GEO datasets; see Materials and Methods) (Fig 5B and S3B Fig). Associated with our precise knowledge of *bab* locus enhancer sequences and with previous genetic data also gained from the literature, our compilation presented in Fig. 10 allows to propose new models for the TF code involved in *Dmel bab* locus regulation: (i) It provides new insights into limb-specific *bab1*/*2* regulation proposing additional direct regulators such as Sp1 in the legs, Hth in the antenna, Scalloped (Sd) in the wing and Ubx in the haltere (ChIP-Seq data shown in S3 Fig); (ii) It suggests that BER also acts as an enhancer region for *bab* gene regulation in other developmental contexts and that common TF sets (notably Abd-B together with Dsx) are acting through distinct *cis*-regulatory elements within BER to drive *bab* gene expression in distinct tissues (e.g., in abdominal histoblast nests versus genitalia); (iii) It proposes a direct Bab2 binding on LAE for *bab* gene auto- and cross regulation (tested above); (iv) Finally, analysis of sequences conserved

among brachyceran *bab* loci identified predicted binding sites for more broadly-expressed transcriptional regulators, i.e., GAF, Pho and CTCF (directly interacting with BER OCS; see Fig 5B, lanes 3, 14 and 19, respectively, as well as S3 Fig for GAF), as well as Eip93F, Eip74EF, Chinmo, all related to chromatin organization whose putative roles in *bab* locus regulation are discussed hereafter.

Discussion

In this work, we have addressed the issue of the emergence and functional diversification of enhancers and promoters from two tandem gene duplicates. Using the *Drosophila bab* locus as a model, we showed that the paralogous genes *bab1-2* originate from an ancient *bab1* duplication in the Muscomorpha/Cyclorrhapha. The early-fixed brachyceran *bab1* LAE has been co-opted lately to regulate also *bab2* expression. Furthermore, this unique enhancer is also responsible for paralog-specific *bab2* expression along the P-D leg axis presumably through privileged interactions with the *bab2* promoter. Finally, LAE regulates only some aspects of *bab1-2* expression in the developing limbs because redundant information has emerged within a large pleiotropic enhancer driving *bab1* and/or *bab2* expression in highly-diverse tissues, by binding common sets of developmental transcription factors. This work brings some cues about (i) how a single enhancer can drive specificity among tandem gene duplicates, (ii) how enhancers evolutionary adapt with distinct cognate gene promoters, and (iii) which functional links can be predicted between dedicated transcription factors and chromatin dynamics during development.

A shared enhancer differentially regulating two tandem gene paralogs through distinct promoter targeting specificities

Here, we have shown that a single enhancer, LAE, regulates two tandem gene paralogs at the same stage and in the same expression pattern. How can this work? It has been proposed that enhancers and their cognate promoters are physically associated within phase-separated nuclear foci composed of high concentrations of TFs and proteins from the basal RNA polymerase II (PolII) initiation machinery inducing strong transcriptional responses (59, 60). Our Hi-C data from eye-antennal discs show a strong interaction between *bab1-2* promoter regions (Fig 5), suggesting that both *bab* promoters could be in close proximity within such phase separated droplets, thus taking advantage of shared transcriptional regulators and allowing concerted gene regulation. In contrast, no strong chromosome contacts could be detected between LAE and any of the two *bab* promoter regions, indicating that this enhancer is not stably associated to the *bab2* or *bab1* promoter in the eye-antennal disc (where only the antennal distal part expresses both genes). It would be interesting to gain Hi-C data from leg discs, in which the *bab1-2* genes are much more broadly expressed.

In addition to be required for *bab1-2* co-expression in proximal tarsal segments, we showed here that the LAE enhancer is also responsible for paralog-specific *bab2* expression along the proximo-distal leg axis. While it has been proposed that expression pattern modifications occur through enhancer emergence, our present work indicates that differential expression of two tandem gene paralogs can depend on a shared pre-existing enhancer (i.e., LAE). How this may work? Relative to its *bab1* paralog, *bab2* expression extends more proximally within the Dac-expressing ts1 cells (44) and more distally in the ts5 segment expressing nuclear Bowl protein, whereas both Dac and Bowl proteins have been proposed to act as *bab2* (and presumably *bab1*) repressors (25, 33, 61). CRISPR/Cas9-mediated LAE excision allowed us to establish that this enhancer is critically required for paralog-specific *bab2* leg expression proximally and distally, in ts1 and ts5 cells, respectively. In this context, we and others have previously proposed that transiently-expressed Rotund activating TF may antagonize Bowl (and eventually Dac)

repressive activity to precisely delimit *bab2* expression among ts1 cells (17, 61). Given that *bab1-2* are distinctly expressed despite being both regulated by Bowl and Rotund, we propose that paralog-specific LAE activity depends on privileged interactions with *bab2* promoter sequences (discussed below). Thus, we speculate that the *bab2* promoter responds to Rotund transcriptional activity differently from its *bab1* counterpart. Consistent with this view, ectopic Rotund expression reveals differential regulatory impacts on the two *bab* gene promoters (S1B Fig). Genetic together with Hi-C experiments indicate that this could occur through specific interactions between LAE-bound TFs (e.g., Rotund) and dedicated proteins within the PolII pre-initiation complex stably-associated to the *bab2* core promoter. We envision that the LAE-bound ZF protein Rotund, the chromatin-remodeling ZF protein GAF (for GAGA-associated Factor) and the PolII-associated TFIID subunit TAF3, the latter known to interact physically with GAF and Bab2 BTB proteins (62, 63), are parts of the underlying promoter targeting molecular mechanism.

In this context, despite that sequence homologies between both promoters (consistent with an ancient duplication event mobilizing the ancestral *bab1* promoter) are still detectable, it is significant that the *bab2* promoter evolves much faster than its *bab1* counterpart. While the *bab1* promoter sequence has been strongly conserved among brachycerans, predating *bab2* gene emergence in the Muscomorpha, the *bab2* promoter sequence has only been fixed recently among Drosophilidae, notably through the Initiator (Inr) sequence duplication, indicating very fast evolutionary drift after the gene duplication process which yielded the *bab2* paralog. We envision that this evolutionary ability has largely contributed to allow novel expression patterns for *bab2*, presumably through differential enhancer-promoter pairwise interplay.

Differential evolutionary conservation of tissue-specific versus pleiotropic enhancers

Our comprehensive phylogenomics analyses from highly diverse Diptera families indicate that the *bab* gene complex has been generated through tandem duplication from an ancestral *bab1*-related gene singleton within the Muscomorpha (Cyclorrhapha), about 100-140 years ago. This result contrasts with published data reporting that the duplication process having yielded the tandem *bab* genes occurred much earlier in the Diptera lineage leading to both the Brachycera (true flies; i.e., with short antenna) and Nematocera (long horned "flies", including mosquitos) suborders (13). In fact, tandem duplication events implicating the *bab* locus did occur in the Bibionomorpha, as reported (13)), and even in the Psychodomorpha with three *bab1*-related gene copies (Figure 8 and S6 Fig), but our phylogenetic analysis supports independent events. Thus, within the Diptera, the ancestral *bab1* singleton had a high propensity to duplicate locally.

In this study, we have shown a strong evolutionary conservation of LAE subsequences among brachycerans, notably its CR2 element containing Dll and Bowl binding sites (S7C Fig). This conservation suggests a long-lasting enhancer function in distal limb-specific regulation of ancestral singleton *bab1* genes. In striking contrast, BER sequence conservation could only be detected among extant muscomorphan *bab* loci. We assume that during evolution large pleiotropic enhancers may better assimilate binding sites for gene-specific transcription factors, thus generating regulatory novelties in distinct imaginal discs.

Gene duplication is a major source to generate phenotypic innovations during evolution, through diverging expression and molecular functions, and eventually from single gene copy translocation to another chromosomal site. Emergence of tissue-specific enhancers not shared between the two gene duplicates, as well as of "shadow" enhancers, have been proposed to be evolutionary novelty sources (64) (6). Our work indicates that the presumably long-lasting brachyceran LAE enhancer has recently been co-opted in drosophilids to allow differential *bab* gene expression. Conversely, the large BER region has apparently accumulated regulatory

546 sequence elements bound by diverse tissue-specific transcription factors (e.g., Dll, Hth, Abd-B
547 and Dsx) acting in different cellular contexts.

548

549 **A pleiotropic enhancer region overlapping with a PcG-response element**

550 ChIP-Seq analysis for histone H3 modifications (H3K4me3, H3K27Ac and H3K4me1
551 enhancer/promoter marks; H3K27me3 chromatin repressive mark) from eye-antennal discs has
552 revealed the pleiotropic BER enhancer region but also an overlapping repressive PcG
553 (Polycomb Group family) domain, indicating that BER encompasses a bivalent chromatin
554 domain, while another one is detected over the *bab2* promoter region. A dual enhancer/silencing
555 function for PcG-Response Element (PRE) during embryogenesis has recently been established
556 genome-wide (65), and the authors have proposed that reuse of enhancer regulatory elements
557 by PcG proteins may help fine-tune gene expression and ensure the timely maintenance of cell
558 identities throughout development. More recently, we have shown widespread enhancer-PcG
559 domain interplay during developmental gene activation through chromatin looping in eye-
560 antennal discs (38). Altogether these data suggest that the *bab1-2* genes might be poised for
561 activation throughout the eye-antennal disc, and possibly other imaginal discs as well.

562 The Pleiohomeotic (Pho) protein is a DNA-binding PcG complex recruiter, critical for gene
563 silencing maintenance during development (66). Pho interaction with several BER subregions,
564 as detected in ChIP-Seq experiments from L3 tissues, as well as the presence of many
565 evolutionarily-conserved predicted Pho binding sites, support a role for Pho in PcG repression
566 throughout BER. We thus propose that Pho-containing PcG repressive complex bound at PREs
567 within the *bab* bivalent locus is counteracted by one or several tissue-specific transcriptional
568 activators identified in this work, which remain(s) to be characterized.

In this context, it is significant that in the eye-antennal disc, the ZF protein CTCF, acting redundantly with other chromatin insulator proteins, strongly interacts directly with the two flanking regions of the TAD covering the *bab* locus and also with several BER OCSs (Fig 5B). Significantly, two of these predicted CTCF interacting sites overlap with putative optimal binding sites for the PcG-recruiter Pho (S18-19 Fig). These data suggest that the CTCF architectural protein and the PcG-recruiter Pho may functionally interact to regulate the *bab* locus chromosome topology. Interestingly, the human Pho homolog (YY1) is a structural enhancer-promoter looping regulator (67) and orchestrates, together with the CTCF protein, a 3D chromatin looping switch during early neural lineage commitment (68). To our knowledge, functional relationships between CTCF and Pho proteins have not been investigated genome-wide in *Drosophila*.

Dynamic *bric-a-brac* locus chromatin accessibility during development

Recent data indicate that chromatin accessibility is dynamic during *Drosophila* larval development, being triggered by the ecdysone hormone (69). Dynamic enhancer activity and chromatin accessibility have been proposed to be regulated by the ecdysone-induced Eip93F (Ecdysone-induced protein 93F, also called E93) transcriptional regulator (70). ChIP data from early pupal wings indicate that Eip93F binds many BER OCS as well as the *bab1* promoter region (70). Consistently, many putative Eip93F binding sites are present in these BER subregions and several have been conserved beyond Drosophilidae (Fig 10C). Interestingly, the human Eip93F homolog interacts with CtBP through a conserved motif (71), and *Drosophila* CtBP is known to recruit diverse chromatin-modifying complexes, notably to participate in Pho-mediated PcG recruitment to PREs (72). Thus, Eip93F binding to BER *cis*-regulatory elements may impact the proposed dual PcG activity at the *bab* locus. In addition to Eip93F,

BER regulatory sequences include many evolutionarily-conserved putative binding sites for the Eip74EF protein (Fig 10C), another ecdysone-induced TF, including one which overlaps with a conserved putative Pho binding site, suggesting again functional correlation between Ecdysone regulation and PcG activity.

Lastly, the *cis*-regulatory landscape within the *bab* locus (i.e., AE, DE, CE, LAE and BER) includes one or several evolutionarily-conserved predicted binding sites for the Chinmo BTB-ZF protein participating to developmental timing, notably through interplay with ecdysone signaling (73, 74). Consistently, ChIP-Seq experiments from embryos (ModENCODE data; http://www.modencode.org/) indicate Chinmo binding to BER sequences (75). Intriguingly, the Chinmo ZF protein is an additional BTB-containing TF prone to regulate directly the *bab* genes, possibly through molecular partnerships with the chromatin organizer GAF (another BTB-ZF protein interacting directly with both *bab* promoter regions; Fig 5B and S3 Fig) and the twin Bab BTB-BabCD proteins themselves. Thus, Chinmo implication in chromatin organization and enhancer activity within the *bab* locus undoubtedly deserves to be investigated.

In summary, the *bab* locus offers a good paradigm to investigate molecularly in great details how chromatin structure, particularly higher-order chromosome organization, impacts on transcriptional memory during development and selective enhancer-promoter interplay in diverse tissular contexts. Indeed, our comprehensive predictive combinatorial code for tissue-specific, as well as broadly-expressed architectural transcription factors (e.g., CTCF, Pho and GAF) regulating two tandem gene paralogs, offers the opportunity to dissect underlying molecular mechanisms, which are prone to be conserved during animal evolution and thus to be of broad biological significance.

Material sand Methods

Fly stocks, culture and genetic manipulations

D. melanogaster stocks were grown on standard yeast extract-sucrose medium. The *vasa*-PhiC31 ZH2A *attP* stock (kindly provided by F. Karch) was used to generate the *LAEpHsp70-GFP* reporter lines and the *BAC69B22* construct as previously described (17). *LAE-GFP* and *LAE-RFP* constructs (including both *Hsp70* and *bab2* core promoters) inserted on the ZH2A (X chromosome) or ZH86Fb (third chromosome) *attP* landing platforms, and displaying identical expression patterns, have been previously described (17, 25). $C15^{2}$/TM6B, Tb^{1} stock was kindly obtained from G. Campbell. Mutant mitotic clones for null alleles of *bowl* and *rotund* were generated with the following genotypes: *y w LAE-GFP*; $DllGal4^{EM2012}$, *UAS-Flp/+; FRT82B, Ub-RFP/FRT82B* rn^{12} (i.e., *rn* mutant clones are RFP negative; Fig 1E) and *y w LAE-RFP*; $DllGal4^{EM2012}$, *UAS-Flp/+*; *Ub-GFP, FRT40A/*$bowl^{1}$ *FRT40A* (i.e., *bowl* mutant clones are GFP negative; Fig 1F), respectively. Rotund protein gain-of-function within the *Dll*-expressing domain was obtained with the following genotype: *y w LAE-GFP*; $DllGal4^{EM2012}$; *UAS-*Rn^{1}/+. The Dll^{EM212}*-Gal4* line was provided by M. Suzanne, while the *UAS-*Rn^{1} line was obtained from the Bloomington stock center. “Flip-out” (FO) mitotic clones over-expressing dsRNA against *lines* were generated by 40 mn heat shocks at 38°C, in mid-late L2 to early-mid L3 larvae of genotypes: *y w LAE-RFP hsFlp*; *UAS-dsRNAlines/pAct>y+>Gal4, UAS-GFP (*i.e., FO clones express GFP in S1C Fig). Mutant mitotic clones for the null bab^{AR07} allele were generated by 30 mn heat shocks at 38°C, in early first to late second-instar larvae of genotypes: y w *LAE-GFP*, hsFlp; FRT80B/bab^{AR07}, FRT80B. FO mitotic clones over-expressing dsRNA against *bab1* or *bab2* were generated by 40 mn heat shocks at 38°C, in early to early-mid L3 larvae of genotypes: *y w LAE-RFP hsFlp*; *UAS-dsbab2 /Pact>y+>Gal4, UAS-GFP* and *y w LAE-RFP, hsFlp*; *Pact>y+>Gal4*, *UAS-GFP*/+; *UAS-dsbab1*/+ (i.e., FO clones express GFP in Fig 7). *UAS-dsRNA* stocks used to obtain interfering RNA against *lines* (#40939), *bab1* (#35707) and *bab2* (#37260) were obtained from the Bloomington stock Center.

642

643 **Immuno-histochemistry and microscopy**

644 Leg discs were dissected from wandering (late third instar stage) larvae (L3). Indirect immuno-
645 fluorescence was carried out as previously described (17) using a LEICA TCS SP5 or SPE
646 confocal microscope. Rat anti-Bab2 (11), rabbit anti-Bab1 (14), rabbit ant-Dll (76), rabbit anti-
647 Bowl (61), and rabbit anti-C15 (31) antibodies were used at 1/2000, 1/500, 1/200, 1/1000 and
648 1/200, respectively.

649

650 **CRISPR/Cas9-mediated chromosomal deletion**

651 Guide RNAs (gRNAs) were designed with CHOPCHOP at the Harvard University website
652 (https://chopchop.cbu.uib.no/). Four gRNA couples were selected that cover two distinct
653 upstream and downstream LAE positions: TGCGTGGAGCCTTCTTCGCCAGG or
654 TGGAGCCTTCTTCGCCAGGCCGG; and TATACTGTTGAGATCCCATGCGG or
655 TTAGGCGCACATAAGGAGGCAGG (the PAM protospacer adjacent motif sequences are
656 underlined), respectively. Targeting tandem chimeric RNAs were produced from annealed
657 oligonucleotides inserted into the pCFD4 plasmid, as described in
658 (http://www.crisprflydesign.org/). Each pCFD4-LAE-KO construct was injected into 50 *Vasa-*
659 *Cas9* embryos (of note the *vasa* promoter sequence is weakly expressed in somatic cells). F0
660 fertile adults and their F1 progeny, with possible somatic LAE-deletion events and candidate
661 mutant chromosomes (balanced with *TM6B, Tb*), respectively, were tested by polymerase chain
662 reactions (PCR) with the following oligonucleotides: AGTTTTTCATCCCCCTTCCA and
663 GTATTTCTTTGCCTTGCCATCG (predicted wild-type amplified DNA: 2167 base pairs).

664

665 **Quantitative RT-PCR analysis**

666 T1-3 leg imaginal discs were dissected from homozygous *white*^{1118} and *bab*$^{\Delta LAE\text{-}M1}$ late L3
667 larvae in PBS 0.1% Tween. 50 discs of each genotype were collected and frozen in nitrogen.
668 Total messenger RNAs were purified using RNeasy kit (Qiagen) and reverse transcribed by
669 SuperScript II (ThermoFisher). *bab1*, *bab2* or *rp49* cDNA levels were monitored by
670 quantitative PCR using the following oligonucleotides: Bab1Fw:
671 CGCCCAAGAGTAACAGAAGC; Bab1Rev: TCTCCTTGTCCTCGTCCTTG; Bab2Fw:
672 CTGCAGGATCCAAGTGAGGT; Bab2Rev: GACTTCACCAGCTCCGTTTC; RP49Fw:
673 GACGCTTCAAGGGACAGTATCTG; RP49Rev: AAACGCGGTTCTGCATGAG. A
674 Wilcoxon test was performed to evaluate the difference between samples.

675

676 **Homology searches, sequence alignments and phylogenetic analyses**

677 Homology searches were done at the NCBI Blast site (https://blast.ncbi.nlm.nih.gov/Blast.cgi).
678 Protein or nucleotide sequence alignments were done using MAFFT (Multiple Alignment using
679 Fast Fourier Transform) (https://mafft.cbrc.jp/alignment/server/). Phylogenetic relationships
680 were inferred through a maximum likelihood analysis with W-IQ-Tree
681 (http://iqtree.cibiv.univie.ac.at/) and visualized with the ETE toolkit
682 (http://etetoolkit.org/treeview/).

683

684 **Transcription factor binding prediction**

685 DNA binding predictions were done using the motif-based sequence analysis tool TomTom
686 from the MEME suite (http://meme-suite.org/tools/tomtom) and the Fly Factor Survey database
687 (http://mccb.umassmed.edu/ffs/).

688

689 **Gene expression omnibus datasets**

690 The following gene expression omnibus (GEO) datasets were extracted from the NCBI website
691 (https://www.ncbi.nlm.nih.gov/gds/): GSE59078; GSM1261348; GSM1426265; GSE126985;
692 GSM3139658; GSM948715; GSE113574; GSM948718; GSM948717; GSE38594;
693 GSM948720; GSM948716; GSM659162; GSM948719; GSE102339; GSE50363.

694

695 **Hi-C and histone tail mark analyses from L3 eye-antennal imaginal discs**

696 Hi-C and histone mark ChIP-Seq analyses from L3 eye-antennal discs have been recently
697 published in (38).

698

699 **Acknowledgments**

700 We thank F. Karch, M. Suzanne, T.M. Williams, G. Boekhoff-Falk, S. Bray, G. Campbell, T.
701 Kojima, F. Laski, J.L. Couderc and the Bloomington Stock Center for fly stocks and reagents.
702 We are grateful to Alain Vincent for his proofreading of the manuscript. We thank Julien Favier
703 for technical assistance, particularly in managing the transgenic facility. Lastly, we
704 acknowledge Brice Ronsin and the Toulouse RIO Imaging platform.

705

706

References

1. Ohno S. **Evolution by Gene Duplication**. Springer-Verlag; 1970.

2. Zhang J. Evolution by gene duplication - an update. Trends Ecol. Evol.; 2003. p. 292-8.

3. Lundin LG. Gene duplications in early metazoan evolution. Semin Cell Dev Biol. 1999;10(5):523-30.

4. He X, Zhang J. Rapid subfunctionalization accompanied by prolonged and substantial neofunctionalization in duplicate gene evolution. Genetics. 2005;169(2):1157-64.

5. Sundström G, Larsson TA, Larhammar D. Phylogenetic and chromosomal analyses of multiple gene families syntenic with vertebrate Hox clusters. BMC Evol Biol. 2008;8:254.

6. Long HK, Prescott SL, Wysocka J. Ever-Changing Landscapes: Transcriptional Enhancers in Development and Evolution. Cell. 2016;167(5):1170-87.

7. Rubinstein M, de Souza FS. Evolution of transcriptional enhancers and animal diversity. Philos Trans R Soc Lond B Biol Sci. 2013;368(1632):20130017.

8. Carroll SB. Evo-devo and an expanding evolutionary synthesis: a genetic theory of morphological evolution. Cell. 2008;134(1):25-36.

9. Levine M. Transcriptional enhancers in animal development and evolution. Curr Biol. 2010;20(17):R754-63.

10. Vlad D, Kierzkowski D, Rast MI, Vuolo F, Dello Ioio R, Galinha C, et al. Leaf shape evolution through duplication, regulatory diversification, and loss of a homeobox gene. Science. 2014;343(6172):780-3.

11. Couderc JL, Godt D, Zollman S, Chen J, Li M, Tiong S, et al. The bric à brac locus consists of two paralogous genes encoding BTB/POZ domain proteins and acts as a homeotic and morphogenetic regulator of imaginal development in Drosophila. Development. 2002;129(10):2419-33.

12. Salomone JR, Rogers WA, Rebeiz M, Williams TM. The evolution of Bab paralog expression and abdominal pigmentation among Sophophora fruit fly species. Evol Dev. 2013;15(6):442-57.

732 13. Roeske MJ, Camino EM, Grover S, Rebeiz M, Williams TM. Cis-regulatory evolution integrated
733 the Bric-à-brac transcription factors into a novel fruit fly gene regulatory network. Elife. 2018;7.
734 14. Williams TM, Selegue JE, Werner T, Gompel N, Kopp A, Carroll SB. The regulation and evolution
735 of a genetic switch controlling sexually dimorphic traits in Drosophila. Cell. 2008;134(4):610-23.
736 15. Gompel N, Carroll SB. Genetic mechanisms and constraints governing the evolution of
737 correlated traits in drosophilid flies. Nature. 2003;424(6951):931-5.
738 16. Kopp A, Duncan I, Carroll SB. Genetic control and evolution of sexually dimorphic characters in
739 Drosophila. Nature. 2000;408(6812):553-9.
740 17. Baanannou A, Mojica-Vazquez LH, Darras G, Couderc JL, Cribbs DL, Boube M, et al. Drosophila
741 distal-less and Rotund bind a single enhancer ensuring reliable and robust bric-a-brac2 expression in
742 distinct limb morphogenetic fields. PLoS Genet. 2013;9(6):e1003581.
743 18. Godt D, Couderc JL, Cramton SE, Laski FA. Pattern formation in the limbs of Drosophila: bric a
744 brac is expressed in both a gradient and a wave-like pattern and is required for specification and proper
745 segmentation of the tarsus. Development. 1993;119(3):799-812.
746 19. Godt D, Laski FA. Mechanisms of cell rearrangement and cell recruitment in Drosophila ovary
747 morphogenesis and the requirement of bric à brac. Development. 1995;121(1):173-87.
748 20. Sahut-Barnola I, Godt D, Laski FA, Couderc JL. Drosophila ovary morphogenesis: analysis of
749 terminal filament formation and identification of a gene required for this process. Dev Biol.
750 1995;170(1):127-35.
751 21. Junion G, Bataillé L, Jagla T, Da Ponte JP, Tapin R, Jagla K. Genome-wide view of cell fate
752 specification: ladybird acts at multiple levels during diversification of muscle and heart precursors.
753 Genes Dev. 2007;21(23):3163-80.
754 22. Camara N, Whitworth C, Dove A, Van Doren M. Doublesex controls specification and
755 maintenance of the gonad stem cell niches in. Development. 2019;146(11).
756 23. Duan J, Zhao Y, Li H, Habernig L, Gordon MD, Miao X, et al. Bab2 Functions as an Ecdysone-
757 Responsive Transcriptional Repressor during Drosophila Development. Cell Rep. 2020;32(4):107972.

758 24. Zhao Y, Duan J, Dziedziech A, Büttner S, Engström Y. Bab2 activates JNK signaling to
759 reprogram *Drosophila* wing disc development. 2021.
760 25. Mojica-Vázquez LH, Benetah MH, Baanannou A, Bernat-Fabre S, Deplancke B, Cribbs DL, et al.
761 Tissue-specific enhancer repression through molecular integration of cell signaling inputs. PLoS Genet.
762 2017;13(4):e1006718.
763 26. Kojima T. The mechanism of Drosophila leg development along the proximodistal axis. Dev
764 Growth Differ. 2004;46(2):115-29.
765 27. Kojima T. Developmental mechanism of the tarsus in insect legs. Curr Opin Insect Sci.
766 2017;19:36-42.
767 28. Estella C, Voutev R, Mann RS. A dynamic network of morphogens and transcription factors
768 patterns the fly leg. Curr Top Dev Biol. 2012;98:173-98.
769 29. Li Q, Barish S, Okuwa S, Maciejewski A, Brandt AT, Reinhold D, et al. A Functionally Conserved
770 Gene Regulatory Network Module Governing Olfactory Neuron Diversity. PLoS Genet.
771 2016;12(1):e1005780.
772 30. Campbell G. Regulation of gene expression in the distal region of the Drosophila leg by the
773 Hox11 homolog, C15. Dev Biol. 2005;278(2):607-18.
774 31. Kojima T, Tsuji T, Saigo K. A concerted action of a paired-type homeobox gene, aristaless, and
775 a homolog of Hox11/tlx homeobox gene, clawless, is essential for the distal tip development of the
776 Drosophila leg. Dev Biol. 2005;279(2):434-45.
777 32. Natori K, Tajiri R, Furukawa S, Kojima T. Progressive tarsal patterning in the Drosophila by
778 temporally dynamic regulation of transcription factor genes. Dev Biol. 2012;361(2):450-62.
779 33. Greenberg L, Hatini V. Essential roles for lines in mediating leg and antennal proximodistal
780 patterning and generating a stable Notch signaling interface at segment borders. Dev Biol.
781 2009;330(1):93-104.
782 34. Prud'homme B, Gompel N, Carroll SB. Emerging principles of regulatory evolution. Proc Natl
783 Acad Sci U S A. 2007;104 Suppl 1:8605-12.

784 35. Hittinger CT, Carroll SB. Gene duplication and the adaptive evolution of a classic genetic switch.
785 Nature. 2007;449(7163):677-81.
786 36. Carroll SB. From pattern to gene, from gene to pattern. Int J Dev Biol. 1998;42(3 Spec No):305-
787 9.
788 37. Lim B, Heist T, Levine M, Fukaya T. Visualization of Transvection in Living Drosophila Embryos.
789 Mol Cell. 2018;70(2):287-96.e6.
790 38. Loubiere V, Papadopoulos GL, Szabo Q, Martinez AM, Cavalli G. Widespread activation of
791 developmental gene expression characterized by PRC1-dependent chromatin looping. Sci Adv.
792 2020;6(2):eaax4001.
793 39. Yeung K, Wang F, Li Y, Wang K, Mardon G, Chen R. Integrative genomic analysis reveals novel
794 regulatory mechanisms of eyeless during Drosophila eye development. Nucleic Acids Res.
795 2018;46(22):11743-58.
796 40. McKay DJ, Lieb JD. A common set of DNA regulatory elements shapes Drosophila appendages.
797 Dev Cell. 2013;27(3):306-18.
798 41. Davie K, Jacobs J, Atkins M, Potier D, Christiaens V, Halder G, et al. Discovery of transcription
799 factors and regulatory regions driving in vivo tumor development by ATAC-seq and FAIRE-seq open
800 chromatin profiling. PLoS Genet. 2015;11(2):e1004994.
801 42. Newcomb S, Voutev R, Jory A, Delker RK, Slattery M, Mann RS. cis-regulatory architecture of a
802 short-range EGFR organizing center in the Drosophila melanogaster leg. PLoS Genet.
803 2018;14(8):e1007568.
804 43. Córdoba S, Requena D, Jory A, Saiz A, Estella C. The evolutionarily conserved transcription
805 factor Sp1 controls appendage growth through Notch signaling. Development. 2016;143(19):3623-31.
806 44. Chu J, Dong PD, Panganiban G. Limb type-specific regulation of bric a brac contributes to
807 morphological diversity. Development. 2002;129(3):695-704.
808 45. Jenett A, Rubin GM, Ngo TT, Shepherd D, Murphy C, Dionne H, et al. A GAL4-driver line resource
809 for Drosophila neurobiology. Cell Rep. 2012;2(4):991-1001.

810 46. Slattery M, Ma L, Négre N, White KP, Mann RS. Genome-wide tissue-specific occupancy of the
811 Hox protein Ultrabithorax and Hox cofactor Homothorax in Drosophila. PLoS One. 2011;6(4):e14686.
812 47. Boube M, Hudry B, Immarigeon C, Carrier Y, Bernat-Fabre S, Merabet S, et al. Drosophila
813 melanogaster Hox Transcription Factors Access the RNA Polymerase II Machinery through Direct
814 Homeodomain Binding to a Conserved Motif of Mediator Subunit Med19. PLoS Genet.
815 2014;10(5):e1004303.
816 48. Estrada B, Sanchez-Herrero E. The Hox gene Abdominal-B antagonizes appendage
817 development in the genital disc of Drosophila. Development. 2001;128(3):331-9.
818 49. Zinzen RP, Girardot C, Gagneur J, Braun M, Furlong EE. Combinatorial binding predicts spatio-
819 temporal cis-regulatory activity. Nature. 2009;462(7269):65-70.
820 50. Arnold CD, Gerlach D, Stelzer C, Boryń Ł, Rath M, Stark A. Genome-wide quantitative enhancer
821 activity maps identified by STARR-seq. Science. 2013;339(6123):1074-7.
822 51. Lours C, Bardot O, Godt D, Laski FA, Couderc JL. The Drosophila melanogaster BTB proteins bric
823 a brac bind DNA through a composite DNA binding domain containing a pipsqueak and an AT-Hook
824 motif. Nucleic Acids Res. 2003;31(18):5389-98.
825 52. Clark AG, Eisen MB, Smith DR, Bergman CM, Oliver B, Markow TA, et al. Evolution of genes and
826 genomes on the Drosophila phylogeny. Nature. 2007;450(7167):203-18.
827 53. Ohler U, Liao GC, Niemann H, Rubin GM. Computational analysis of core promoters in the
828 Drosophila genome. Genome Biol. 2002;3(12):RESEARCH0087.
829 54. Meers MP, Adelman K, Duronio RJ, Strahl BD, McKay DJ, Matera AG. Transcription start site
830 profiling uncovers divergent transcription and enhancer-associated RNAs in Drosophila melanogaster.
831 BMC Genomics. 2018;19(1):157.
832 55. Gilchrist DA, Dos Santos G, Fargo DC, Xie B, Gao Y, Li L, et al. Pausing of RNA polymerase II
833 disrupts DNA-specified nucleosome organization to enable precise gene regulation. Cell.
834 2010;143(4):540-51.

835 56. Muse GW, Gilchrist DA, Nechaev S, Shah R, Parker JS, Grissom SF, et al. RNA polymerase is
836 poised for activation across the genome. Nat Genet. 2007;39(12):1507-11. Epub 2007 Nov 11.
837 57. Lee C, Li X, Hechmer A, Eisen M, Biggin MD, Venters BJ, et al. NELF and GAGA factor are linked
838 to promoter-proximal pausing at many genes in Drosophila. Mol Cell Biol. 2008;28(10):3290-300.
839 58. Kwak H, Fuda NJ, Core LJ, Lis JT. Precise maps of RNA polymerase reveal how promoters direct
840 initiation and pausing. Science. 2013;339(6122):950-3.
841 59. Kim S, Shendure J. Mechanisms of Interplay between Transcription Factors and the 3D
842 Genome. Mol Cell. 2019;76(2):306-19.
843 60. Sabari BR, Dall'Agnese A, Young RA. Biomolecular Condensates in the Nucleus. Trends Biochem
844 Sci. 2020.
845 61. de Celis Ibeas JM, Bray SJ. Bowl is required downstream of Notch for elaboration of distal limb
846 patterning. Development. 2003;130(24):5943-52.
847 62. Pointud JC, Larsson J, Dastugue B, Couderc JL. The BTB/POZ domain of the regulatory proteins
848 Bric à brac 1 (BAB1) and Bric à brac 2 (BAB2) interacts with the novel Drosophila TAF(II) factor
849 BIP2/dTAF(II)155. Dev Biol. 2001;237(2):368-80.
850 63. Chopra VS, Srinivasan A, Kumar RP, Mishra K, Basquin D, Docquier M, et al. Transcriptional
851 activation by GAGA factor is through its direct interaction with dmTAF3. Dev Biol. 2008;317(2):660-70.
852 64. Hong JW, Hendrix DA, Levine MS. Shadow enhancers as a source of evolutionary novelty.
853 Science. 2008;321(5894):1314.
854 65. Erceg J, Pakozdi T, Marco-Ferreres R, Ghavi-Helm Y, Girardot C, Bracken AP, et al. Dual
855 functionality of. Genes Dev. 2017;31(6):590-602.
856 66. Schuettengruber B, Bourbon HM, Di Croce L, Cavalli G. Genome Regulation by Polycomb and
857 Trithorax: 70 Years and Counting. Cell. 2017;171(1):34-57.
858 67. Weintraub AS, Li CH, Zamudio AV, Sigova AA, Hannett NM, Day DS, et al. YY1 Is a Structural
859 Regulator of Enhancer-Promoter Loops. Cell. 2017;171(7):1573-88.e28.

860 68. Beagan JA, Duong MT, Titus KR, Zhou L, Cao Z, Ma J, et al. YY1 and CTCF orchestrate a 3D
861 chromatin looping switch during early neural lineage commitment. Genome Res. 2017;27(7):1139-52.
862 69. Uyehara CM, Nystrom SL, Niederhuber MJ, Leatham-Jensen M, Ma Y, Buttitta LA, et al.
863 Hormone-dependent control of developmental timing through regulation of chromatin accessibility.
864 Genes Dev. 2017;31(9):862-75.
865 70. Nystrom SL, Niederhuber MJ, McKay DJ. Expression of E93 provides an instructive cue to
866 control dynamic enhancer activity and chromatin accessibility during development. Development.
867 2020;147(6).
868 71. Quinlan KG, Verger A, Kwok A, Lee SH, Perdomo J, Nardini M, et al. Role of the C-terminal
869 binding protein PXDLS motif binding cleft in protein interactions and transcriptional repression. Mol
870 Cell Biol. 2006;26(21):8202-13.
871 72. Basu A, Atchison ML. CtBP levels control intergenic transcripts, PHO/YY1 DNA binding, and PcG
872 recruitment to DNA. J Cell Biochem. 2010;110(1):62-9.
873 73. Marchetti G, Tavosanis G. Steroid Hormone Ecdysone Signaling Specifies Mushroom Body
874 Neuron Sequential Fate via Chinmo. Curr Biol. 2017;27(19):3017-24.e4.
875 74. Narbonne-Reveau K, Maurange C. Developmental regulation of regenerative potential in
876 Drosophila by ecdysone through a bistable loop of ZBTB transcription factors. PLoS Biol.
877 2019;17(2):e3000149.
878 75. Nègre N, Brown CD, Ma L, Bristow CA, Miller SW, Wagner U, et al. A cis-regulatory map of the
879 Drosophila genome. Nature. 2011;471(7339):527-31.
880 76. Panganiban G, Sebring A, Nagy L, Carroll S. The development of crustacean limbs and the
881 evolution of arthropods. Science. 1995;270(5240):1363-6.
882 77. Jory A, Estella C, Giorgianni MW, Slattery M, Laverty TR, Rubin GM, et al. A survey of 6,300
883 genomic fragments for cis-regulatory activity in the imaginal discs of Drosophila melanogaster. Cell
884 Rep. 2012;2(4):1014-24.

885 78. Slattery M, Voutev R, Ma L, Nègre N, White KP, Mann RS. Divergent transcriptional regulatory
886 logic at the intersection of tissue growth and developmental patterning. PLoS Genet.
887 2013;9(9):e1003753.

888

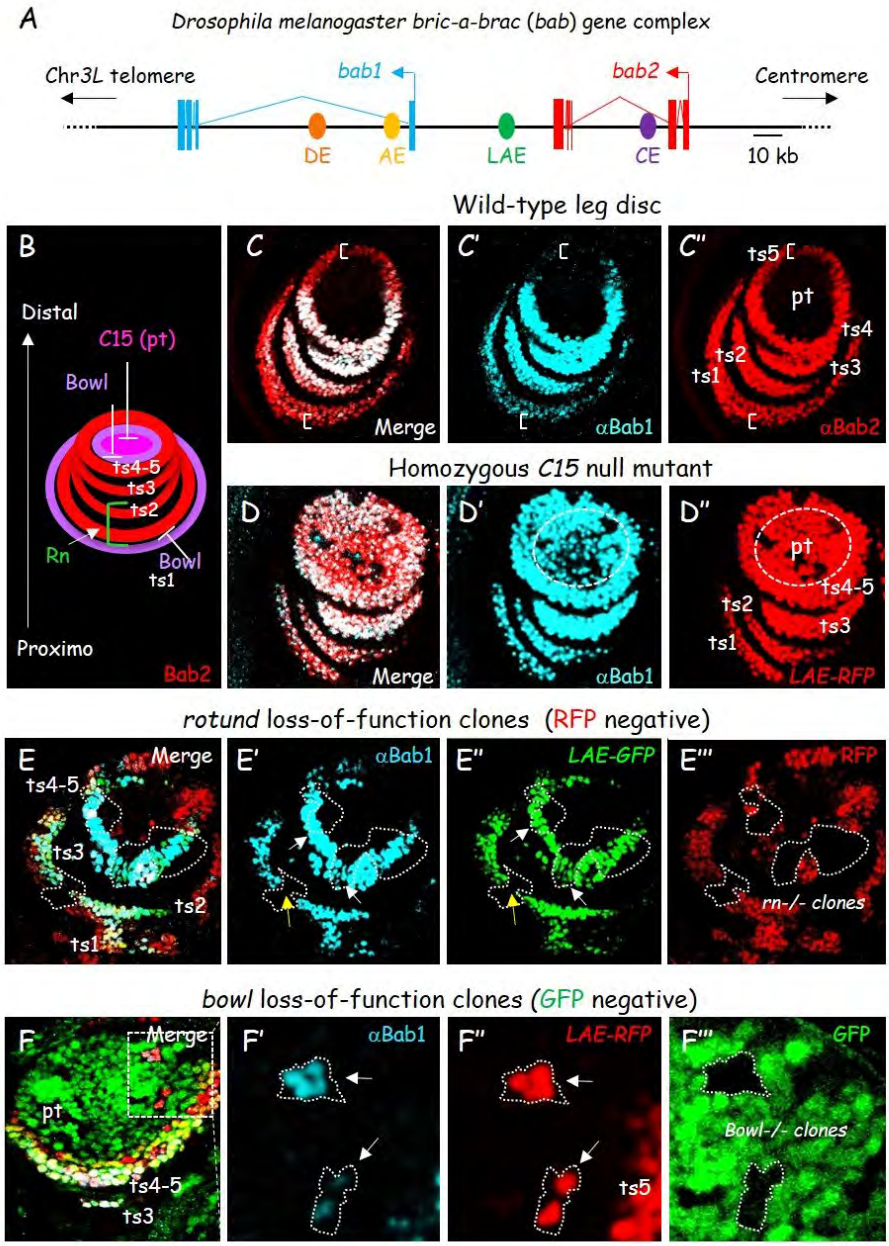

Fig 1. *C15*, *rotund* and *bowl* all regulate both *bab1* and *bab2*. (A) Schematic view of the *Dmel bab* locus on the 3L chromosomal arm (Chr*3L*). The tandem *bab1* (blue) and *bab2* (red) transcription units (filled boxes and broken lines represent exons and introns, respectively), the previously known CRE/enhancers are depicted by filled dots (abdominal DE and AE in dark and light orange, respectively; leg/antennal LAE in dark green and cardiac CE in purple), and the telomere and centromere directions are indicated by arrows. **(B)** A scheme depicted C15, Bowl and Rn TF activities in regulating *bab2* expression as a four-ring pattern within the developing distal leg, is shown. **(C)** Medial confocal view of a wild-type L3 leg disc. Merged Bab1 (blue) and Bab2 (red) immunostainings, as well as each marker in isolation in (C') and (C"), respectively, are shown. Positions of *bab2*-expressing ts1-5 cells and the pretarsal (pt) field are indicated in (C"). Brackets indicate paralog-specific expression in proximalmost and distalmost *bab2*-expressing cells. **(D)** Distal confocal view of a homozygous $C15^{2}$ mutant L3 leg disc expressing *LAE-RFP*. Merged Bab1 immunostaining (in blue) and RFP fluorescence (red), and each marker in isolation in (D') and (D"), are shown. Bab2-expressing mutant pt cells are circled with a dashed line in (D') and (D"). **(E)** Medial confocal view of a mosaic L3 leg disc expressing *LAE-GFP* and harboring *rotund* mutant clones. Merged Bab1 (blue) immunostaining, GFP (green) and RFP (red) fluorescence, as well as each marker in isolation in (E'), (E") and (E"'), respectively, are shown. Mutant clones are detected as black areas, owing to the loss of RFP. The respective ts1-5 fields are indicated in (E). White and yellow arrows indicate *bab1* (*bab2*) still- and non-expressing *rotund-/-* clones, respectively. **(F)** Distal confocal view of a mosaic L3 leg disc expressing *LAE-RFP* and harboring *bowl* mutant clones. Merged Bab1 (blue) immunostaining, RFP (red) and GFP (green) fluorescence, as well as a higher magnification of the boxed area for each marker in isolation in (F'), (F") and (F"'), respectively, are shown. Mutant clones are detected as black areas, owing to the loss of GFP. White arrows indicate pretarsal *bowl-/-* clones ectopically expressing both *bab1* and *LAE-RFP* (*bab2*).

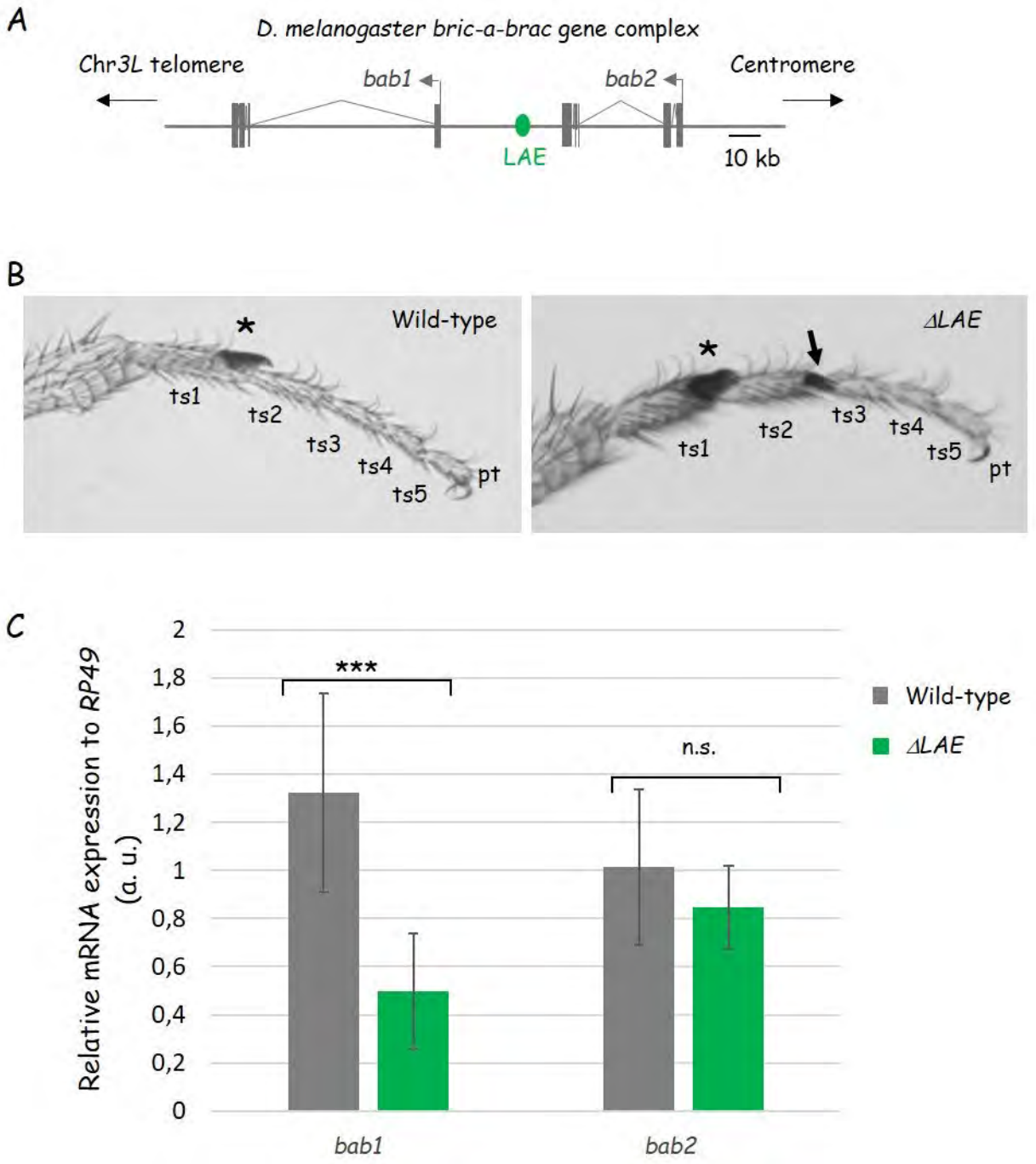

Fig 2. LAE is not critically required for tarsal segmentation and for overall *bab2* expression in the leg disc. **(A)** Schematic view of the *Dmel bab* locus on the 3L chromosomal arm (Chr*3L*). The tandem *bab1* and *bab2* transcription units (filled boxes and broken lines represent exons and introns, respectively), the intergenic LAE enhancer (in green), as well as the telomere and centromere directions, are depicted as in Fig 1A, except that both genes are depicted in grey. The small CRISPR/Cas9-mediated chromosomal deficiency ($bab^{\Delta LAE}$) is shown in beneath (deleted LAE is depicted as a broken line). **(B)** Photographs of wild-type and homozygous $bab^{\Delta LAE}$ T1 distal legs from adult males. The regular sex-comb (an array of about 10 specialized bristles on the male forelegs) on distal ts1 is indicated with asterisks, while ectopic sex-comb bristles on distal ts2 from the mutant leg (right) is indicated by an arrow. Note that the five tarsal segments remain individualized in homozygous $bab^{\Delta LAE}$ mutant legs. **(C)** Overall *bab1-2* expression from wild-type and homozygous $bab^{\Delta LAE}$ L3 leg discs, as determined from reverse transcription quantitative PCR analyses. The *bab1-2* expression levels were quantified relative to *rp49* mRNA abundance.

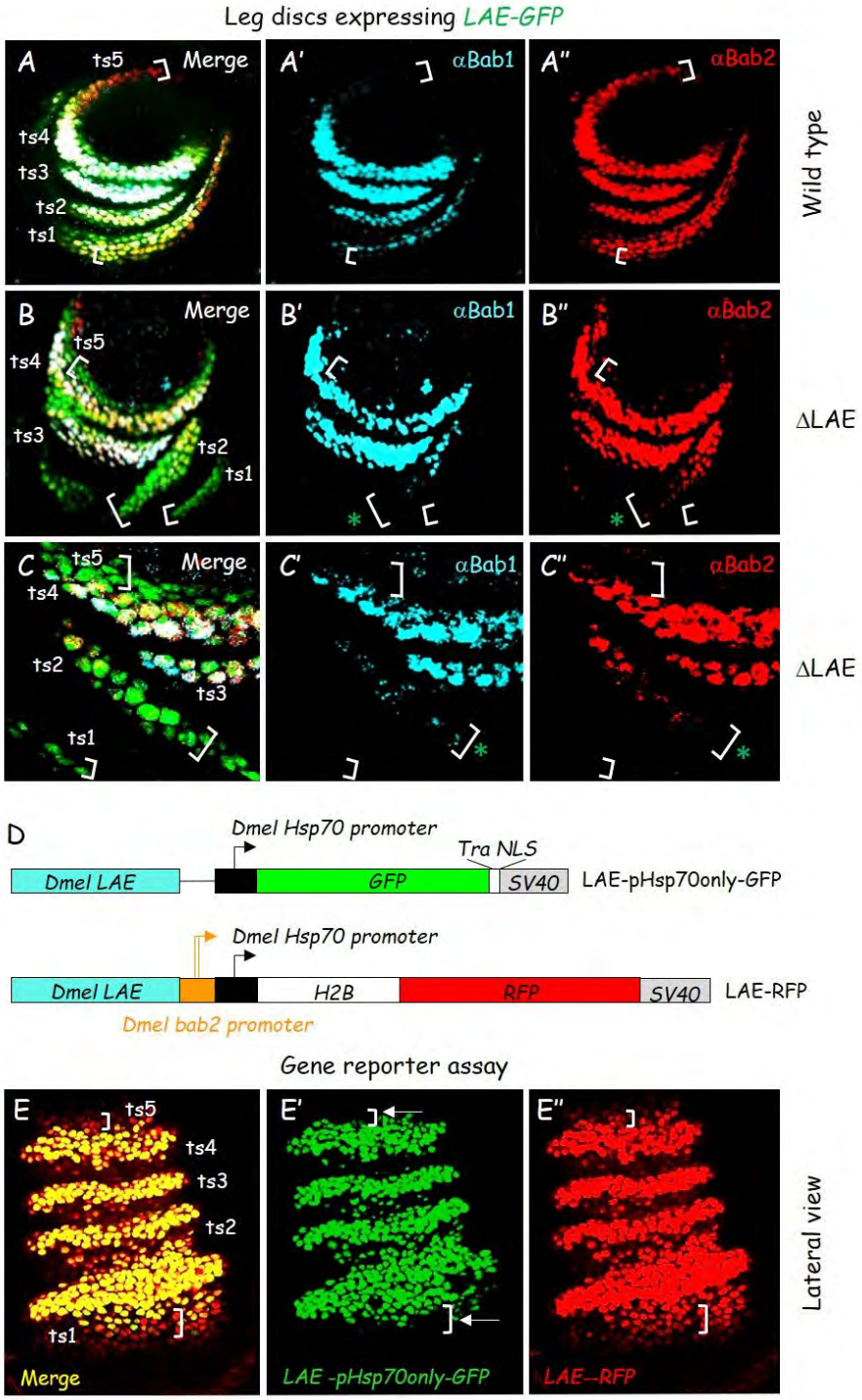

Fig 3. LAE is mostly critically required for paralog-specific *bab2* expression in the developing distal legs. (A-C) Medial (A-B) and distal (C) confocal views of wild-type (A) and homozygous bab^{DLAE} mutant (B and C) L3 leg discs expressing *LAE-GFP*. Merged GFP fluorescence (green), Bab1 (blue) and Bab2 (red) immunostainings, as well as the two latter in isolation in (A'-C') and (A"-C"), respectively, are shown. Brackets indicate positions of paralog-specific expression in proximalmost (ts1) and distalmost (ts5) *bab2*-expressing (GFP+) cells. Green asterisks in (B'-B") and (C'-C") indicate weaker expression of both *bab* paralogs in GFP+ ts2 cells. **(D)** Modular structures of the *LAE-pHsp70onlyGFP* and *LAE-RFP* reporter constructs. GFP (green box) and RFP (red box) open-reading frames (ORFs) have been fused with ORFs for the Transformer (Tra) nuclear localization signal (NLS) and the histone H2B, respectively (see white boxes). The *SV40* polyadenylation signal region is boxed in grey. The *Dmel* LAE sequence is boxed in blue. The classical non-heat-inducible basal *Hsp70* promoter sequence is boxed in black, while the *bab2* core promoter sequence is depicted in orange. Note that both promoters are juxtaposed in the *LAE-RFP* construct. **(E)** LAE activity requires functionally the *bab2* promoter to ensure paralog-specific expression in the developing legs. A lateral confocal view of merged GFP (green) and RFP (red) fluorescence, as well as each marker in isolation in (E') and (E"), respectively, of the distal part of an early pupal leg expressing both the *LAE-pHsp70onlyGFP*^{ZH2A} and *LAE-RFP*^{ZH86Fb} reporter constructs (depicted in (D)), are shown. Brackets indicate tarsal RFP+ cells expressing *bab2* in a paralog-specific manner, which never express the *LAE-pHsp70onlyGFP*^{ZH2A} reporter which lacks *bab2* core promoter sequences (see white arrows).

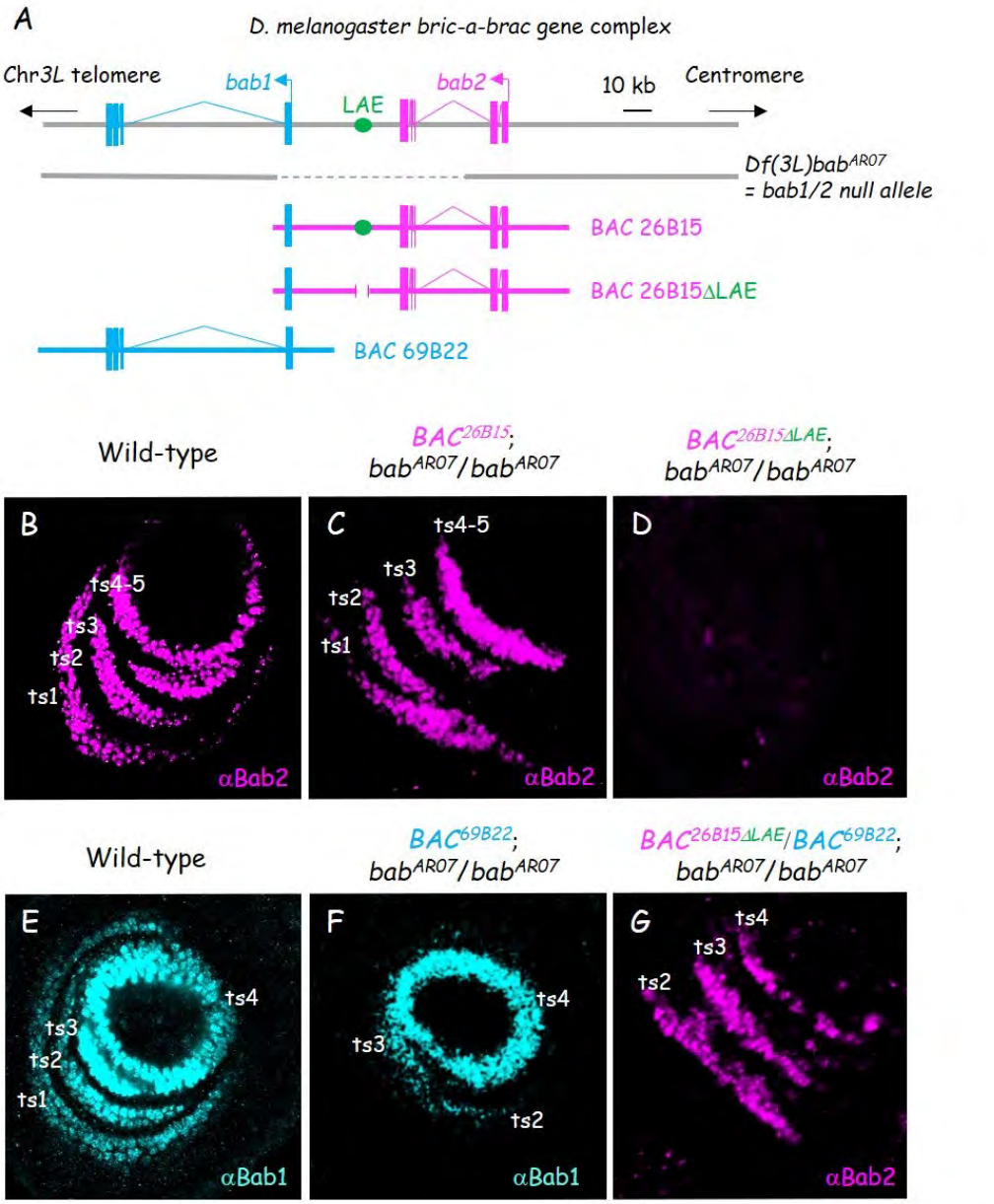

Fig 4. *bab1* includes partially-redundant limb-specific *cis*-regulatory information. (A) Chromosomal deficiency and BAC constructs covering the *bab* locus. The tandem gene paralogs and intergenic LAE are depicted as shown in Fig. 1A, except that *bab2* is depicted in pink instead of red. The *bab*^{AR07} *3L* chromosomal deficiency is shown in beneath, with known deleted portion indicated by a dashed line. Note that the breakpoints have not been precisely mapped. The two overlapping BAC constructs *69B22* and *26B15*, as well as a mutant derivative of the latter specifically-deleted for LAE, are shown further in beneath. **(B-G)** Medial confocal views of wild-type (B-E) and homozygous *bab*^{AR07} mutant (C-D and F-G) L3 leg discs, harboring singly or combined X-linked BAC construct(s) shown in (A), as indicated above each panel. Bab2 (pink) and Bab1 (blue) immunostainings are shown. Positions of *bab1*- and *bab2*-expressing ts1-4 cells are indicated. Note stochastic *bab2* expression in (G).

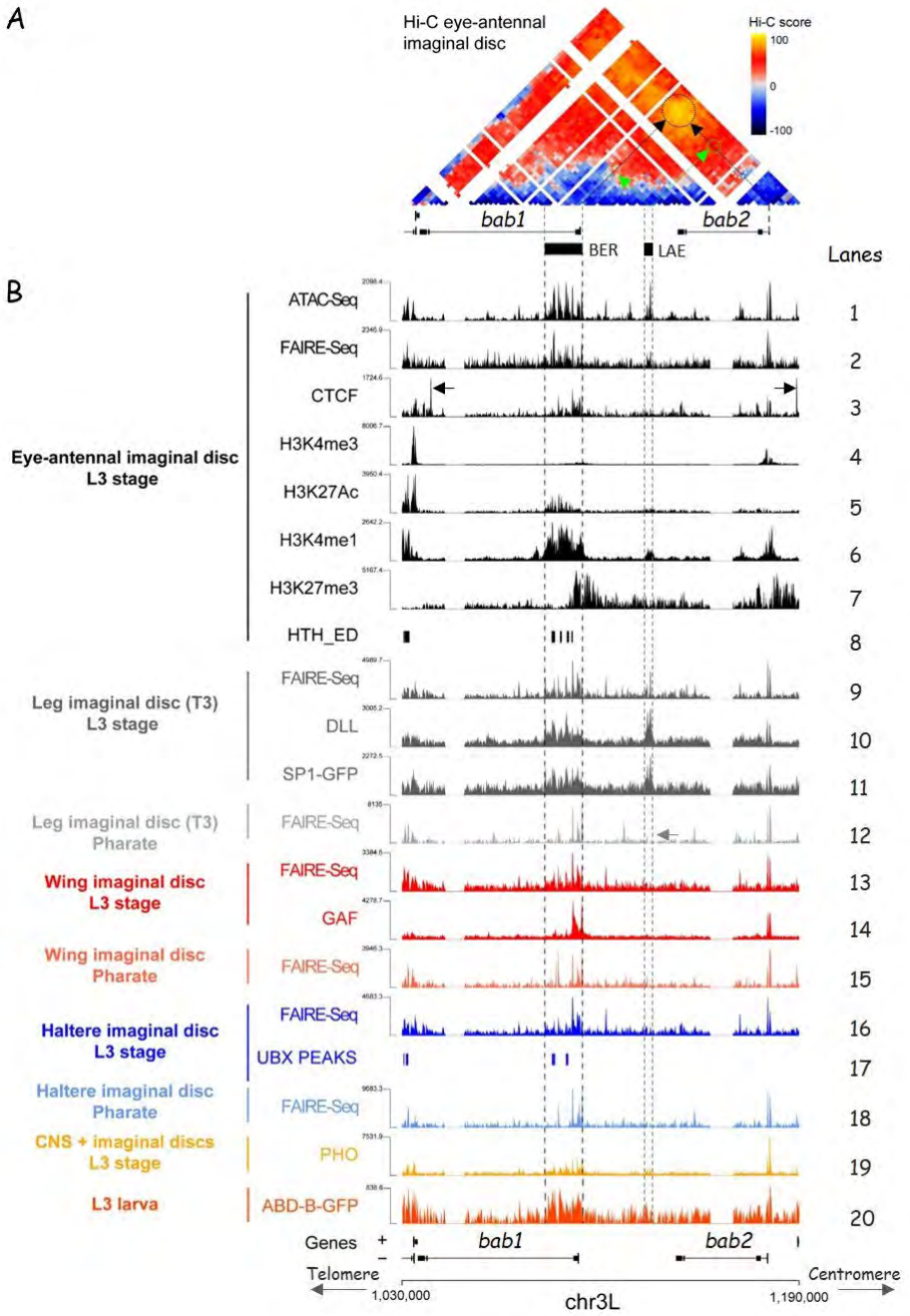

Fig 5. A topologically-associating domain encompasses the *bab* locus in the eye-antennal disc and genome-wide chromatin features identify an enhancer signature region (BER) within *bab1*. (A) Hi-C screenshot of a 160 kb region covering the *Dmel bab* gene complex. Score scale is indicated on the right (yellow to dark blue from positive to negative). **(B)** ATAC-, FAIRE- and/or ChIP-Seq profiles from L3 eye-antennal (ED), leg, wing and haltere discs as well as from adult pharate appendages (leg, wing and haltere) and from whole larval tissues, as indicated on the left side. As referred in the main text, lanes are numbered on the right side. ChIP-Seq peak calling data are shown in lanes 8, 17-18. Otherwise, normalized open chromatin, histone H3 post-translational modifications and TF binding profiles are shown. Positions of the tandem *bab1-2* genes are indicated on the bottom. The respective locations of the BER and LAE sequences are highlighted with vertical dashed lines. Of note, according to normalized FAIRE-Seq signals, LAE is not fully accessible in the pharate T3 leg (see grey arrow in lane 12). Strongest CTCF ChIP-Seq signals are indicated by horizontal black arrows (lane 3).

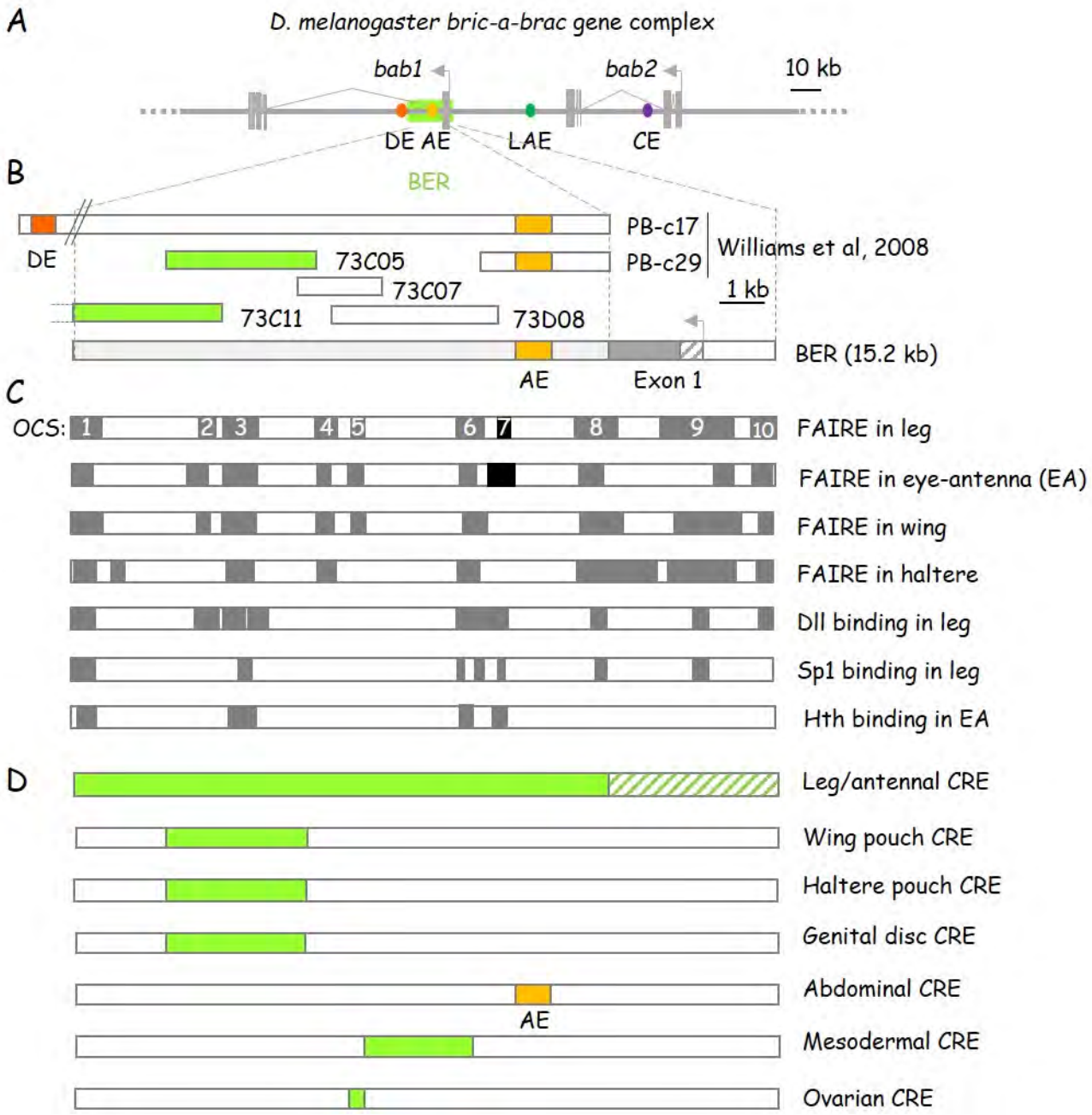

Fig 6. BER behaves as a composite pleiotropic enhancer. (A) The BER enhancer signature region includes the abdominal AE enhancer. Organization of the *Dmel bab* locus, with the tandem gene paralogs as depicted as in Fig. 2A. The characterized enhancers are depicted by filled dots (abdominal DE and AE in dark and light orange, respectively; leg/antennal LAE in dark green and cardiac CE in purple). BER is boxed in light green. The genomic portions of the overlapping *69B22* and *26B15* BAC constructs are shown in beneath. **(B)** Transgenic lines covering BER identify *cis*-regulatory elements driving reporter gene expression in diverse larval imaginal tissues. Genomic fragments covered by relevant Janelia Farm FlyLight reporter lines [77] and the DE- and/or AE-containing PB-c17 and PB-c29 genomic constructs, described in [14], are shown above a scheme of the BER region. *bab1* protein coding and 5'-untranslated sequences within the first exon are filled or hatched in dark grey, respectively, while the intronic region is in light gray. The AE sequence is in orange, as depicted in (A). FlyLight reporter lines driving reporter expression in diverse imaginal discs (see S4 Fig) are filled in light green. **(C)** BER includes open chromatin sequences (OCS) and is bound by Dll, Sp1, Hth TFs in diverse developing appendages (leg, eye-antenna, wing and haltere). OCS and TF-bound sequences are depicted by filled grey/black boxes. Numbers refer to OCSs detected in the leg discs (see main text). The black boxes represent OCSs detected in the eye-antennal (EA) and leg but not in wing and haltere discs. OCS and Dll or Sp1-bound regions, as determined from peak calling (FAIRE-Seq GSE38727 and ChIP-Seq GSE113574 GEO dataset series, respectively), are from [40] and [42], respectively. ChIP-Seq data for Hth are from [78]. **(D)** BER includes pleiotropic *cis*-regulatory elements (CREs). Locations of predicted CREs (see text) are indicated by light green boxes. The hatched part of the predicted leg/antennal CRE is inferred from data obtained with the PB-c17 construct reported in [14].

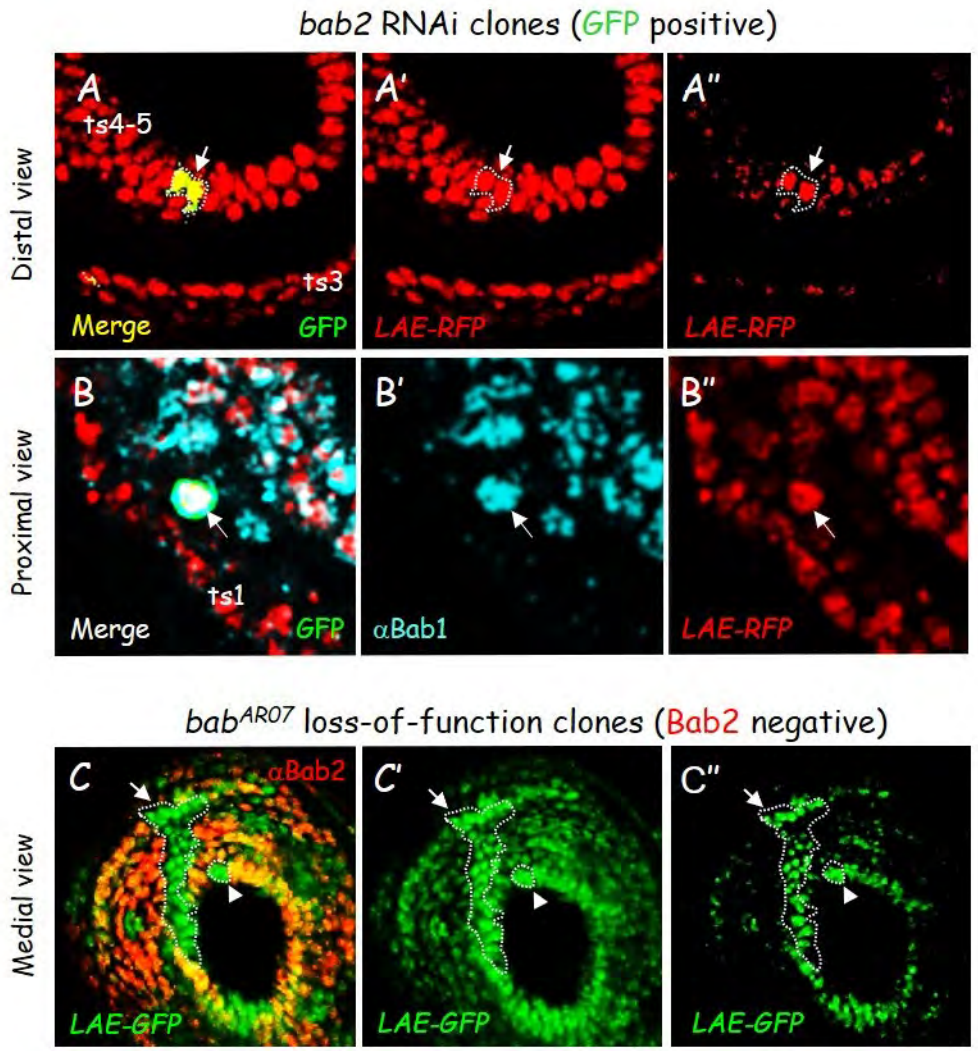

Fig 7. Auto- and cross-regulation among the two *bab* paralogs in the developing legs. (A) Distal confocal view of a L3 leg disc expressing *LAE-RFP* and harboring flip-out (FO) clones expressing interfering RNA against *bab2*. Merged RFP (red) and GFP (green) fluorescence, as well as the former in isolation and under two distinct signal magnification (A' and A"), are shown. A FO clone (GFP+) within *LAE-RFP* (*bab2*)-expressing ts4 cells is circled with a dashed line (see arrow). **(B)** Proximal confocal view of a L3 leg disc expressing *LAE-RFP* and harboring FO clones expressing interfering RNA against *bab2*. Merged Bab1 (blue) immunostaining, RFP (red) and GFP (green) fluorescence, as well as the two formers in isolation, in (B') and (B"), respectively, are shown. Note that a single-cell FO clone (GFP+), within *LAE-RFP* (*bab2*)-expressing ts1 cells, is sufficient to upregulate *bab1* (see arrows). **(C-D)** L3 leg (C) and eye-antennal (D) discs expressing *LAE-GFP* and harboring mutant clones for the protein null allele bab^{AR07}. Merged Bab2 (red) immunostaining and GFP (green) fluorescence as well as the latter in isolation under two distinct signal magnifications (C'-C" and D'-D"), are shown. Tiny and larger clones (Bab2 negative) are circled with dashed lines (arrowheads and arrows, respectively).

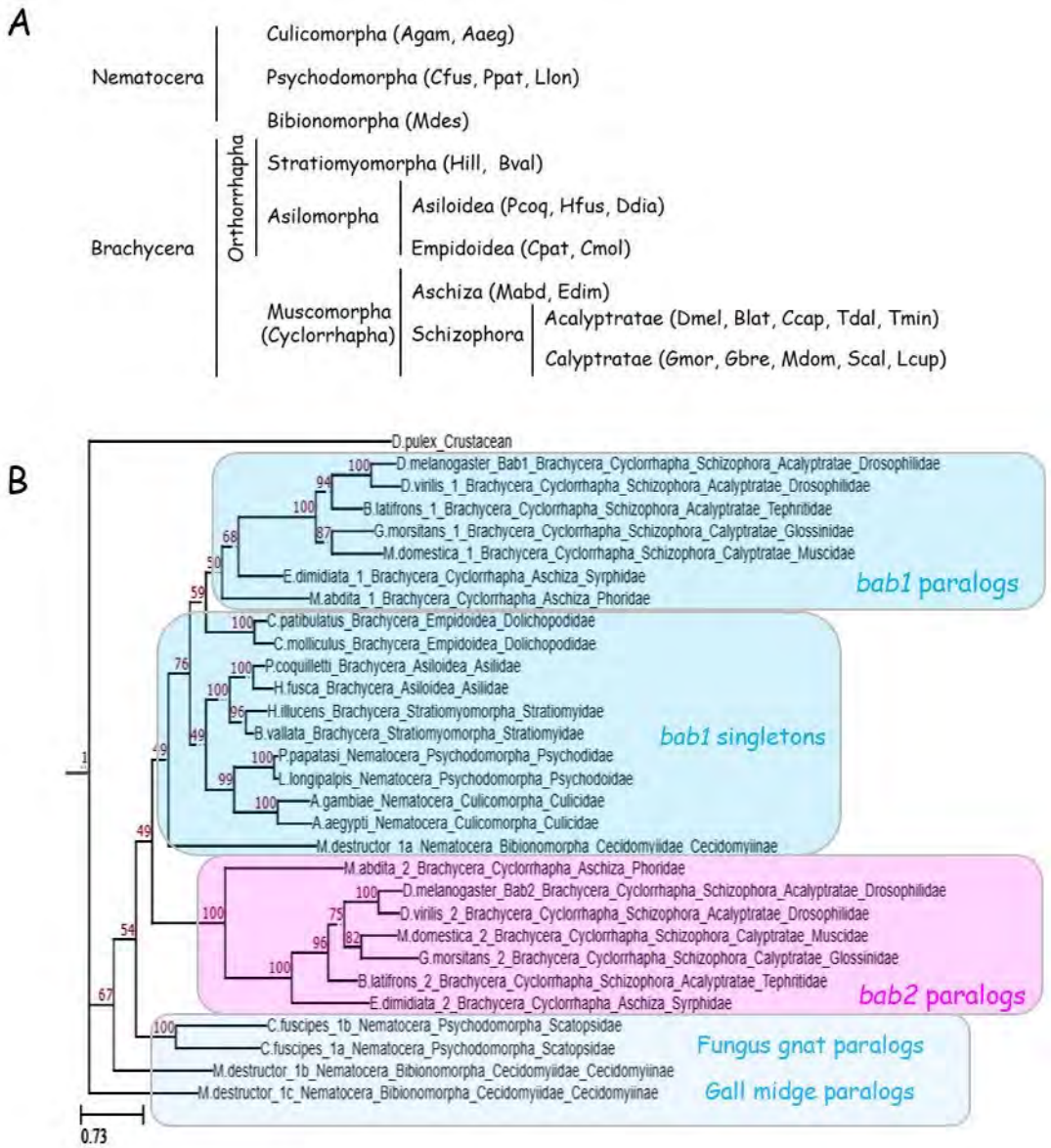

Fig 8. Phylogenetic relationships among dipteran *bab* paralogs and orthologs. (A) Dipteran families studied in this work. Species abbreviations are described in Supplementary data. **(B)** Phylogenetic relationships of the *bab* paralogs and orthologs inferred from a maximum likelihood consensus tree constructed from 1000 bootstrap replicates. Support values (percentage of replicate trees) are shown in red. Scale bar represents substitution per site. Clustered positions of *bab2* paralogs and *bab1* paralogs/orthologs are shown in pink and light blue, respectively.

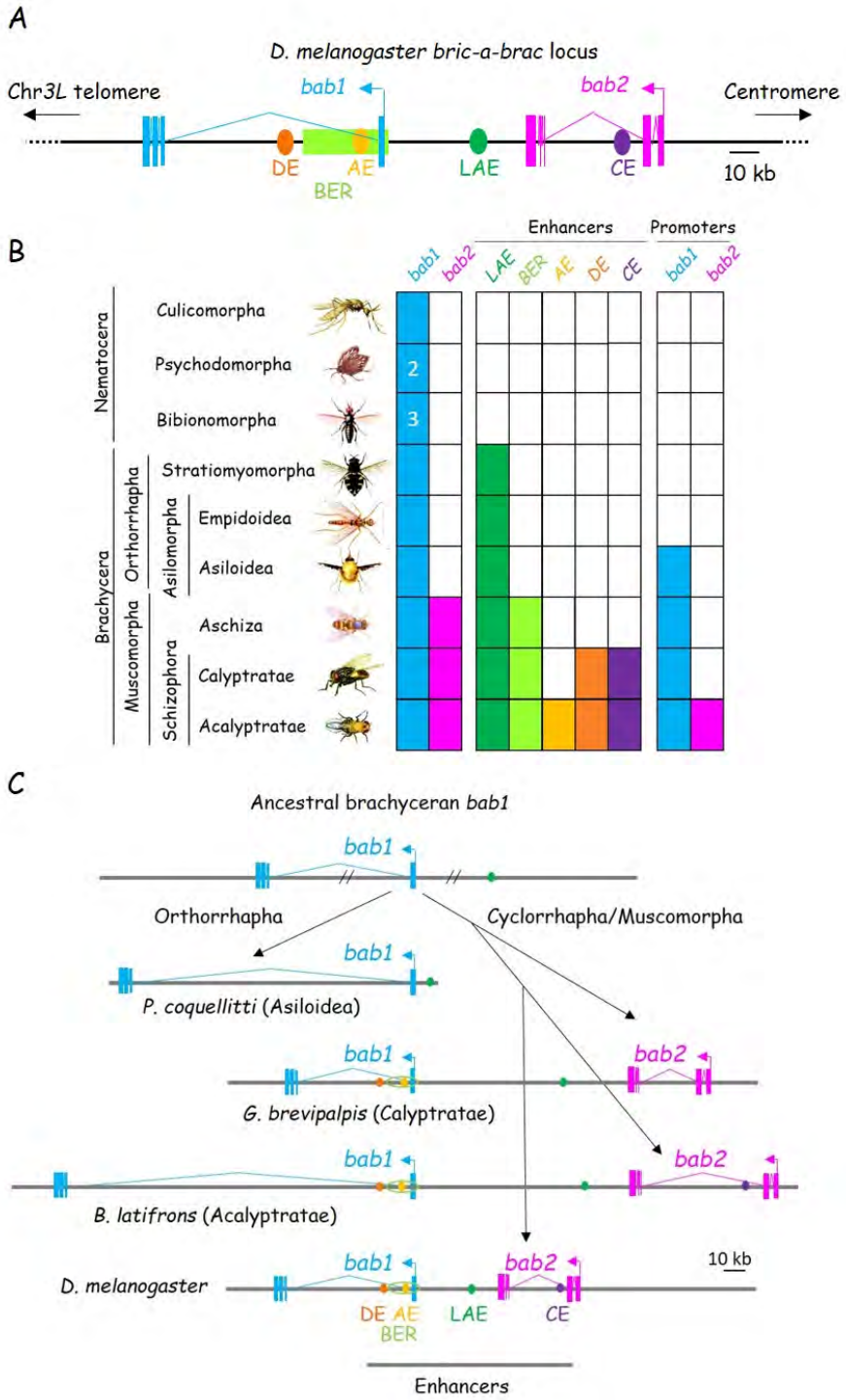

Fig 9. Conservation of enhancer/promoter sequences and evolutionary history of the *bab* locus among the Brachycera. (A) Organization of the *Dmel bab* gene paralogs and enhancers. The locus is depicted as in Fig 1A, except that *bab2* is represented in pink instead of red. **(B)** Evolutionary conservation of the *bab* gene paralogs, enhancers and promoters among diverse dipterans. Infraorders, sections, subsections and superfamilies are indicated on the left, arranged in a phylogenetic series from the "lower" Nematocera to the "higher" Brachycera suborders. Presence of *bab1* and/or *bab2* paralogs and conservation of enhancer and promoter sequences are indicated by filled or hatched boxes colored as depicted in (A). **(C)** Evolutionary scenario for the *bab* locus within the Brachycera suborders. A scheme depicting chromosomal fate of an ancestral *bab1*-like gene which gives rise to derived extant orthorrhaphan singletons (Asilomorpha) and Muscomorpha-specific paralogous (Calyptratae and Acalyptratae) genes. Locations of conserved enhancer sequences are shown, as depicted in (A).

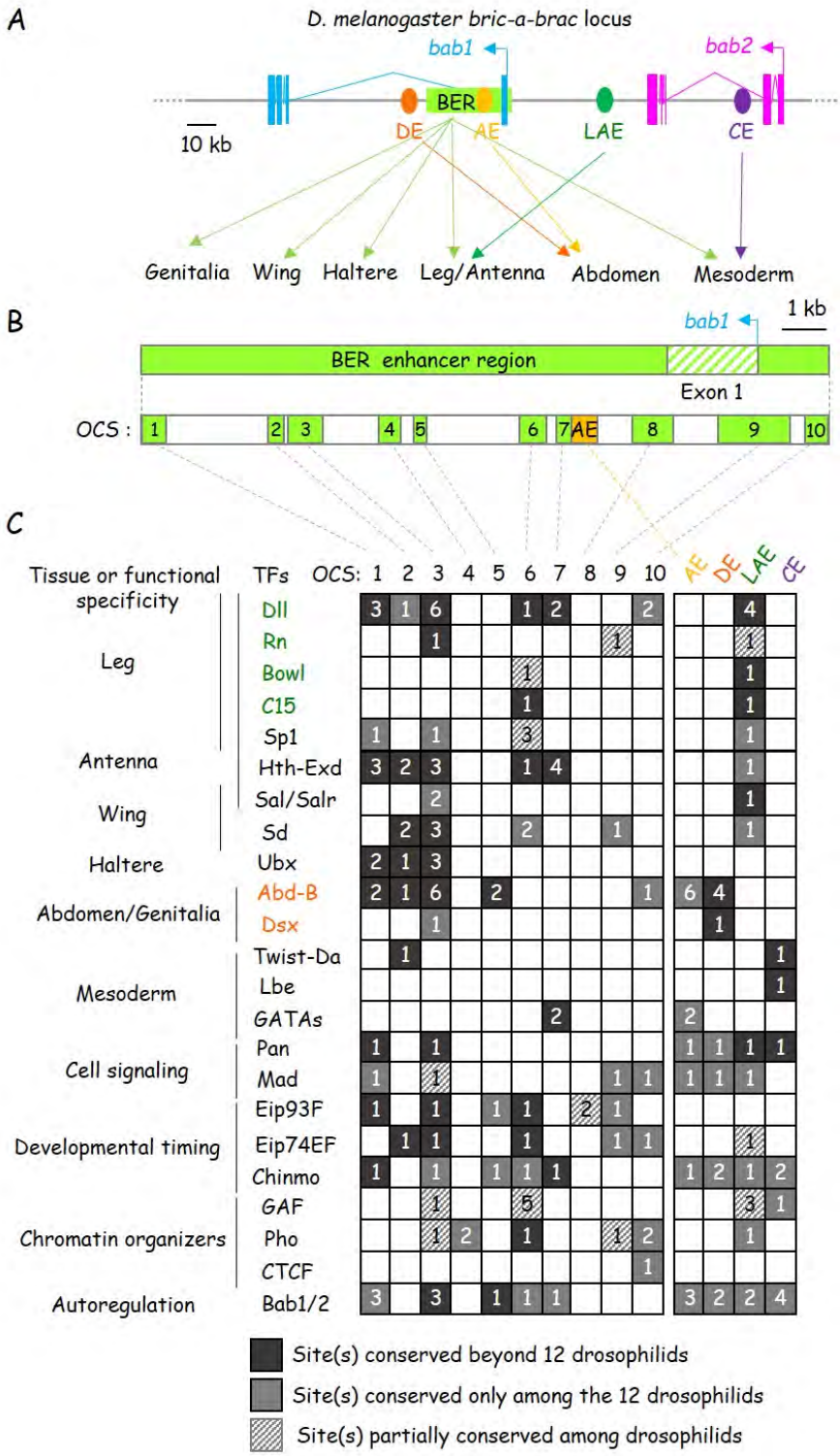

Fig 10. A comprehensive predictive tissue-specific TF code governing *bab* paralog expression. (A) Organization of the *Dmel bab* gene paralogs and enhancers, as depicted in Fig 9A. Expression tissue specificities conferred by each enhancer are shown in beneath. **(B)** BER structural and chromatin state organizations. The *bab1* first exon is hatched. OCS regions (see Fig 6C), as defined in leg tissues; are represented by light green boxes. The abdominal AE CRE (not detected in FAIRE-Seq data from leg and eye-antennal discs) is depicted as a light orange box. **(C)** Evolutive conservation of predicted TF binding sites within *Dmel bab cis*-regulatory sequences. Site conservation among and beyond drosophilids of transcriptional regulators involved in tissue-specific morphogenetic processes, cell signaling, developmental timing and chromatin organization. Predicted/validated TF site numbers are indicated within colored or hatched boxes reflecting their relative conservation are indicated in beneath. Experimentally-validated direct *bab* regulators are colored according to their well characterized bound-enhancer sequences (see A).

Wild-type leg disc

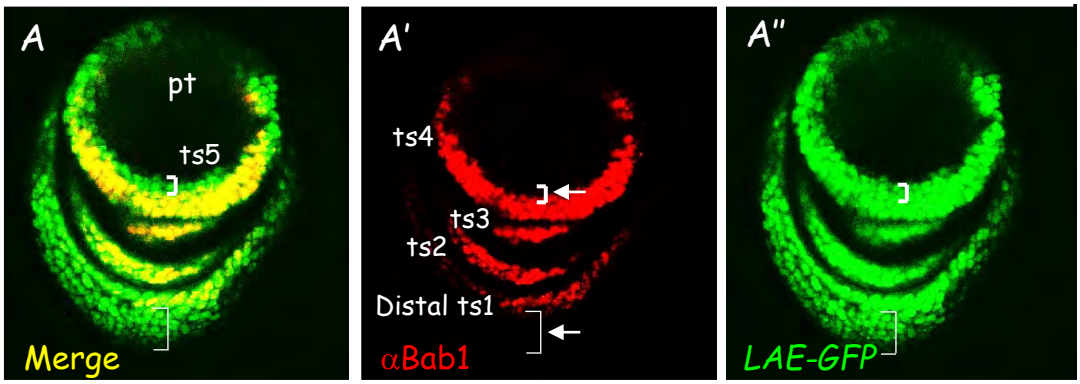

rotund gain-of-function (Dll domain)

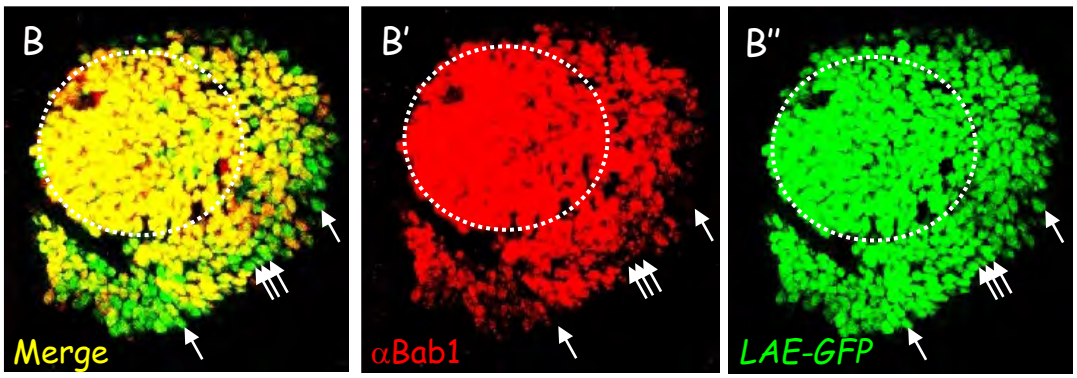

bowl gain-of-function clones (FO *lines* RNAi; GFP+)

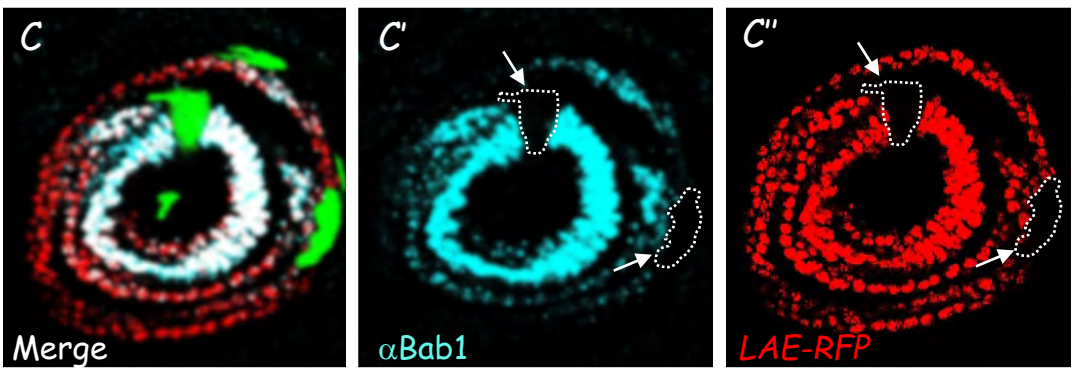


LAE _
Up targeted site
Down targeted site
Wt TAGGGTATTTGCGTGGAGCCTTCTTCGCCAGGCCGGCCTTTTGTTTTATTTCCTTGACTC//CCGGTTGTTCTAATTGTTGGCTAGTTAGGCGCACATAAGGAGGCAGGTCTCTGAACCC
M1 TAGGGTATTTGCGT----------//----------caaaagagtcaGTCTCTGAACCC
M2 TAGGGTATTTGCGTGGAGCaaat----------//----------agagaCTGAACCC
M3 TAGGGTATTTGCGTGGAGCCTTC----------//----------ttcgcAGGTCTCTGAACCC
M4 TAGGGTATTTGCGTGGAGCCTTC----------//----------tagacctgcGCAGGTCTCTGAACCC
M5 TAGGGTATTTGCGTGGAGCCTTCTTgcgcaaaat----------//----------
M6 TAGGGTATTTGCGTGGAGCCTTCTTCGC----------//----------gcGGCAGGTCTCTGAACCC

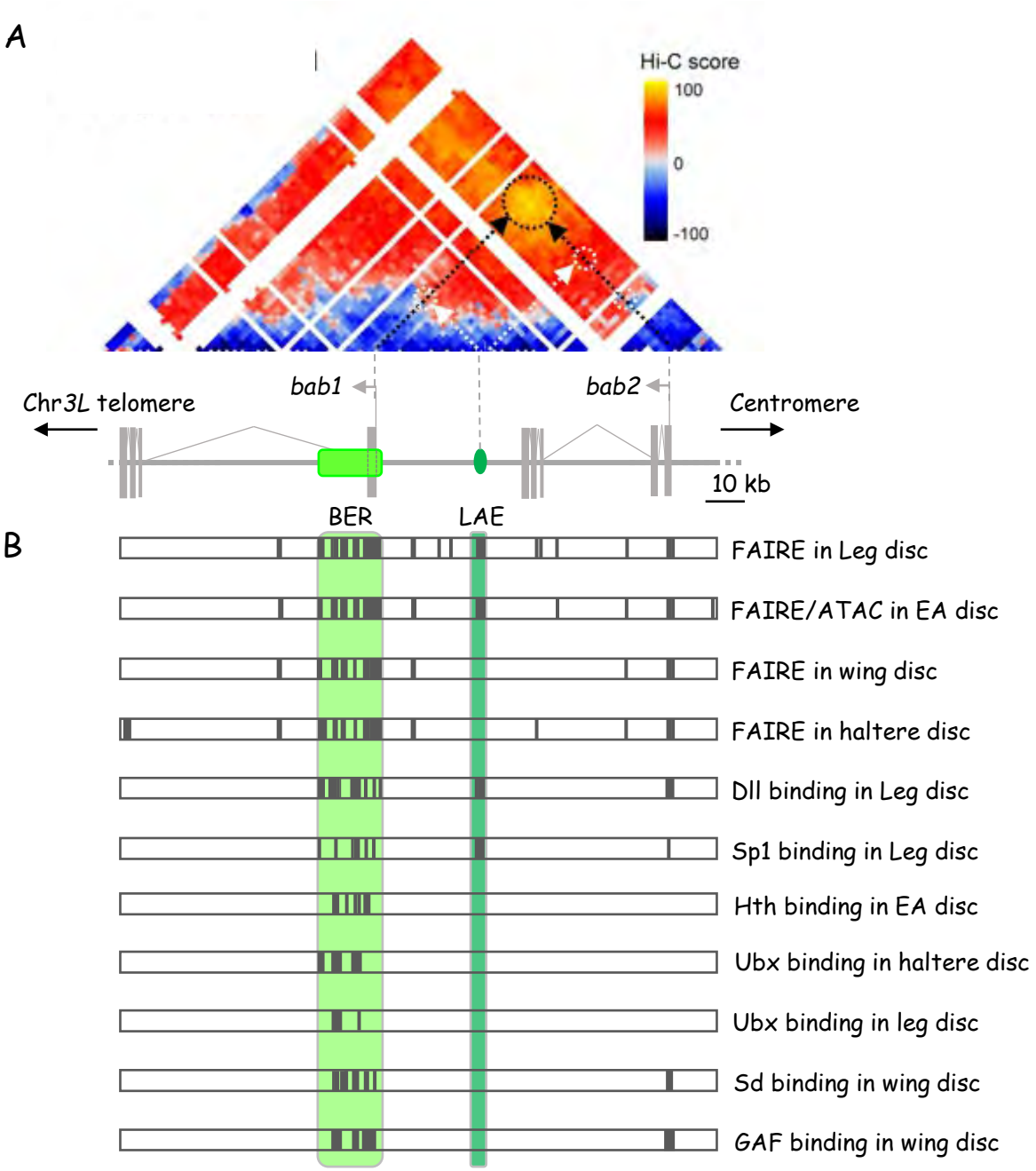
A
Hi-C score
100
0
-100
bab1
bab2
Chr3L telomere
Centromere
10 kb
B
BER
LAE
FAIRE in Leg disc
FAIRE/ATAC in EA disc
FAIRE in wing disc
FAIRE in haltere disc
Dll binding in Leg disc
Sp1 binding in Leg disc
Hth binding in EA disc
Ubx binding in haltere disc
Ubx binding in leg disc
Sd binding in wing disc
GAF binding in wing disc

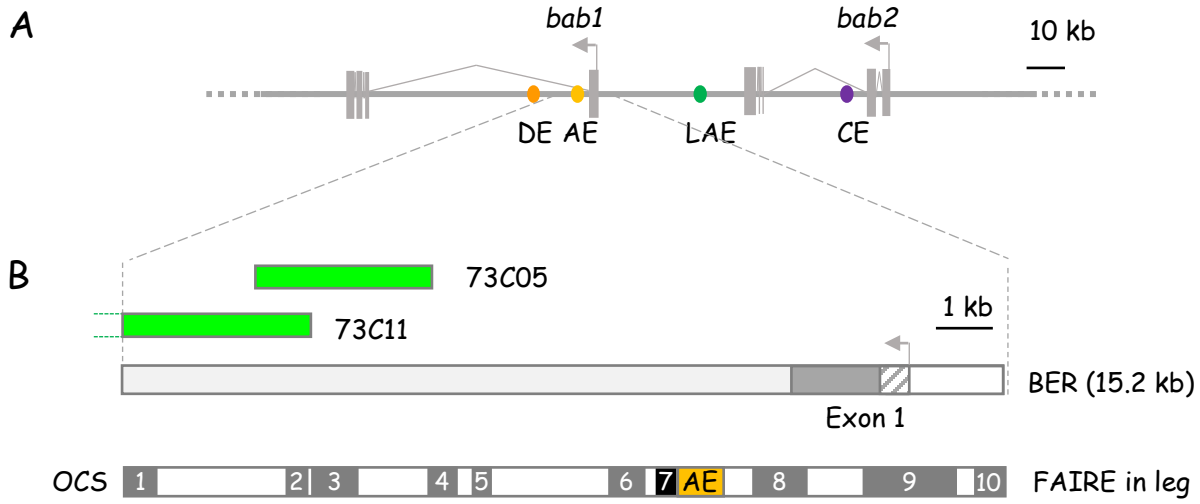

73C11-Gal4 + UAS-GFP

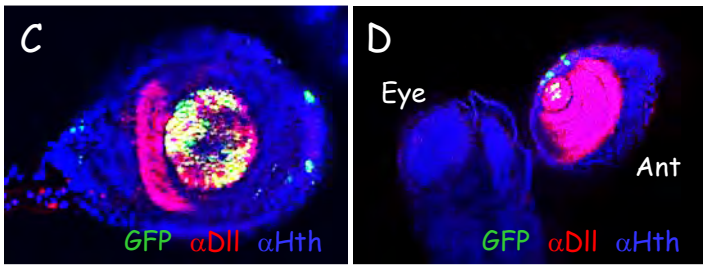

Leg disc Eye-antennal disc

73C05-Gal4 + UAS-GFP

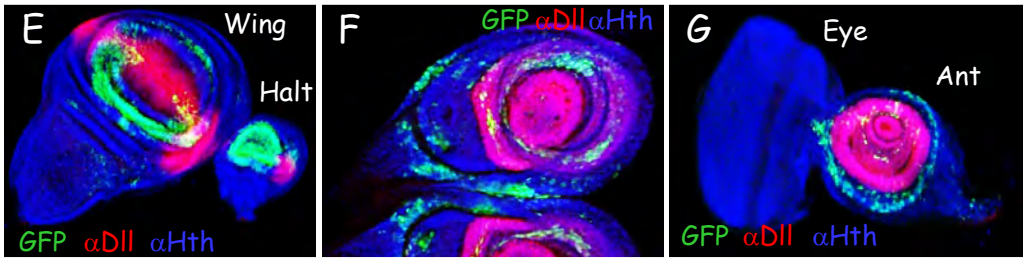

Wing, leg and haltere discs Leg discs Eye-antennal disc

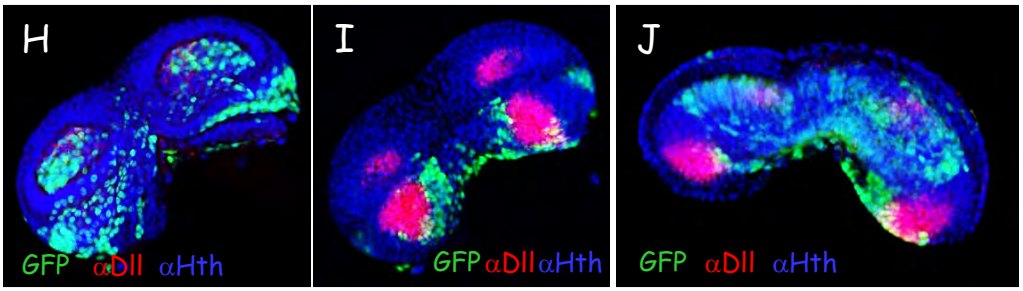

Female genital discs Male genital disc

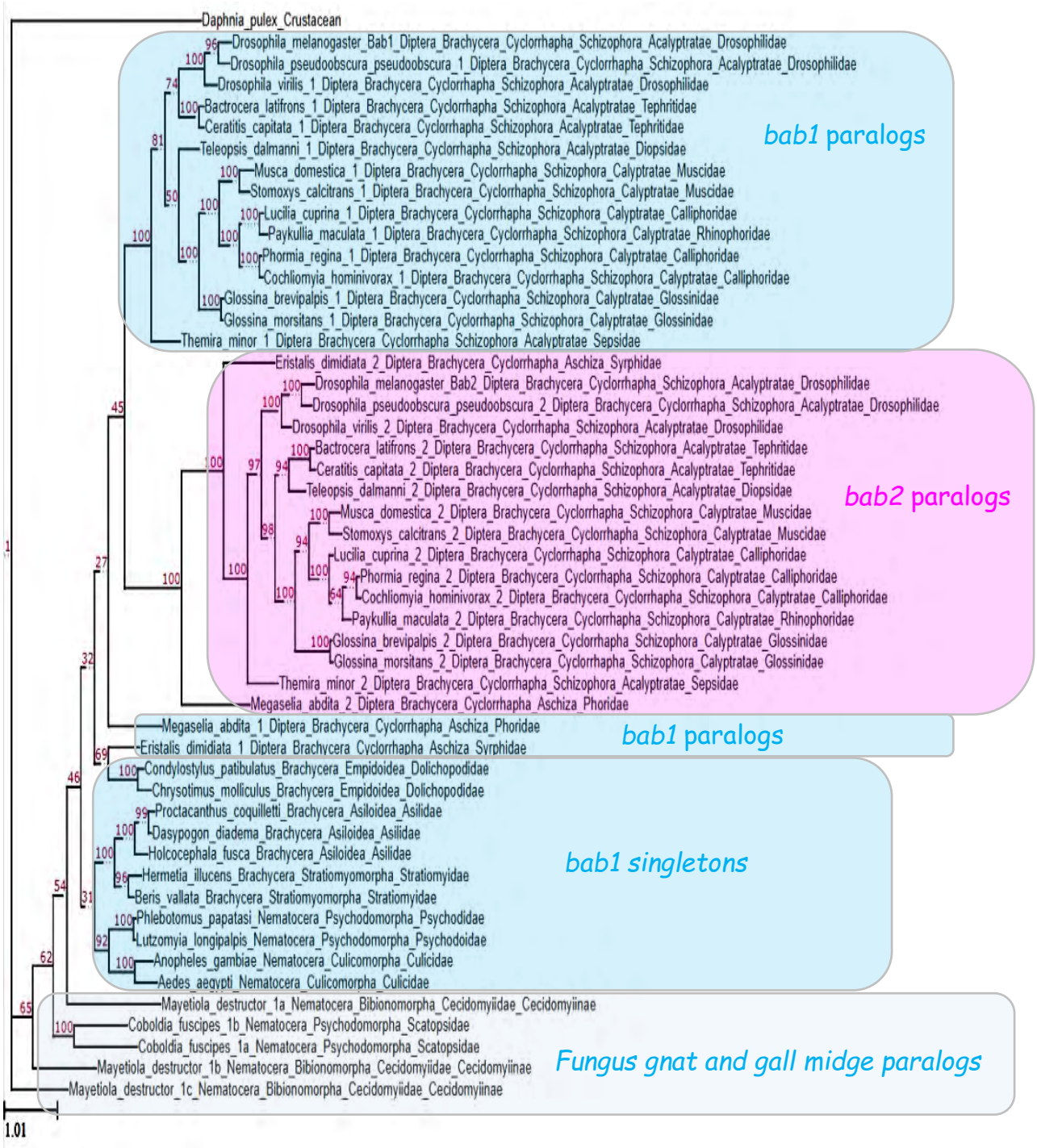
Daphnia_pulex_Crustacean
Drosophila_melanogaster_Bab1_Diptera_Brachycera_Cyclorrhapha_Schizophora_Acalyptratae_Drosophilidae
Drosophila_pseudoobscura_pseudoobscura_1_Diptera_Brachycera_Cyclorrhapha_Schizophora_Acalyptratae_Drosophilidae
Drosophila_virilis_1_Diptera_Brachycera_Cyclorrhapha_Schizophora_Acalyptratae_Drosophilidae
Bactrocera_latifrons_1_Diptera_Brachycera_Cyclorrhapha_Schizophora_Acalyptratae_Tephritidae
Ceratitis_capitata_1_Diptera_Brachycera_Cyclorrhapha_Schizophora_Acalyptratae_Tephritidae
Teleopsis_dalmanni_1_Diptera_Brachycera_Cyclorrhapha_Schizophora_Acalyptratae_Diopsidae
Musca_domestica_1_Diptera_Brachycera_Cyclorrhapha_Schizophora_Calyptratae_Muscidae
Stomoxys_calcitrans_1_Diptera_Brachycera_Cyclorrhapha_Schizophora_Calyptratae_Muscidae
Lucilia_cuprina_1_Diptera_Brachycera_Cyclorrhapha_Schizophora_Calyptratae_Calliphoridae
Paykullia_maculata_1_Diptera_Brachycera_Cyclorrhapha_Schizophora_Calyptratae_Rhinophoridae
Phormia_regina_1_Diptera_Brachycera_Cyclorrhapha_Schizophora_Calyptratae_Calliphoridae
Cochliomyia_hominivorax_1_Diptera_Brachycera_Cyclorrhapha_Schizophora_Calyptratae_Calliphoridae
Glossina_brevipalpis_1_Diptera_Brachycera_Cyclorrhapha_Schizophora_Calyptratae_Glossinidae
Glossina_morsitans_1_Diptera_Brachycera_Cyclorrhapha_Schizophora_Calyptratae_Glossinidae
Themira_minor_1_Diptera_Brachycera_Cyclorrhapha_Schizophora_Acalyptratae_Sepsidae
bab1 paralogs
Eristalis_dimidiata_2_Diptera_Brachycera_Cyclorrhapha_Aschiza_Syrphidae
Drosophila_melanogaster_Bab2_Diptera_Brachycera_Cyclorrhapha_Schizophora_Acalyptratae_Drosophilidae
Drosophila_pseudoobscura_pseudoobscura_2_Diptera_Brachycera_Cyclorrhapha_Schizophora_Acalyptratae_Drosophilidae
Drosophila_virilis_2_Diptera_Brachycera_Cyclorrhapha_Schizophora_Acalyptratae_Drosophilidae
Bactrocera_latifrons_2_Diptera_Brachycera_Cyclorrhapha_Schizophora_Acalyptratae_Tephritidae
Ceratitis_capitata_2_Diptera_Brachycera_Cyclorrhapha_Schizophora_Acalyptratae_Tephritidae
Teleopsis_dalmanni_2_Diptera_Brachycera_Cyclorrhapha_Schizophora_Acalyptratae_Diopsidae
Musca_domestica_2_Diptera_Brachycera_Cyclorrhapha_Schizophora_Calyptratae_Muscidae
Stomoxys_calcitrans_2_Diptera_Brachycera_Cyclorrhapha_Schizophora_Calyptratae_Muscidae
Lucilia_cuprina_2_Diptera_Brachycera_Cyclorrhapha_Schizophora_Calyptratae_Calliphoridae
Phormia_regina_2_Diptera_Brachycera_Cyclorrhapha_Schizophora_Calyptratae_Calliphoridae
Cochliomyia_hominivorax_2_Diptera_Brachycera_Cyclorrhapha_Schizophora_Calyptratae_Calliphoridae
Paykullia_maculata_2_Diptera_Brachycera_Cyclorrhapha_Schizophora_Calyptratae_Rhinophoridae
Glossina_brevipalpis_2_Diptera_Brachycera_Cyclorrhapha_Schizophora_Calyptratae_Glossinidae
Glossina_morsitans_2_Diptera_Brachycera_Cyclorrhapha_Schizophora_Calyptratae_Glossinidae
Themira_minor_2_Diptera_Brachycera_Cyclorrhapha_Schizophora_Acalyptratae_Sepsidae
Megaselia_abdita_2_Diptera_Brachycera_Cyclorrhapha_Aschiza_Phoridae
bab2 paralogs
Megaselia_abdita_1_Diptera_Brachycera_Cyclorrhapha_Aschiza_Phoridae
Eristalis_dimidiata_1_Diptera_Brachycera_Cyclorrhapha_Aschiza_Syrphidae
bab1 paralogs
Condylostylus_patibulatus_Brachycera_Empidoidea_Dolichopodidae
Chrysotimus_molliculus_Brachycera_Empidoidea_Dolichopodidae
Proctacanthus_coquilletti_Brachycera_Asiloidea_Asilidae
Dasypogon_diadema_Brachycera_Asiloidea_Asilidae
Holocephala_fusca_Brachycera_Asiloidea_Asilidae
Hermetia_illucens_Brachycera_Stratiomyomorpha_Stratiomyidae
Beris_vallata_Brachycera_Stratiomyomorpha_Stratiomyidae
Phlebotomus_papatasi_Nematocera_Psychodomorpha_Psychodidae
Lutzomyia_longipalpis_Nematocera_Psychodomorpha_Psychodoidae
Anopheles_gambiae_Nematocera_Culicomorpha_Culicidae
Aedes_aegypti_Nematocera_Culicomorpha_Culicidae
bab1 singletons
Mayetiola_destructor_1a_Nematocera_Bibionomorpha_Cecidomyiidae_Cecidomyiinae
Coboldia_fuscipes_1b_Nematocera_Psychodomorpha_Scatopsidae
Coboldia_fuscipes_1a_Nematocera_Psychodomorpha_Scatopsidae
Mayetiola_destructor_1b_Nematocera_Bibionomorpha_Cecidomyiidae_Cecidomyiinae
Mayetiola_destructor_1c_Nematocera_Bibionomorpha_Cecidomyiidae_Cecidomyiinae
Fungus gnat and gall midge paralogs
1.01

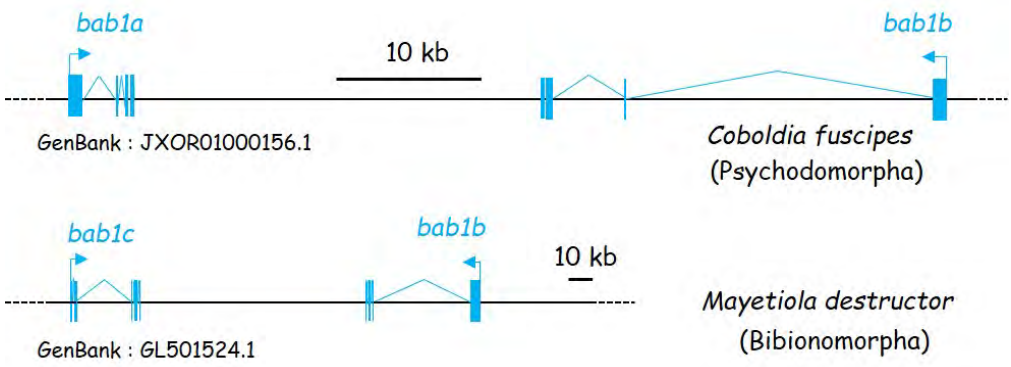
bab1a
10 kb
bab1b
GenBank : JXOR01000156.1
Coboldia fuscipes
(Psychodomorpha)
bab1c
bab1b
10 kb
GenBank : GL501524.1
Mayetiola destructor
(Bibionomorpha)

A


CR1
2
Dmel LAE
3

B

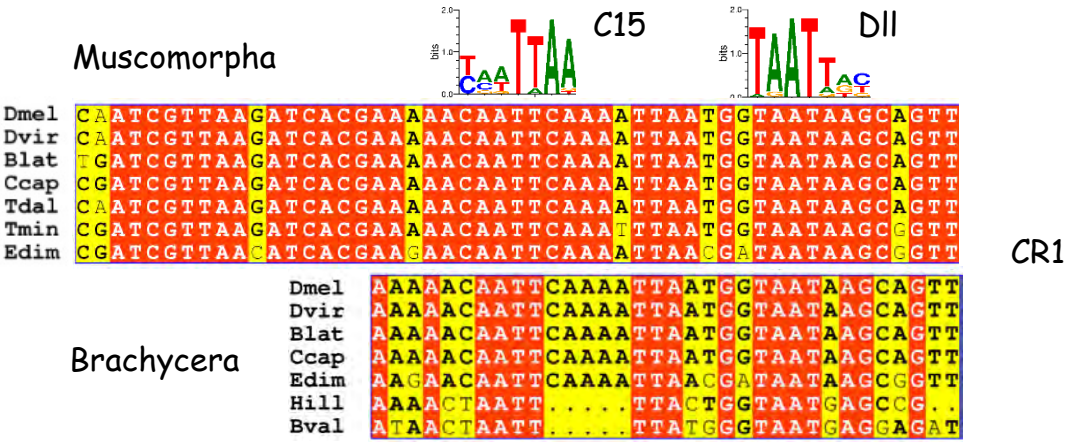
Muscomorpha
C15
Dll
Dmel
Dvir
Blat
Ccap
Tdal
Tmin
Edim
CR1
Brachycera
Dmel
Dvir
Blat
Ccap
Edim
Hill
Bval

C

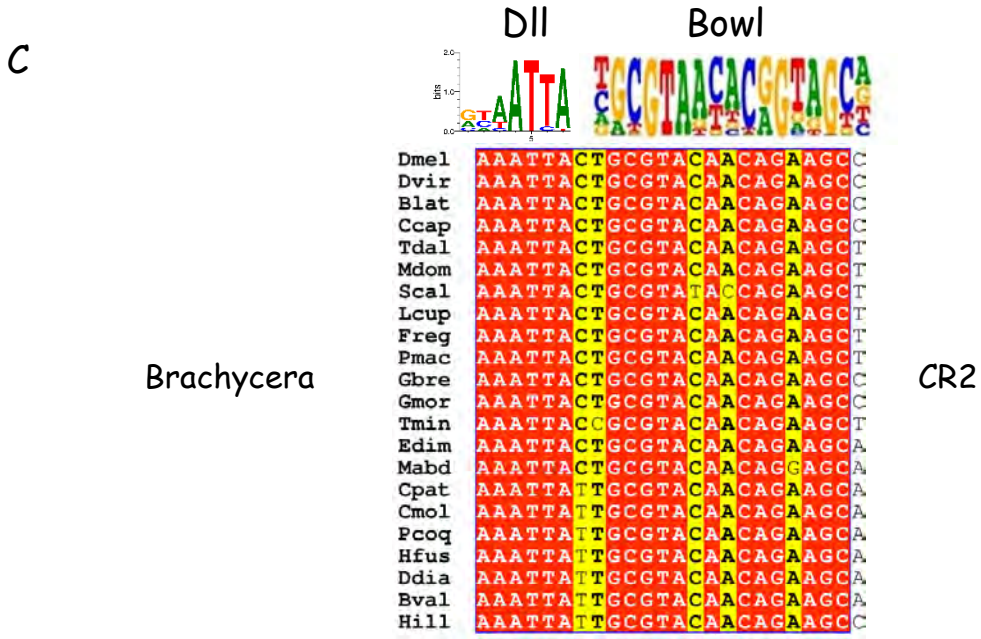
Dll
Bowl
Brachycera
Dmel
Dvir
Blat
Ccap
Tdal
Mdom
Scal
Lcup
Freg
Pmac
Gbre
Gmor
Tmin
Edim
Mabd
Cpat
Cmol
Pcoq
Hfus
Ddia
Bval
Hill
CR2

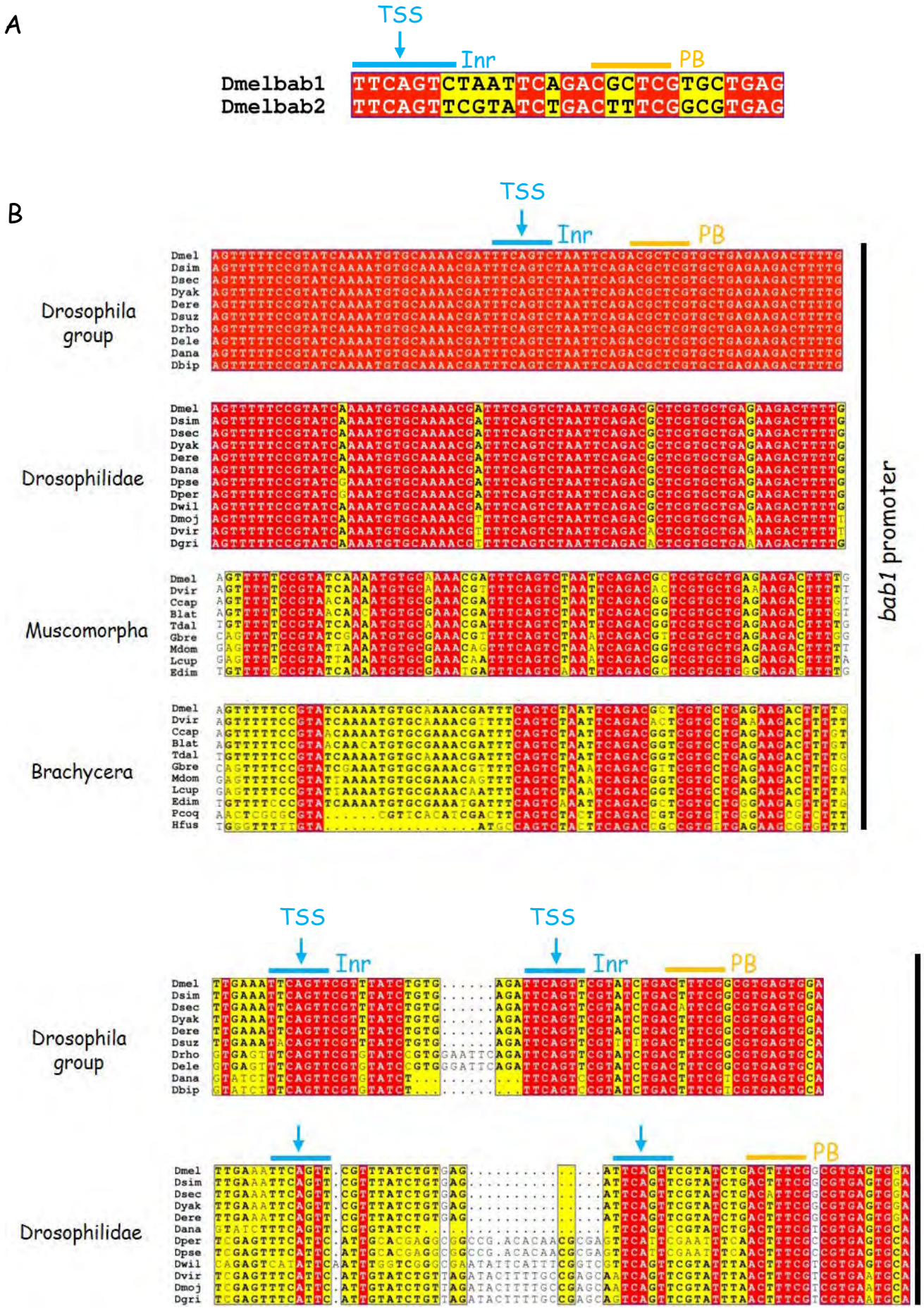
A
TSS
Inr
PB
Dmelbab1
Dmelbab2
TTCAGTCTAATTCAGACGCTCGTGCTGAG
TTCAGTTCGTATCTGACTTTCGGCGTGAG
B
TSS
Inr
PB
Drosophila group
Drosophilidae
Muscomorpha
Brachycera
bab1 promoter
TSS
TSS
Inr
Inr
PB
Drosophila group
Drosophilidae
bab2 promoter

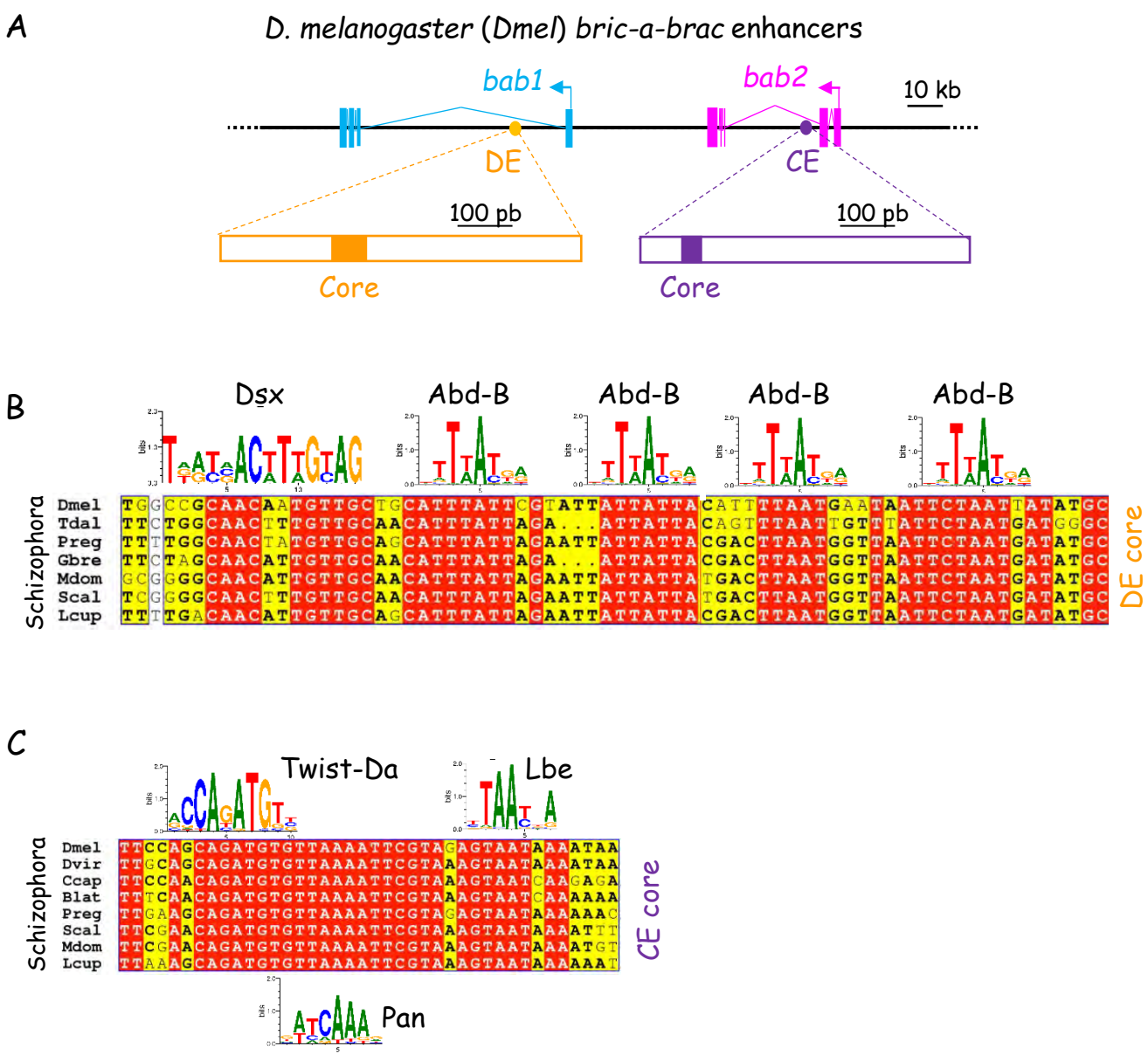
A
D. melanogaster (Dmel) bric-a-brac enhancers
bab1
bab2
10 kb
DE
CE
100 pb
100 pb
Core
Core
B
Dsx
Abd-B
Abd-B
Abd-B
Abd-B
Schizophora
Dmel
Tdal
Preg
Gbre
Mdom
Scal
Lcup
DE core
C
Twist-Da
Lbe
Schizophora
Dmel
Dvir
Ccap
Blat
Preg
Scal
Mdom
Lcup
CE core
Pan

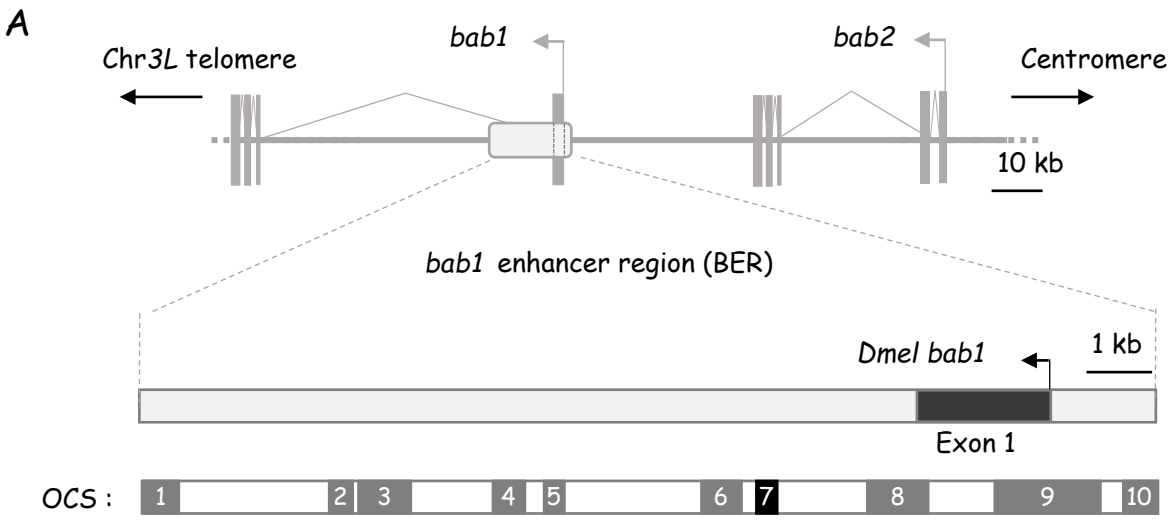

B

		Muscomorphan families	OCS : 1	2	3	4	5	6	7	8	9	10
Schizophora	Acalyptratae	Drosophilidae	4	2	8	1	4	3	6	2	4	3
		Tephritidae (Blat, Ccap)	2	1	5		1	1	5		1	
		Diopsidae (Tdal)	2	1	5		1	1	5		1	
		Sepsidae (Tmin)	1		2			1	1		1	
	Calyptratae	Glossinidae (Gbre, Gmor)	1		3			1	3		1	
		Muscidae (Mdom, Scal)		1	1			1	1		1	
		Calliphoridae (Lcup, Preg)		1	2			1	3		1	
		Rhinophoridae (Pmac)		1	2			1	2		1	
Aschiza		Syrphidae (Edim)			1						1	
		Phoridae (Mabd)			1						1	

Sequence element(s) conserved among 12 Drosophilids (dubbed CS)

CS element(s) conserved beyond Drosophilidae

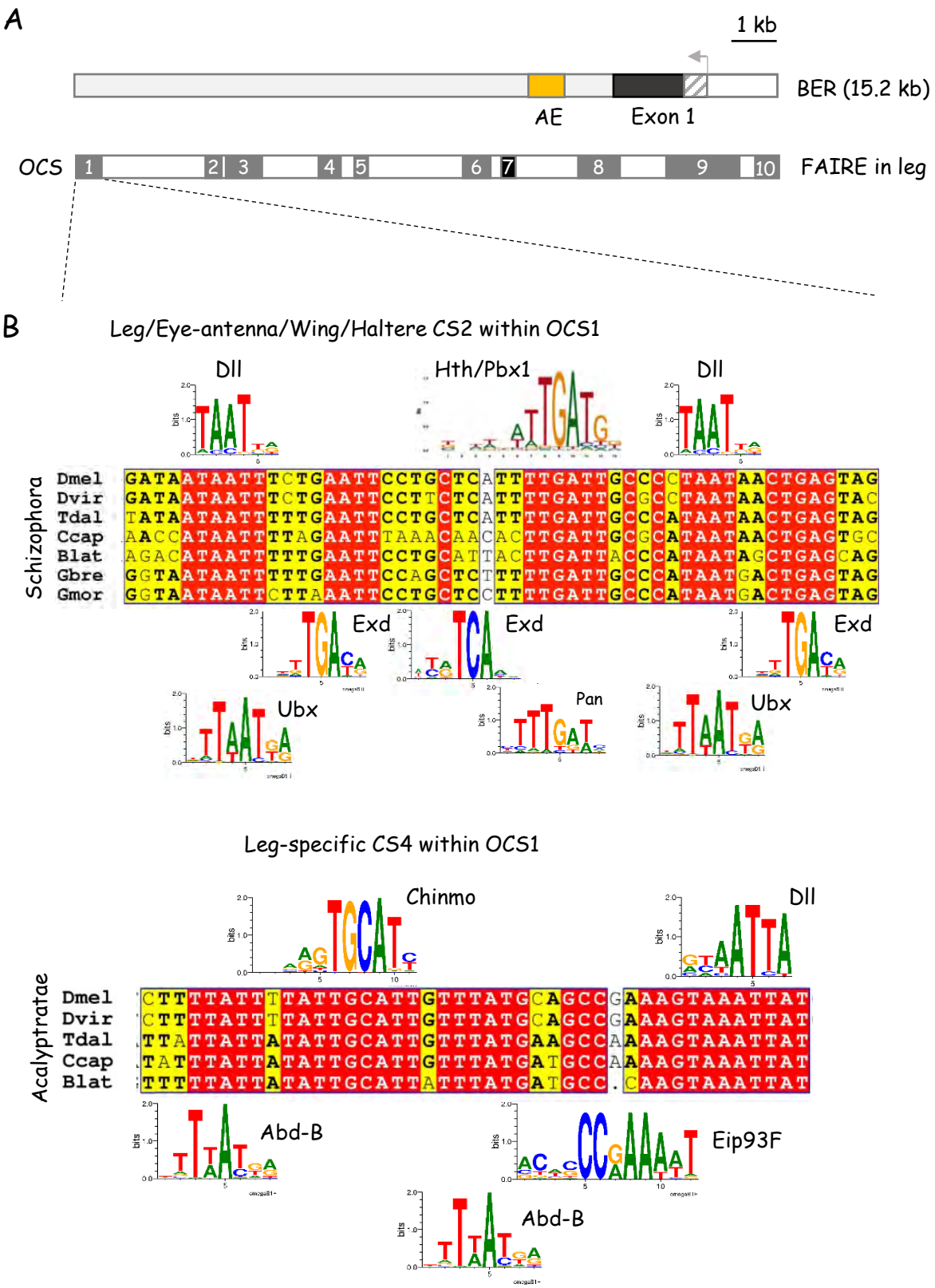
A
1 kb
BER (15.2 kb)
AE
Exon 1
OCS
1
2
3
4
5
6
7
8
9
10
FAIRE in leg
B
Leg/Eye-antenna/Wing/Haltere CS2 within OCS1
Dll
Hth/Pbx1
Dll
Schizophora
Dmel
Dvir
Tdal
Ccap
Blat
Gbre
Gmor
Exd
Exd
Exd
Ubx
Pan
Ubx
Leg-specific CS4 within OCS1
Chinmo
Dll
Acalyptratae
Dmel
Dvir
Tdal
Ccap
Blat
Abd-B
Eip93F
Abd-B

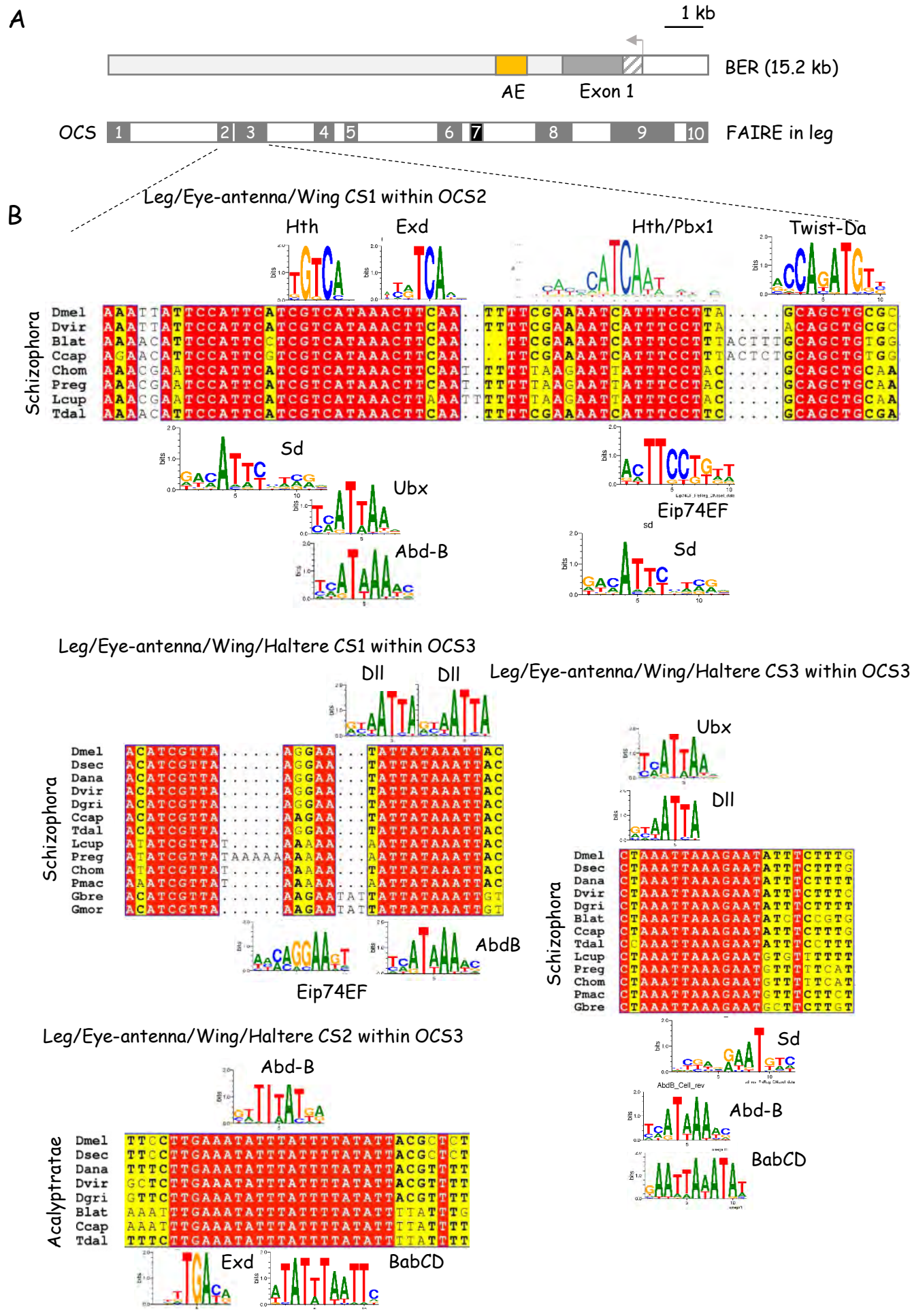
A
1 kb
BER (15.2 kb)
AE
Exon 1
OCS
1
2
3
4
5
6
7
8
9
10
FAIRE in leg
B
Leg/Eye-antenna/Wing CS1 within OCS2
Hth
Exd
Hth/Pbx1
Twist-Da
Schizophora
Dmel
Dvir
Blat
Ccap
Chom
Preg
Lcup
Tdal
Sd
Ubx
Abd-B
Eip74EF
sd
Leg/Eye-antenna/Wing/Haltere CS1 within OCS3
Dll
Dll
Dmel
Dsec
Dana
Dvir
Dgri
Ccap
Tdal
Lcup
Preg
Chom
Pmac
Gbre
Gmor
AbdB
Eip74EF
Leg/Eye-antenna/Wing/Haltere CS3 within OCS3
Ubx
Dll
Schizophora
Sd
Abd-B
BabCD
Leg/Eye-antenna/Wing/Haltere CS2 within OCS3
Abd-B
Acalyptratae
Exd
BabCD

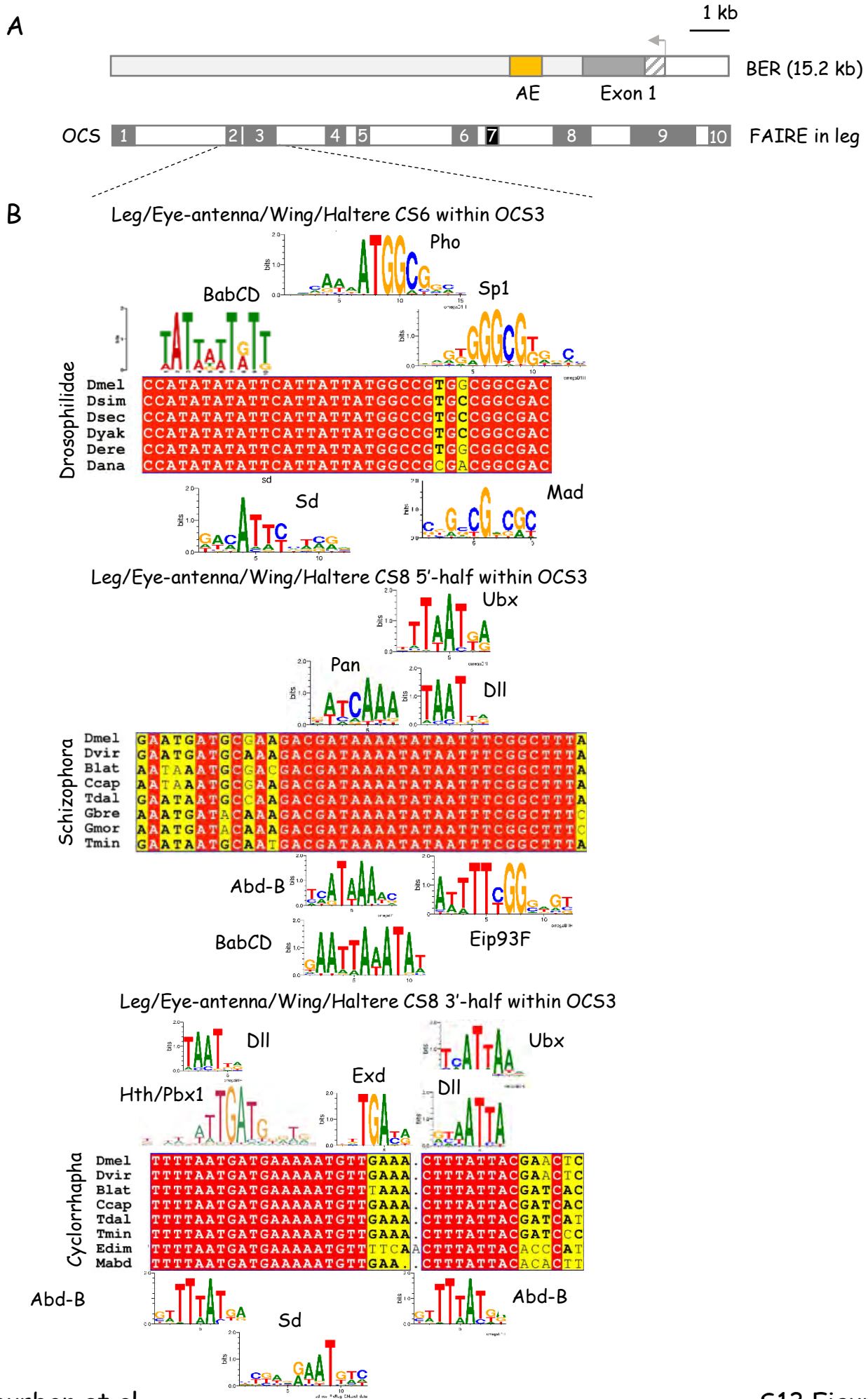
A
1 kb
BER (15.2 kb)
AE
Exon 1
OCS
1
2
3
4
5
6
7
8
9
10
FAIRE in leg
B
Leg/Eye-antenna/Wing/Haltere CS6 within OCS3
Pho
BabCD
Sp1
Drosophilidae
Dmel
Dsim
Dsec
Dyak
Dere
Dana
Sd
Sd
Mad
Leg/Eye-antenna/Wing/Haltere CS8 5'-half within OCS3
Ubx
Pan
Dll
Schizophora
Dmel
Dvir
Blat
Ccap
Tdal
Gbre
Gmor
Tmin
Abd-B
BabCD
Eip93F
Leg/Eye-antenna/Wing/Haltere CS8 3'-half within OCS3
Dll
Ubx
Exd
Hth/Pbx1
Dll
Cyclorrhapha
Dmel
Dvir
Blat
Ccap
Tdal
Tmin
Edim
Mabd
Abd-B
Sd
Abd-B

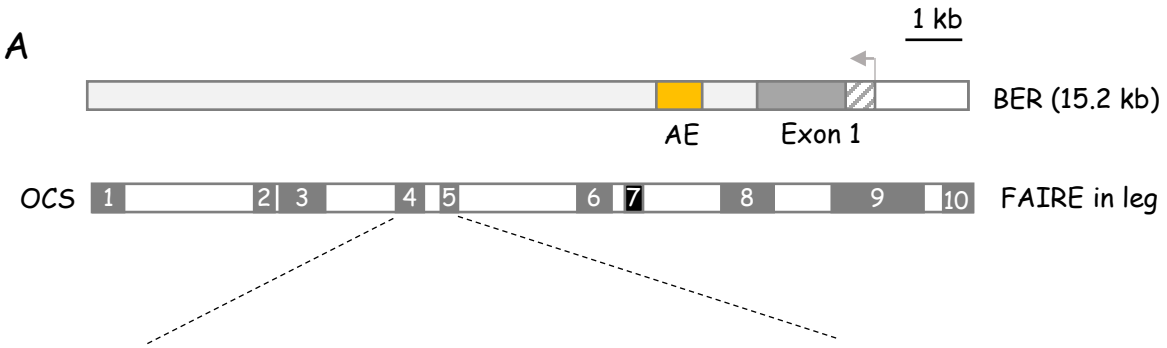

B

Leg/Eye-antenna/Wing/Haltere CS1 within OCS4

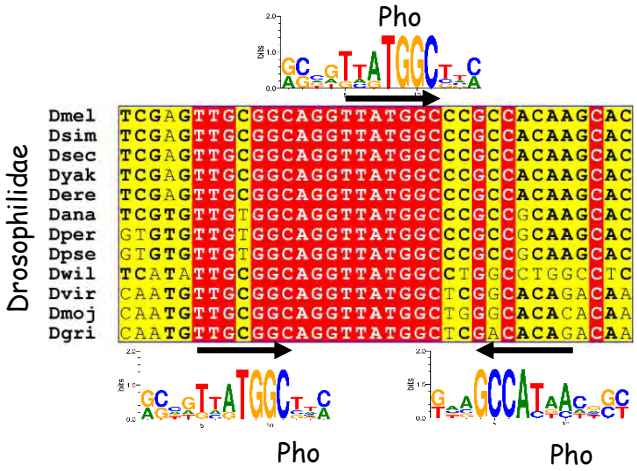

Leg/Eye-antenna/Wing CS1 within OCS5

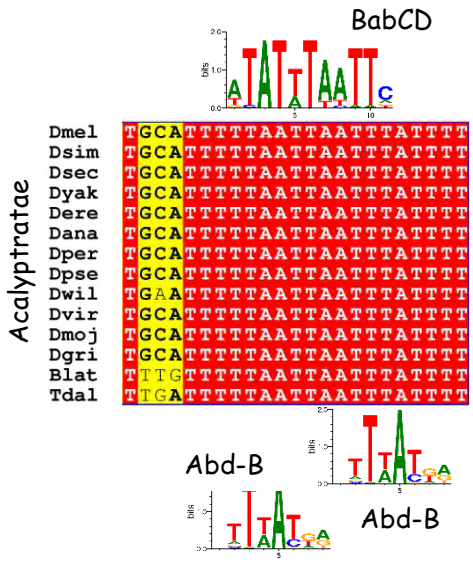

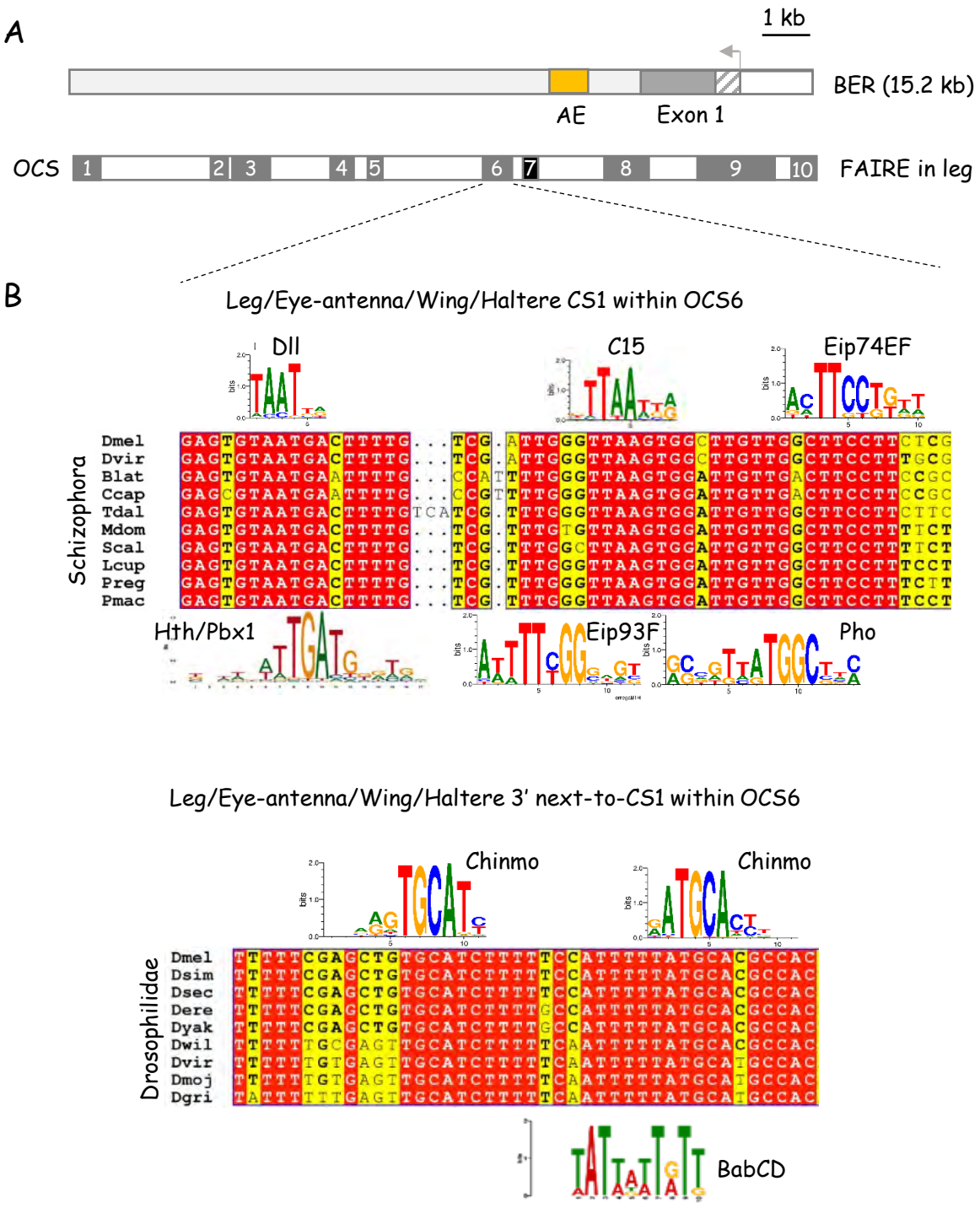
A
1 kb
BER (15.2 kb)
AE
Exon 1
OCS
1
2
3
4
5
6
7
8
9
10
FAIRE in leg
B
Leg/Eye-antenna/Wing/Haltere CS1 within OCS6
Dll
C15
Eip74EF
Schizophora
Dmel
Dvir
Blat
Ccap
Tdal
Mdom
Scal
Lcup
Preg
Pmac
Hth/Pbx1
Eip93F
Pho
Leg/Eye-antenna/Wing/Haltere 3' next-to-CS1 within OCS6
Chinmo
Chinmo
Drosophilidae
Dmel
Dsim
Dsec
Dere
Dyak
Dwil
Dvir
Dmoj
Dgri
BabCD

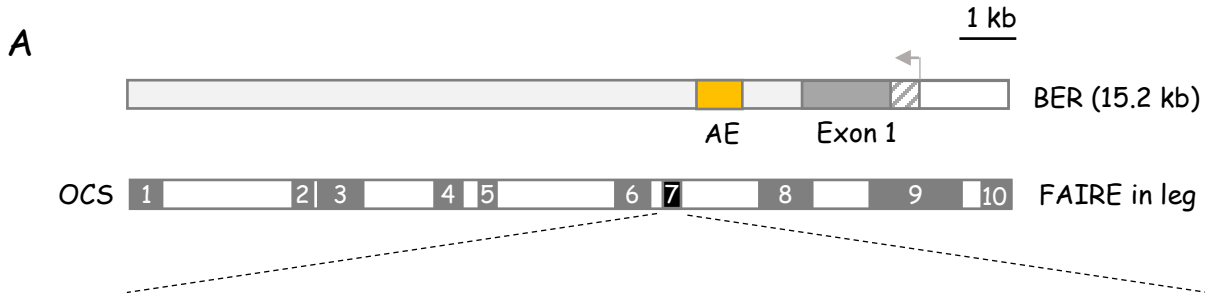

B Leg and eye-antennal-specific CS4 within OCS7

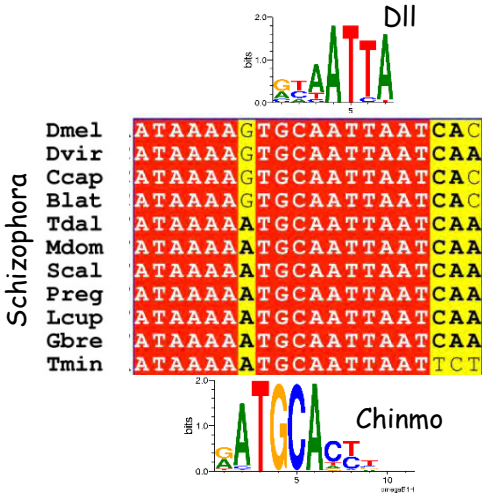

Leg and eye-antennal-specific CS5 within OCS7

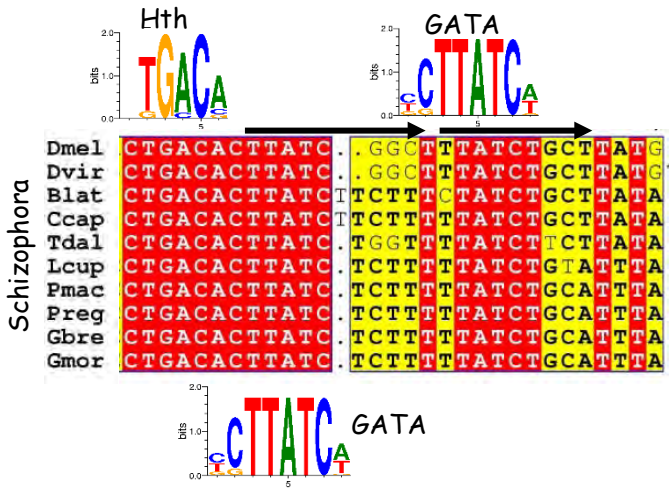

Eye-antenna-specific CS1 within OCS7

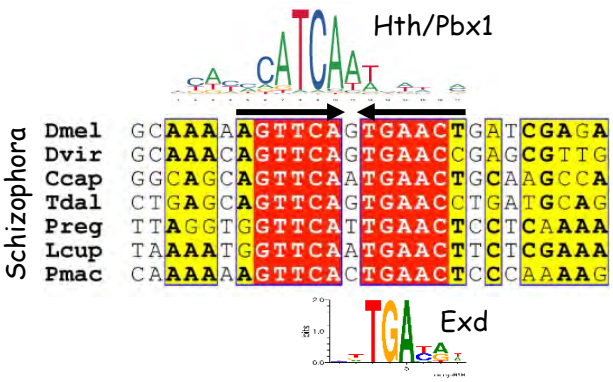

Eye-antenna-specific CS2 within OCS7

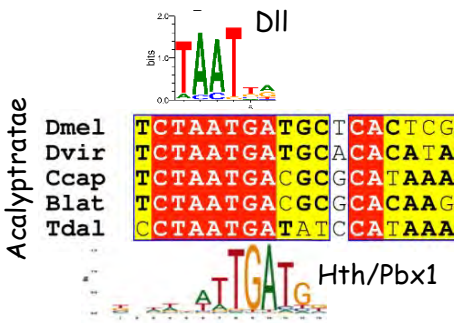

Eye-antenna-specific CS6 within OCS7

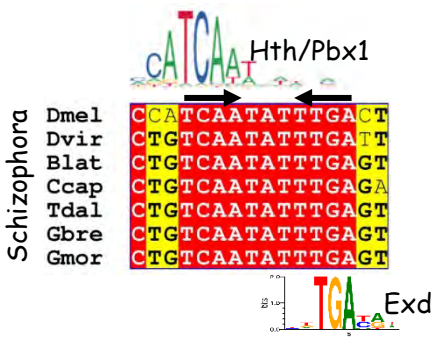

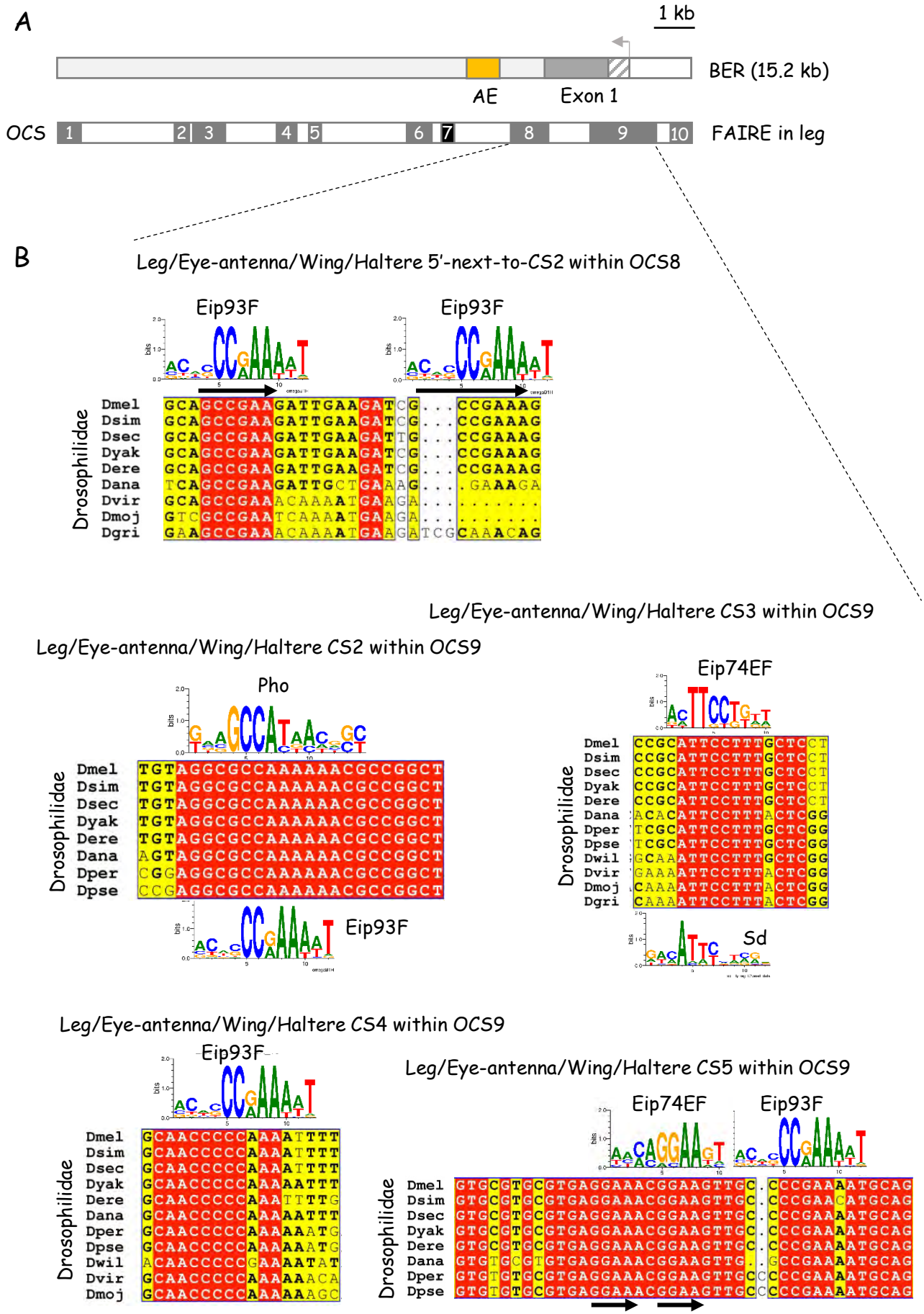
A
1 kb
BER (15.2 kb)
AE
Exon 1
OCS
1
2
3
4
5
6
7
8
9
10
FAIRE in leg
B
Leg/Eye-antenna/Wing/Haltere 5'-next-to-CS2 within OCS8
Eip93F
Eip93F
Drosophilidae
Dmel
Dsim
Dsec
Dyak
Dere
Dana
Dvir
Dmoj
Dgri
Leg/Eye-antenna/Wing/Haltere CS3 within OCS9
Leg/Eye-antenna/Wing/Haltere CS2 within OCS9
Pho
Eip74EF
Eip93F
Dper
Dpse
Dwil
Sd
Leg/Eye-antenna/Wing/Haltere CS4 within OCS9
Eip93F
Leg/Eye-antenna/Wing/Haltere CS5 within OCS9
Eip74EF
Eip93F

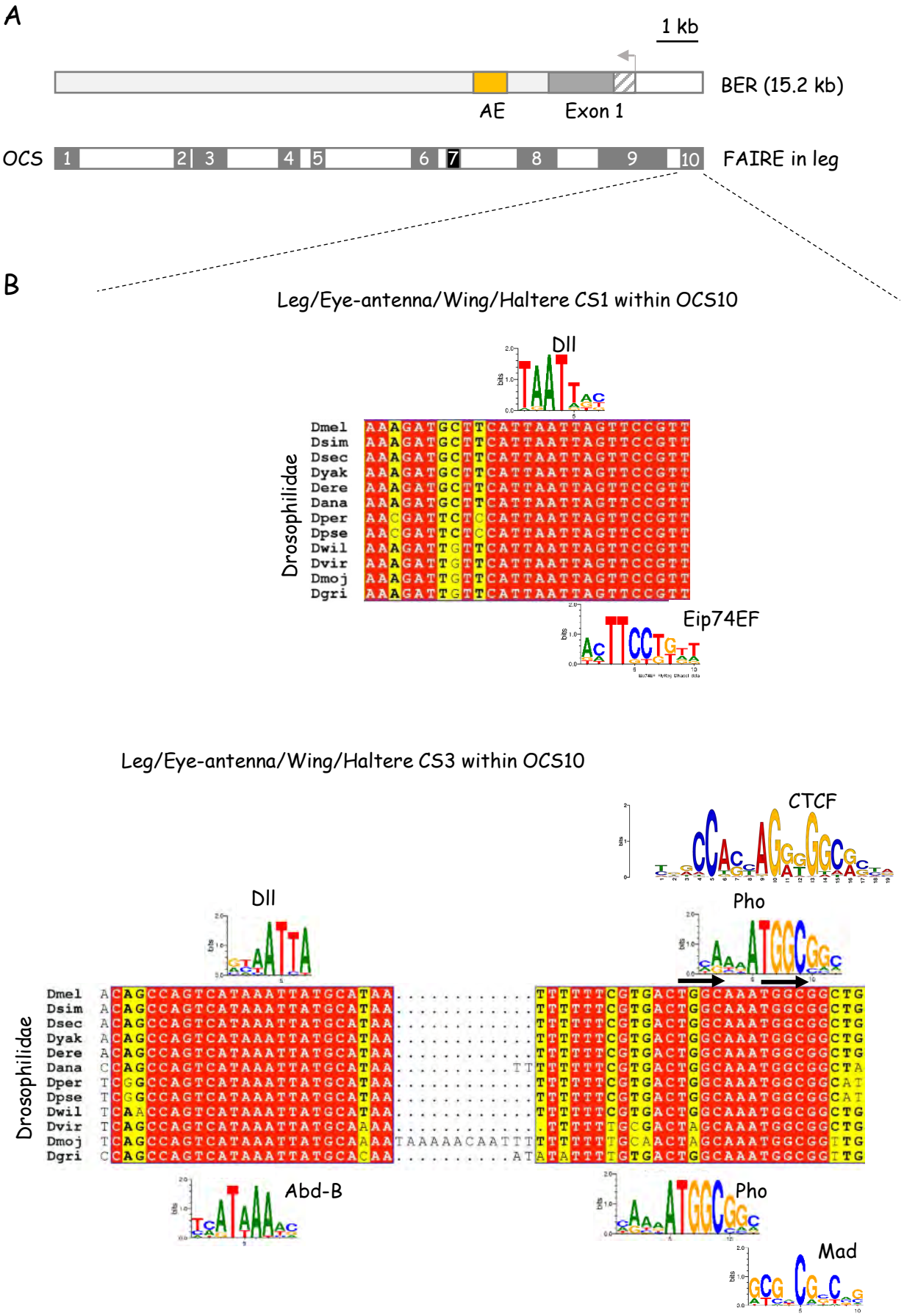
A
1 kb
BER (15.2 kb)
AE
Exon 1
OCS
1
2
3
4
5
6
7
8
9
10
FAIRE in leg
B
Leg/Eye-antenna/Wing/Haltere CS1 within OCS10
Dll
Drosophilidae
Dmel AAAGATGCTTCATTAATTAGTTCCGTT
Dsim AAAGATGCTTCATTAATTAGTTCCGTT
Dsec AAAGATGCTTCATTAATTAGTTCCGTT
Dyak AAAGATGCTTCATTAATTAGTTCCGTT
Dere AAAGATGCTTCATTAATTAGTTCCGTT
Dana AAAGATGCTTCATTAATTAGTTCCGTT
Dper AACGATTCTCCATTAATTAGTTCCGTT
Dpse AACGATTCTCCATTAATTAGTTCCGTT
Dwil AAAGATTGTTCATTAATTAGTTCCGTT
Dvir AAAGATTGTTCATTAATTAGTTCCGTT
Dmoj AAAGATTGTTCATTAATTAGTTCCGTT
Dgri AAAGATTGTTCATTAATTAGTTCCGTT
Eip74EF
Leg/Eye-antenna/Wing/Haltere CS3 within OCS10
CTCF
Dll
Pho
Drosophilidae
Dmel ACAGCCAGTCATAAATTATGCATAA.....TTTTTTTCGTGACTGGCAAATGGCGGCTG
Dsim ACAGCCAGTCATAAATTATGCATAA.....TTTTTTTCGTGACTGGCAAATGGCGGCTG
Dsec ACAGCCAGTCATAAATTATGCATAA.....TTTTTTTCGTGACTGGCAAATGGCGGCTG
Dyak ACAGCCAGTCATAAATTATGCATAA.....TTTTTTTCGTGACTGGCAAATGGCGGCTG
Dere ACAGCCAGTCATAAATTATGCATAA.....TTTTTTTCGTGACTGGCAAATGGCGGCTG
Dana CCAGCCAGTCATAAATTATGCATAA.....TTTTTTTCGTGACTGGCAAATGGCGGCTA
Dper TCGGCCAGTCATAAATTATGCATAA.....TTTTTTTCGTGACTGGCAAATGGCGGCAT
Dpse TCGGCCAGTCATAAATTATGCATAA.....TTTTTTTCGTGACTGGCAAATGGCGGCAT
Dwil TCAACCAGTCATAAATTATGCATAA.....TTTTTTTCGTGACTGGCAAATGGCGGCTG
Dvir TCAGCCAGTCATAAATTATGCAAAA.....TTTTTTTTGCGACTAGCAAATGGCGGCTG
Dmoj TCAGCCAGTCATAAATTATGCAAAATAAAAACAATTTTTTTTTTTGCAACTAGCAAATGGCGGTTG
Dgri CCAGCCAGTCATAAATTATGCACAA.....ATATATTTTGTGACTGGCAAATGGCGGITG
Abd-B
Pho
Mad

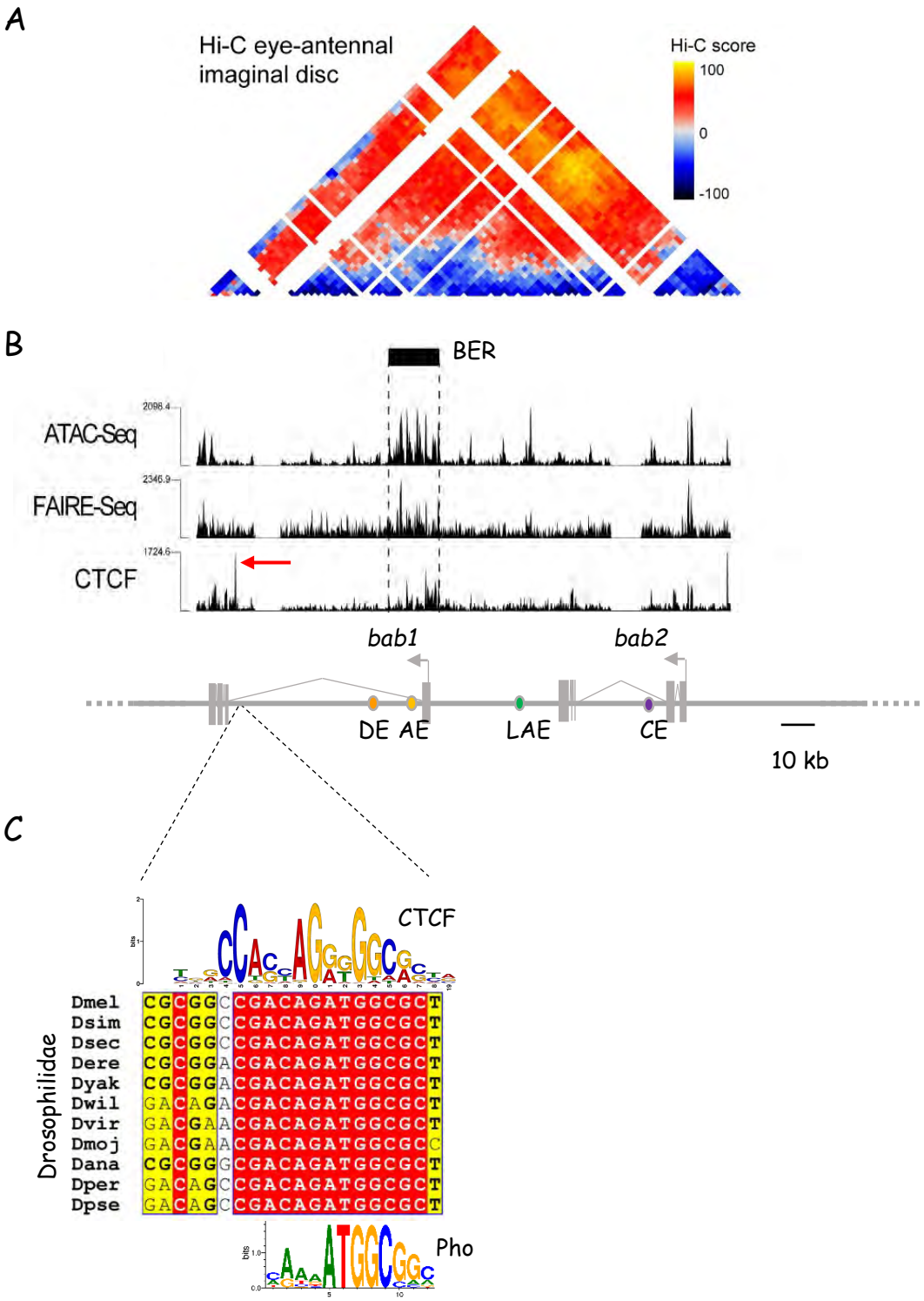
A
Hi-C eye-antennal imaginal disc
Hi-C score
100
0
-100
B
BER
ATAC-Seq
FAIRE-Seq
CTCF
bab1
bab2
DE
AE
LAE
CE
10 kb
C
CTCF
Drosophilidae
Dmel
Dsim
Dsec
Dere
Dyak
Dwil
Dvir
Dmoj
Dana
Dper
Dpse
Pho

Supplementary data

Sequence conservation between paralogous Bab1/2 proteins among muscomorphans. The four-letter species abbreviations are as listed below (page 2). Strictly conserved amino-acid residues are indicated by white characters on a red background while partially conserved ones are in black characters on a yellow background. Locations of the strongly-conserved BTB and BabCD domains are indicated along the right side (see black lines).

Conservation among twelve reference drosophilids of *D. melanogaster* BER OCS1-10 as well as LAE, CE, AE and DE sequences. The four-letter Drosophilidae species abbreviations are as listed below (page 2). Locations of conserved sequence elements (CS) are indicated by underneath black bars. Sequence LOGOs of predicted binding sites for the Dll, Bowl, C15, Sp1, Rn, Sal/Salr, BabCD, GAF, Pho, Eip74EF, Dsx, Abd-B, Sd, Chinmo, Pan, Mad, GATA factors, Twist-Da and Lbe transcription factors are depicted above or below the alignments.

Four letter abbreviations for investigated species

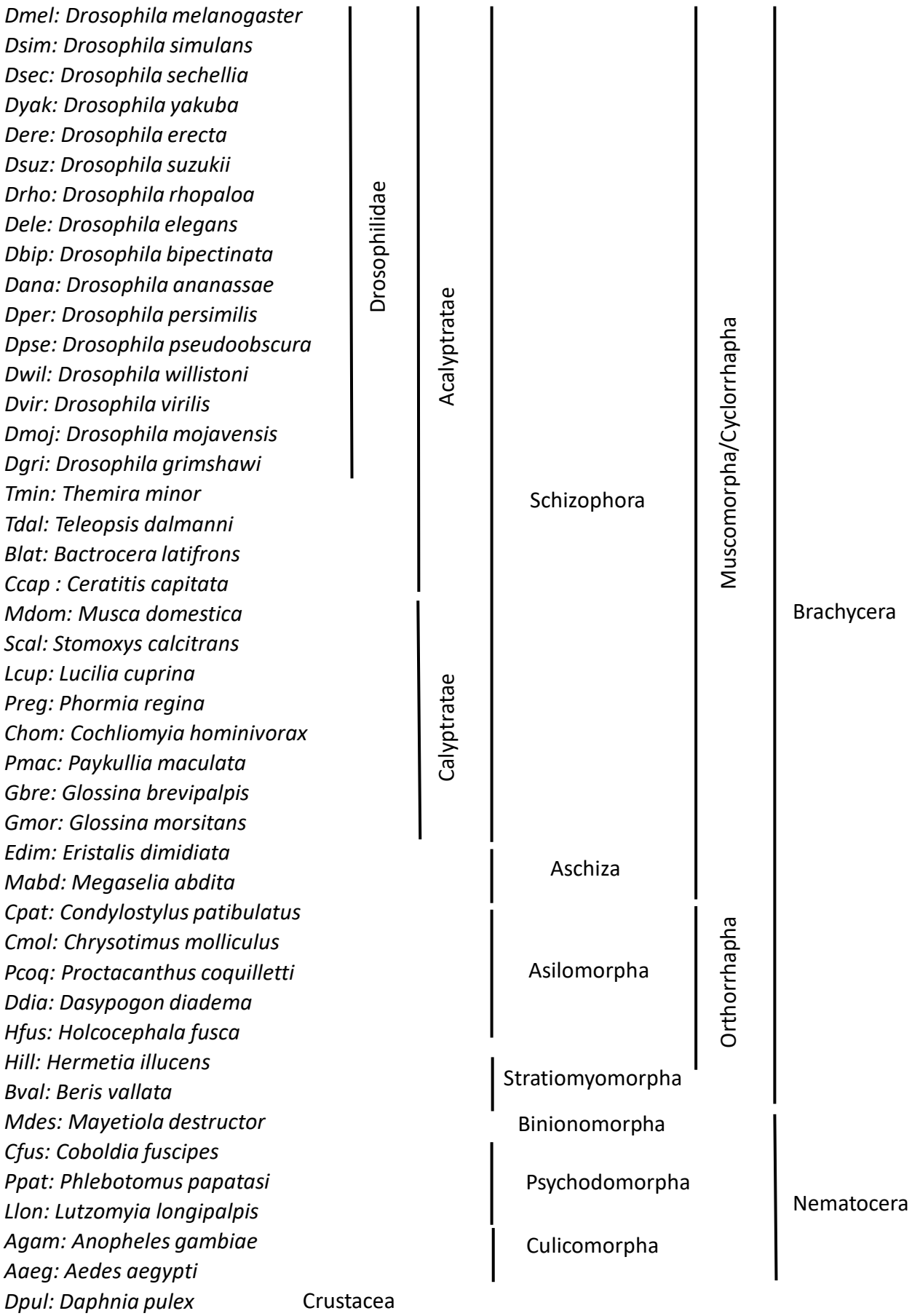

Bab1 sequence conservation among muscomorphans (Part1)

Bab1 sequence conservation among muscomorphans (Part2)

Bab2 sequence conservation among muscomorphs (Part1)

Bab2 sequence conservation among muscomorphans (Part2)

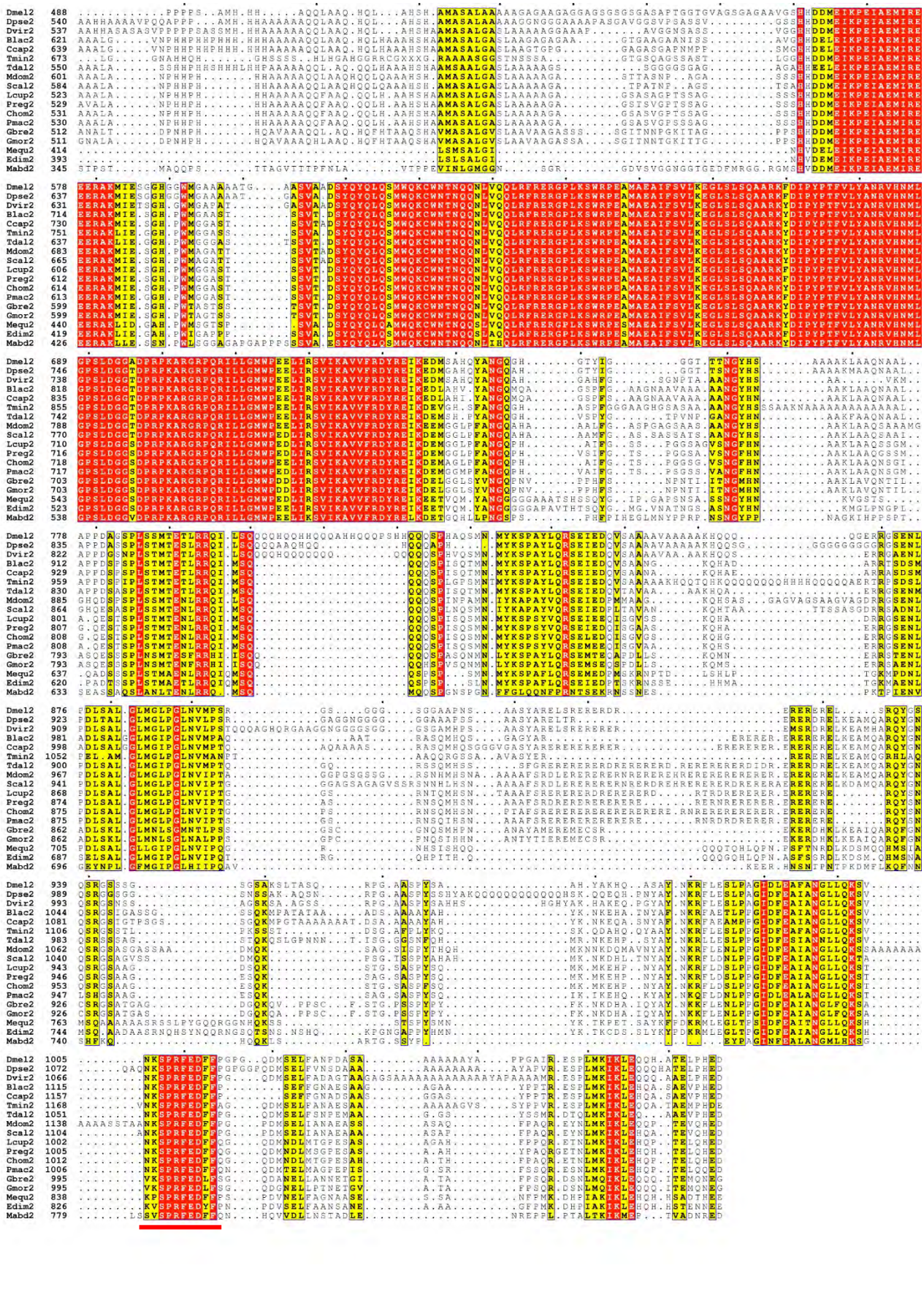

Sequence conservation between Bab1/2 paralogs (Part1)

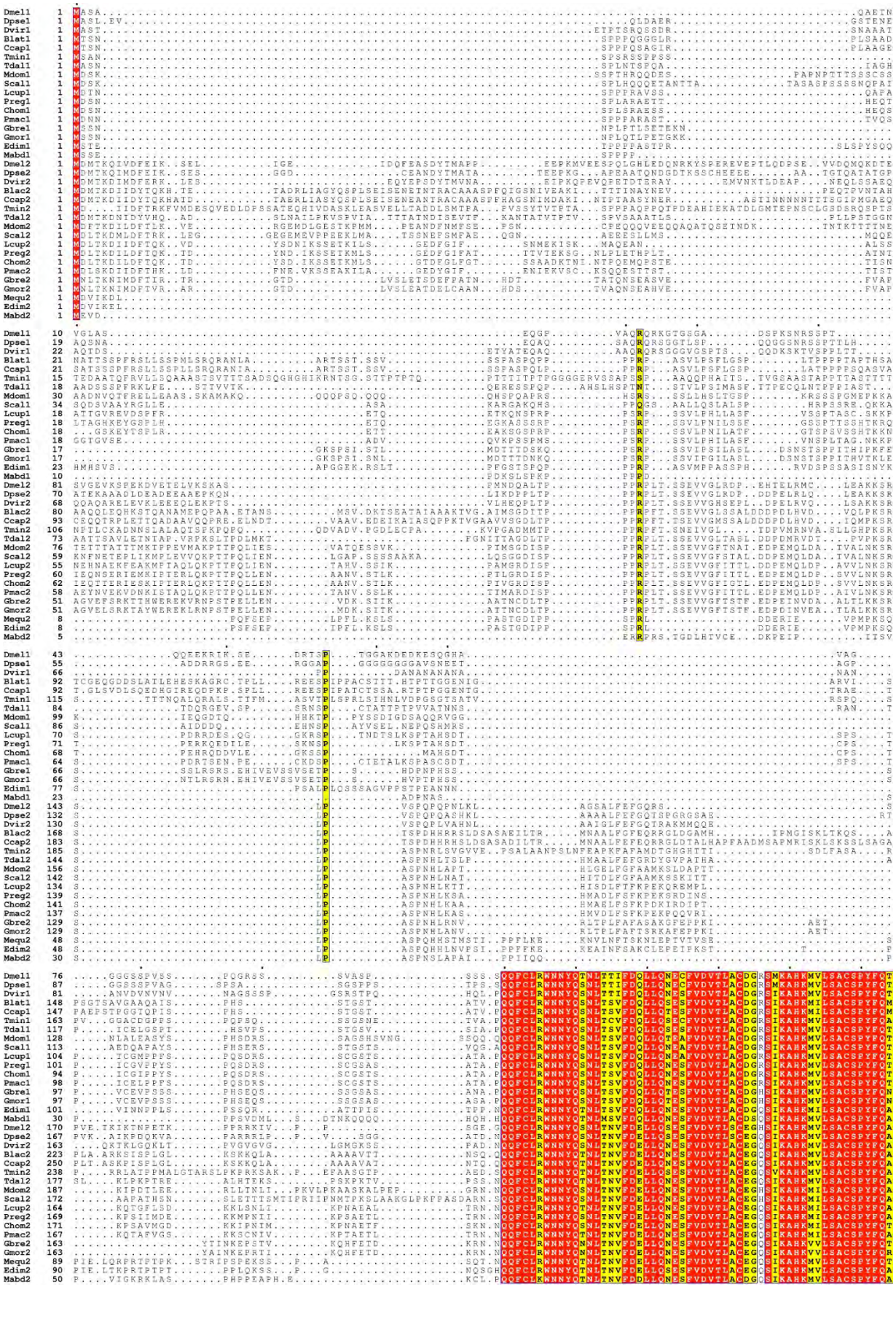

Sequence conservation between Bab1/2 paralogs (Part2)

Sequence conservation between Bab1/2 paralogs (Part3)

Sequence conservation between Bab1/2 paralogs (Part4)

Sequence conservation between Bab1/2 paralogs (Part5)

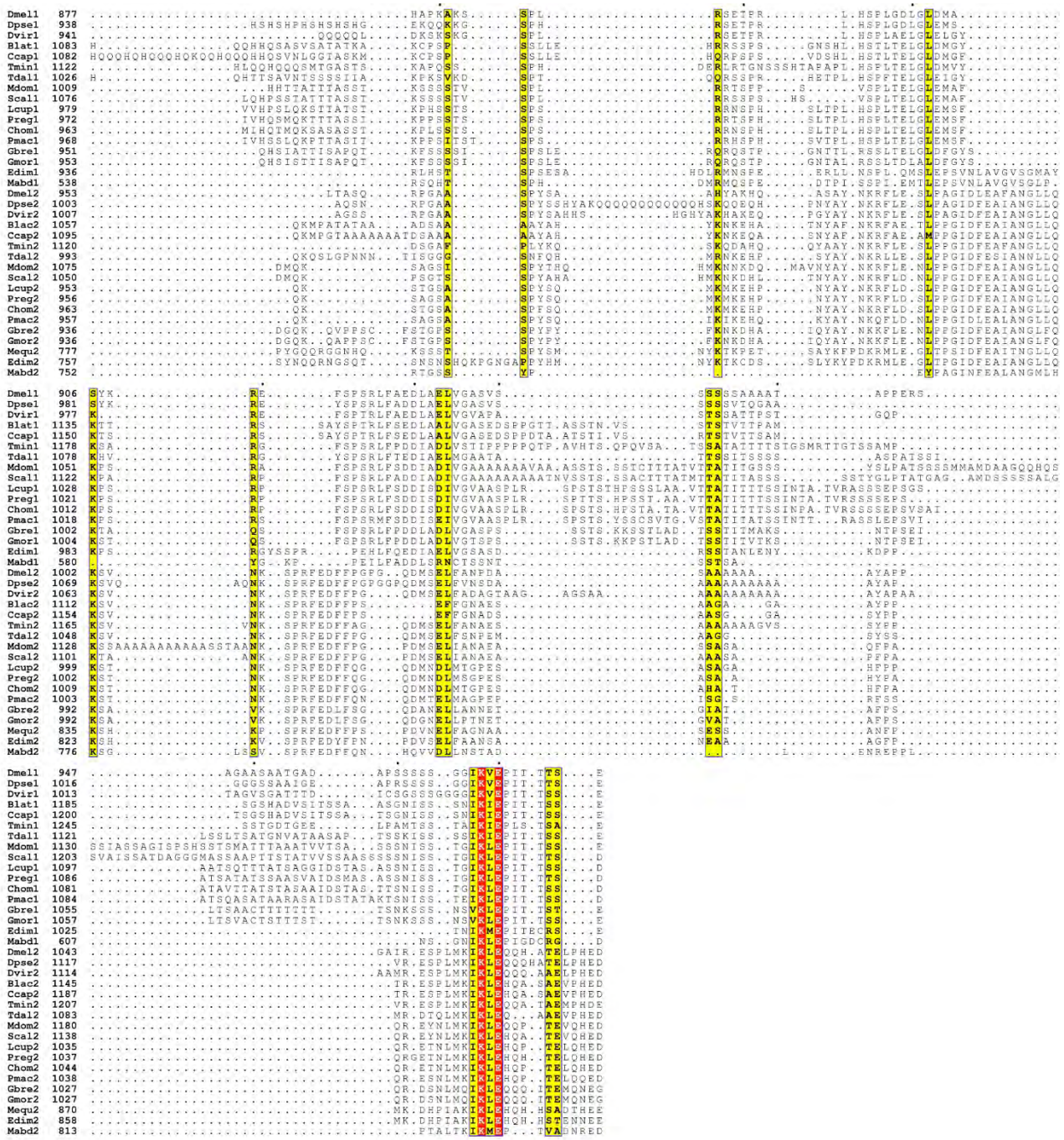

BER^{OCS1} sequence conservation among Drosophilidae (Part1)

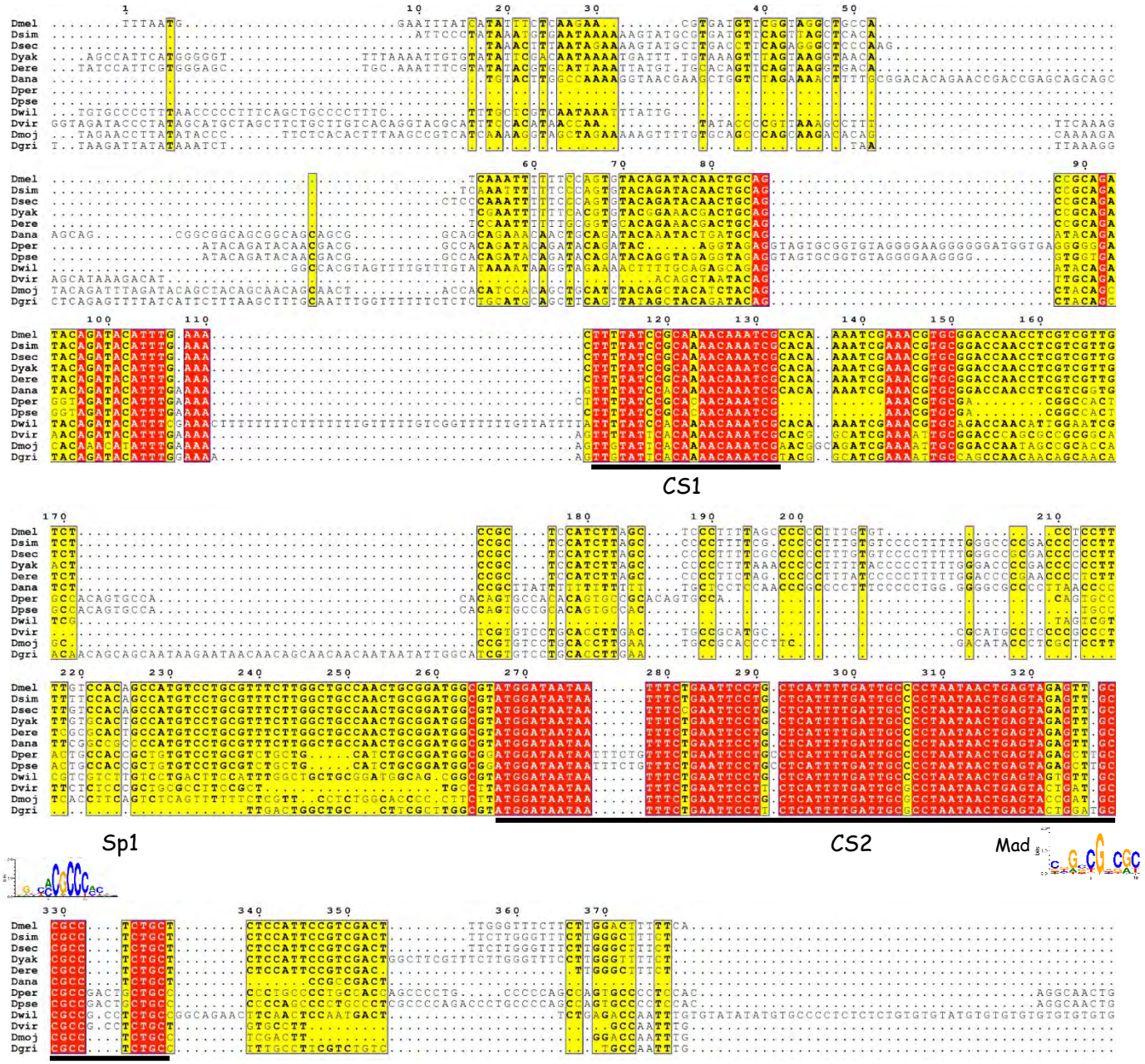

BER^{OCS1} sequence conservation among Drosophilidae (Part2)

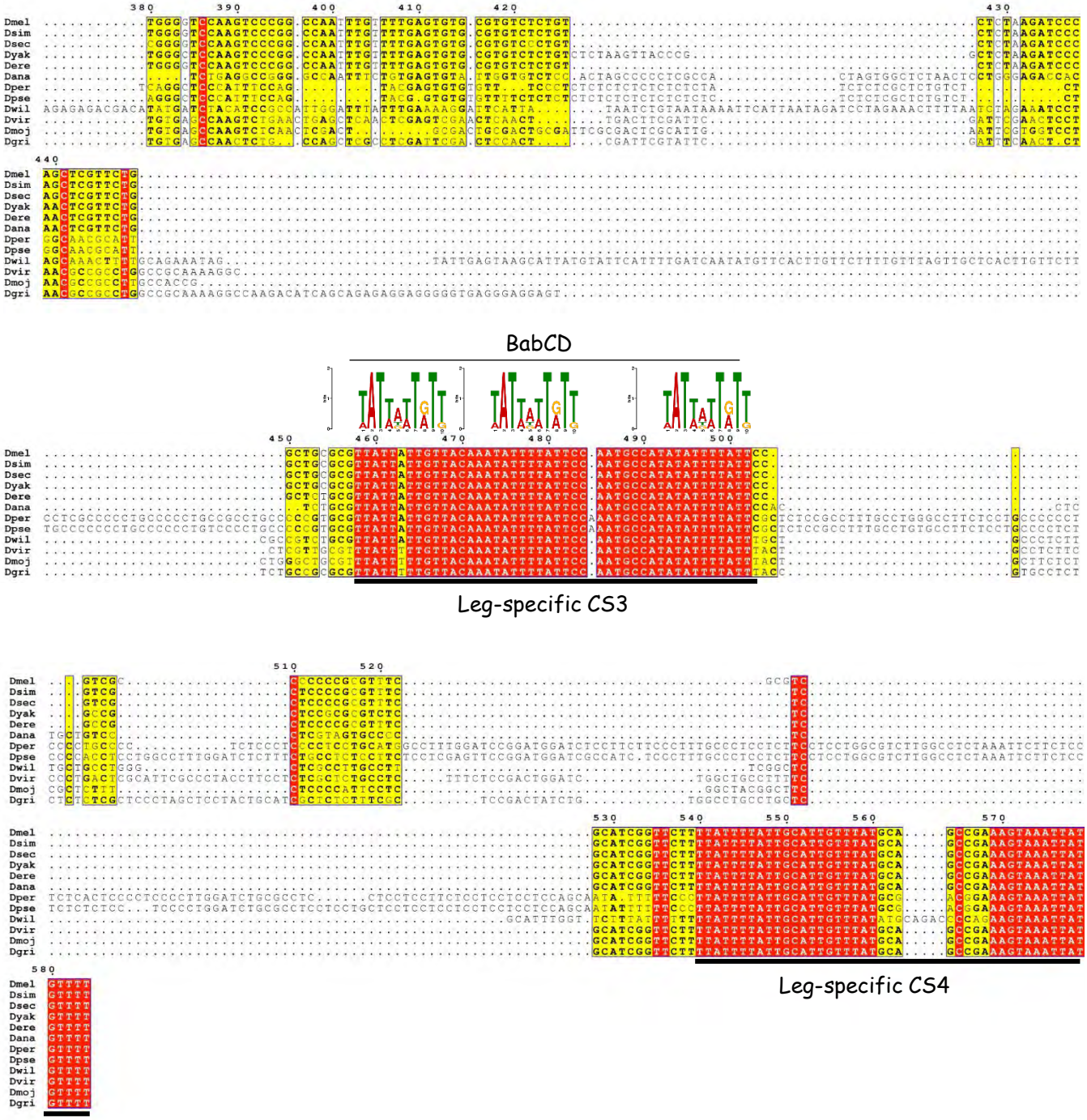

BER^{OCS2} sequence conservation among Drosophilidae

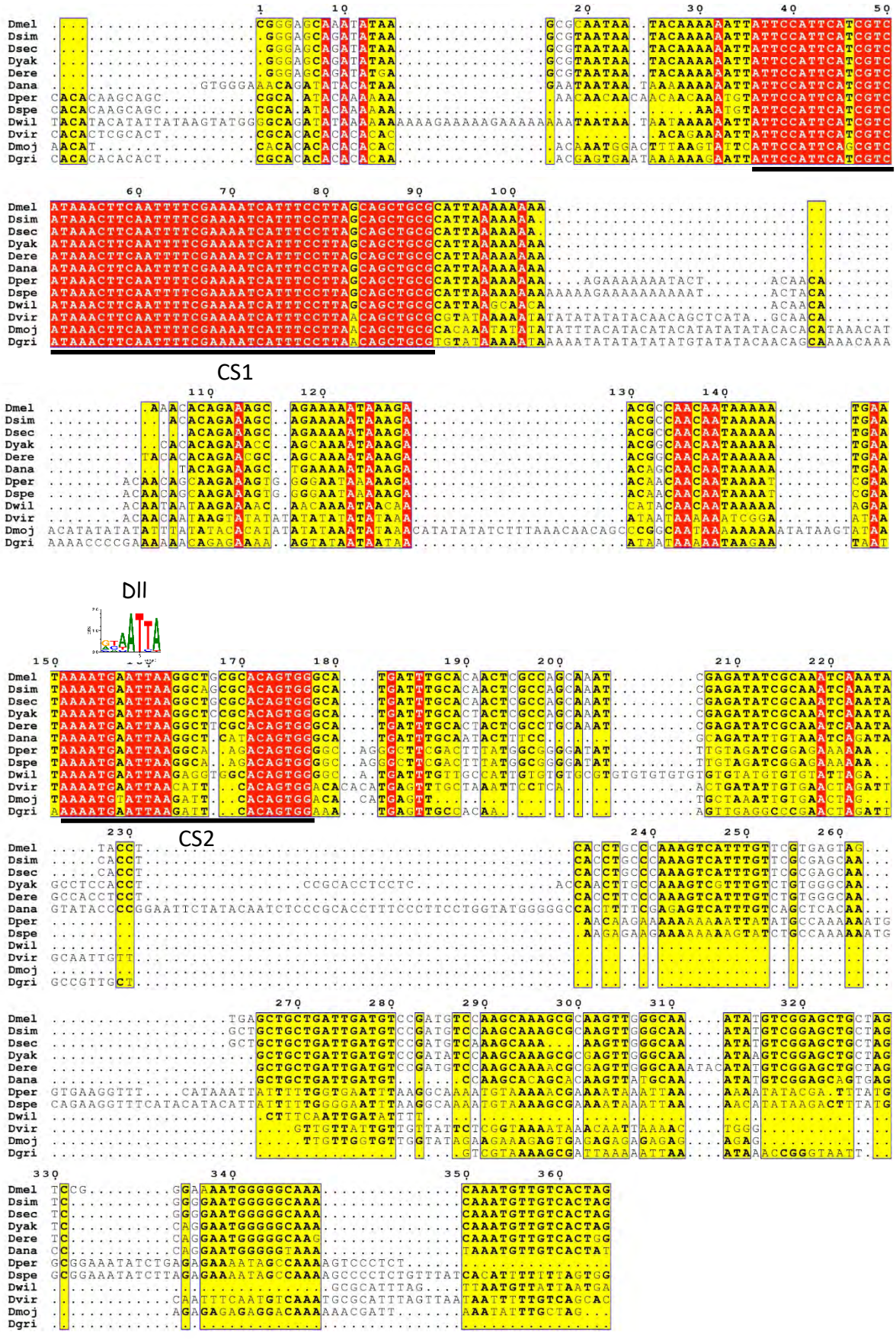

BER^{OCS3} sequence conservation among Drosophilidae (Part1)

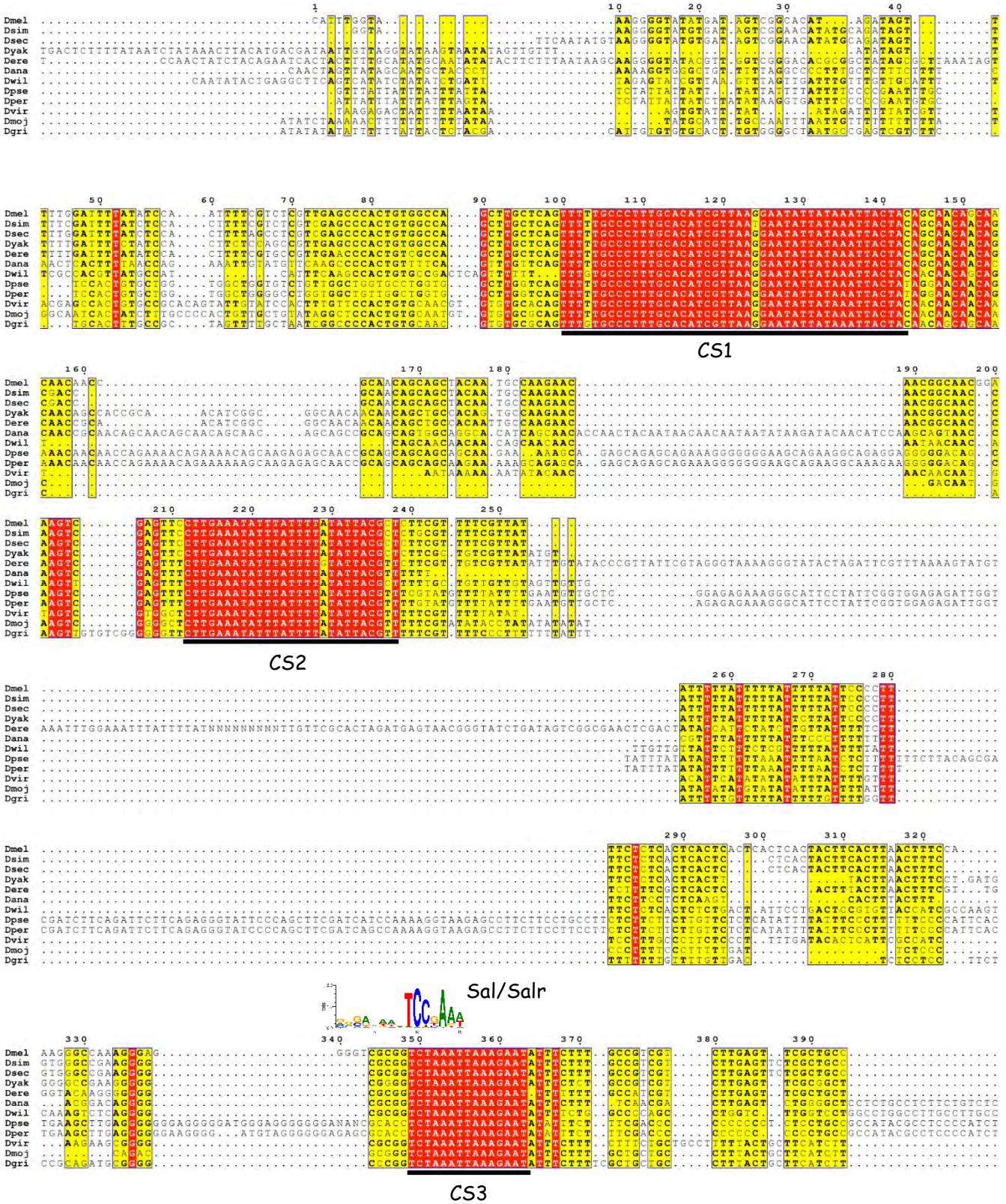

BER^{OCS3} sequence conservation among Drosophilidae (Part2)

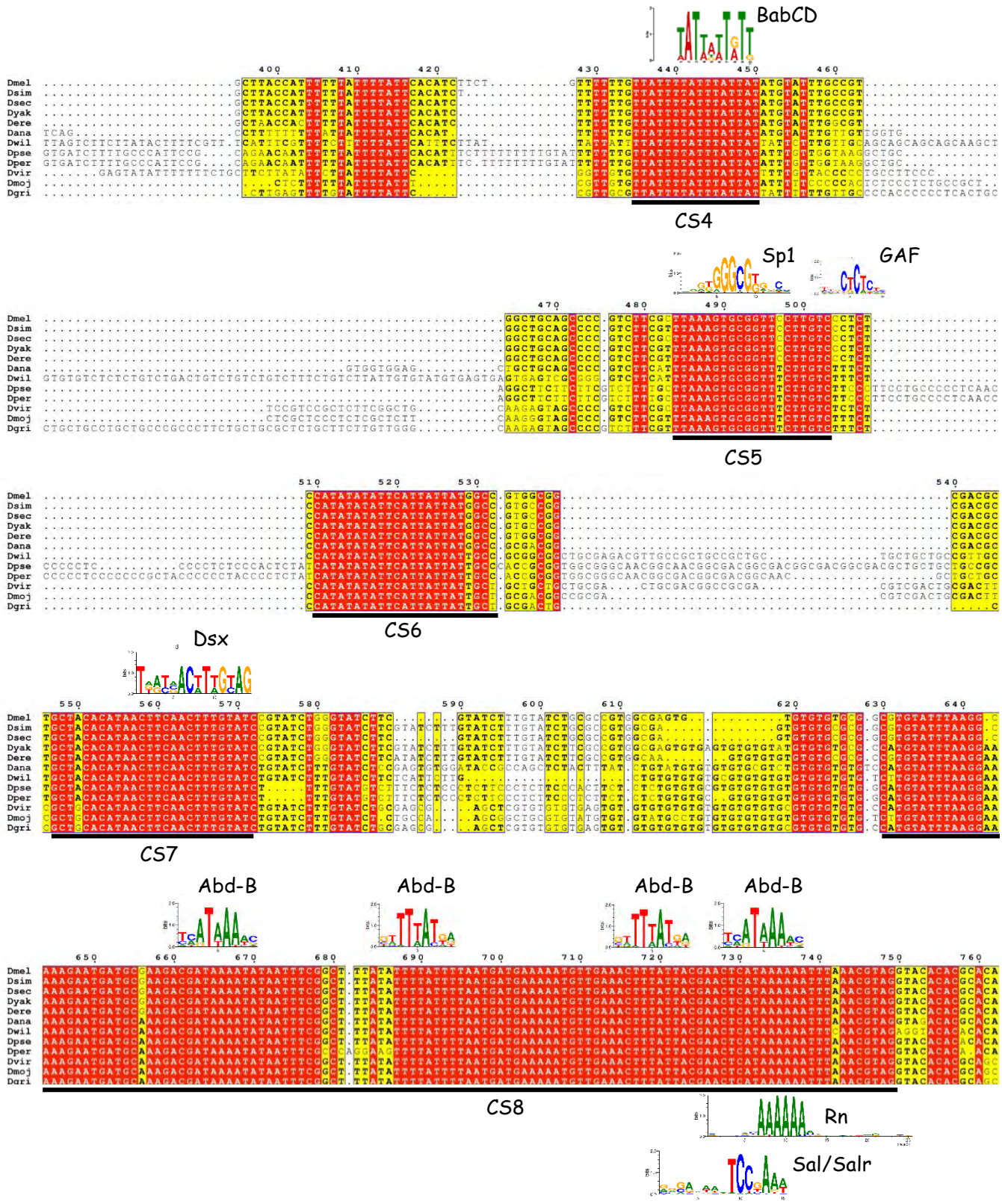

BER^{OCS4} sequence conservation among Drosophilidae

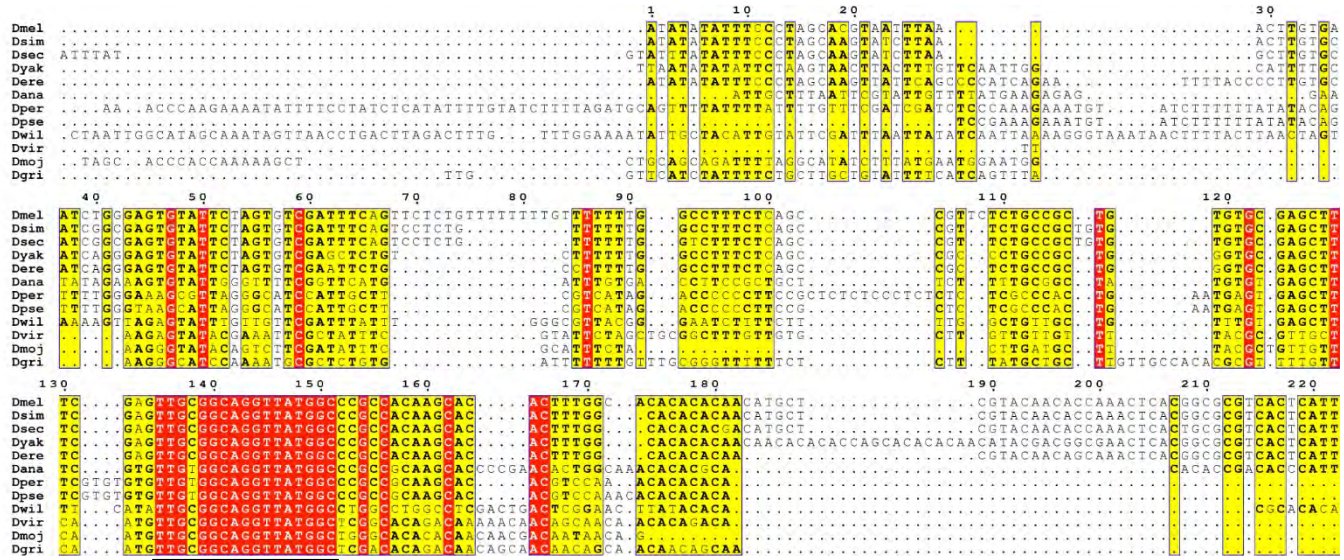

CS1

BER^{OCS5} sequence conservation among Drosophilidae

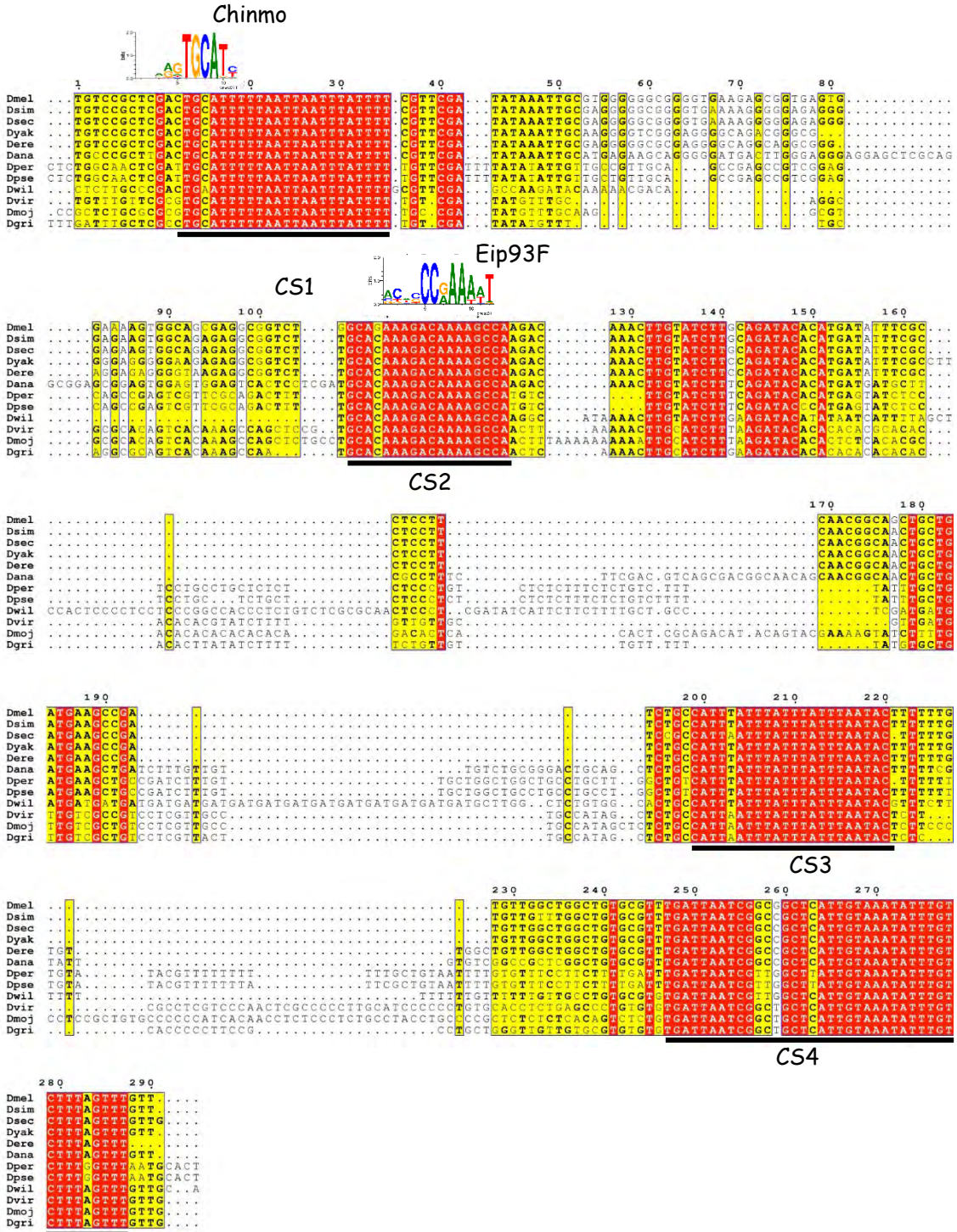

BER^{OCS6} sequence conservation among Drosophilidae (Part1)

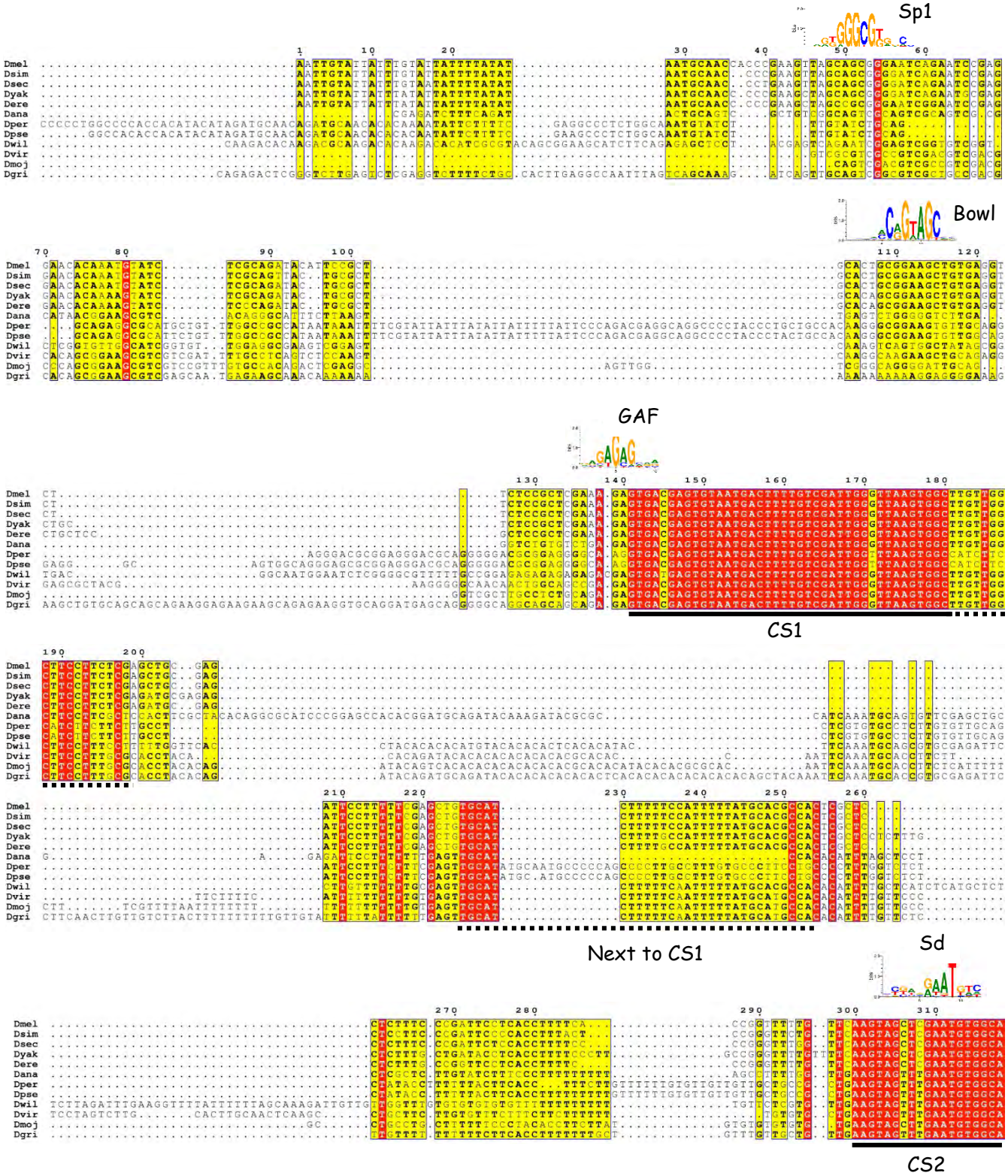

BER^{OCS6} sequence conservation among Drosophilidae (Part2)

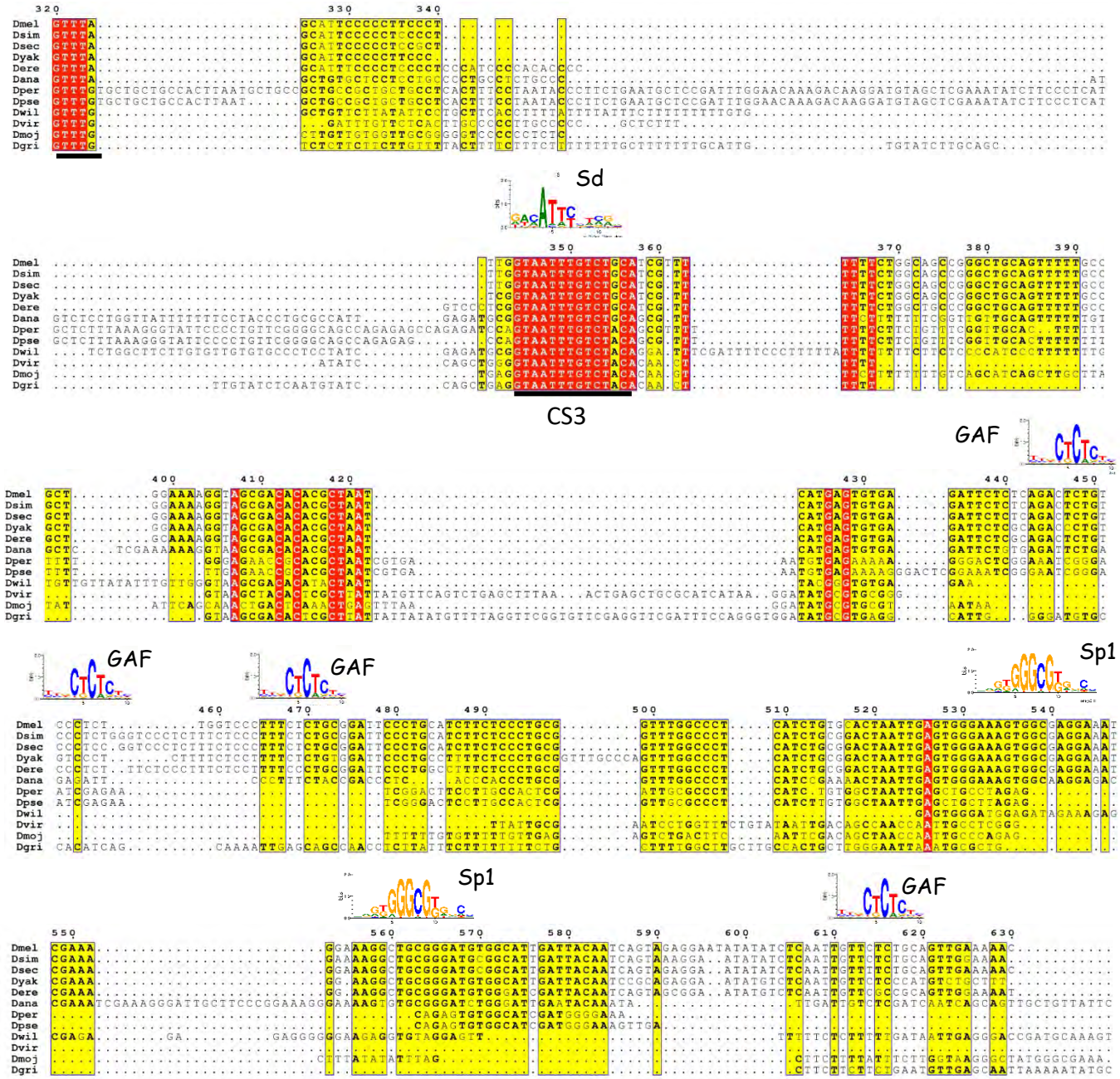

BER^{OCS7} sequence conservation among Drosophilidae (Part1)

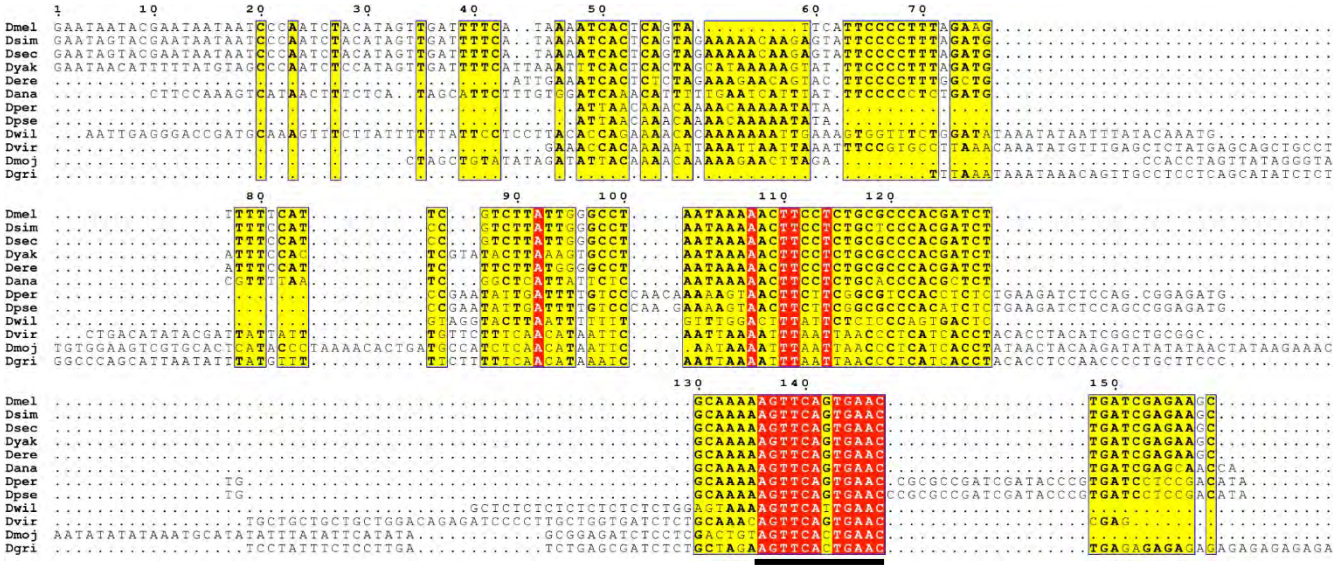

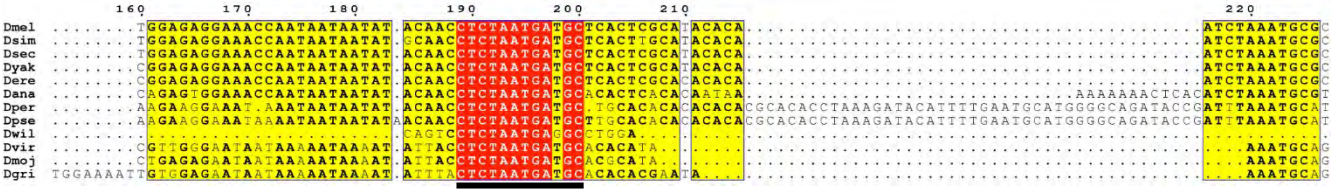

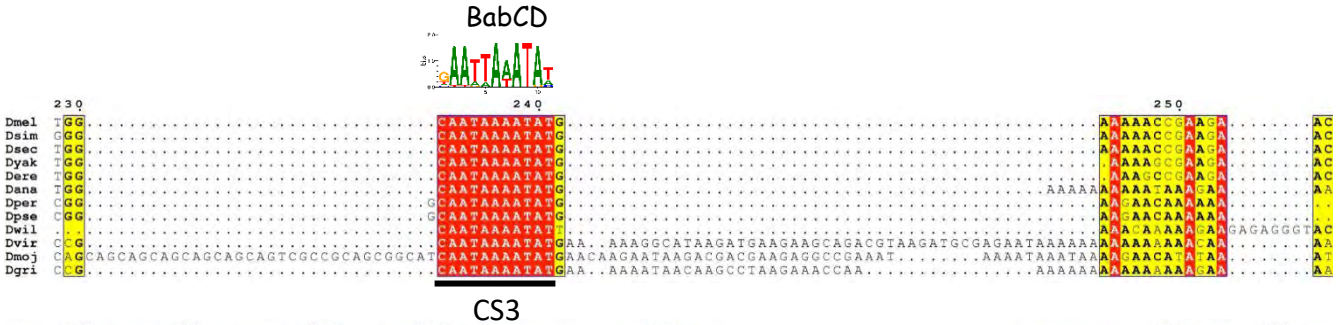

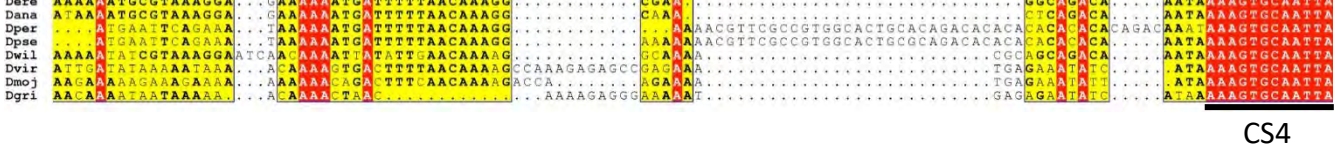

BER^{OCS7} sequence conservation among Drosophilidae (Part2)

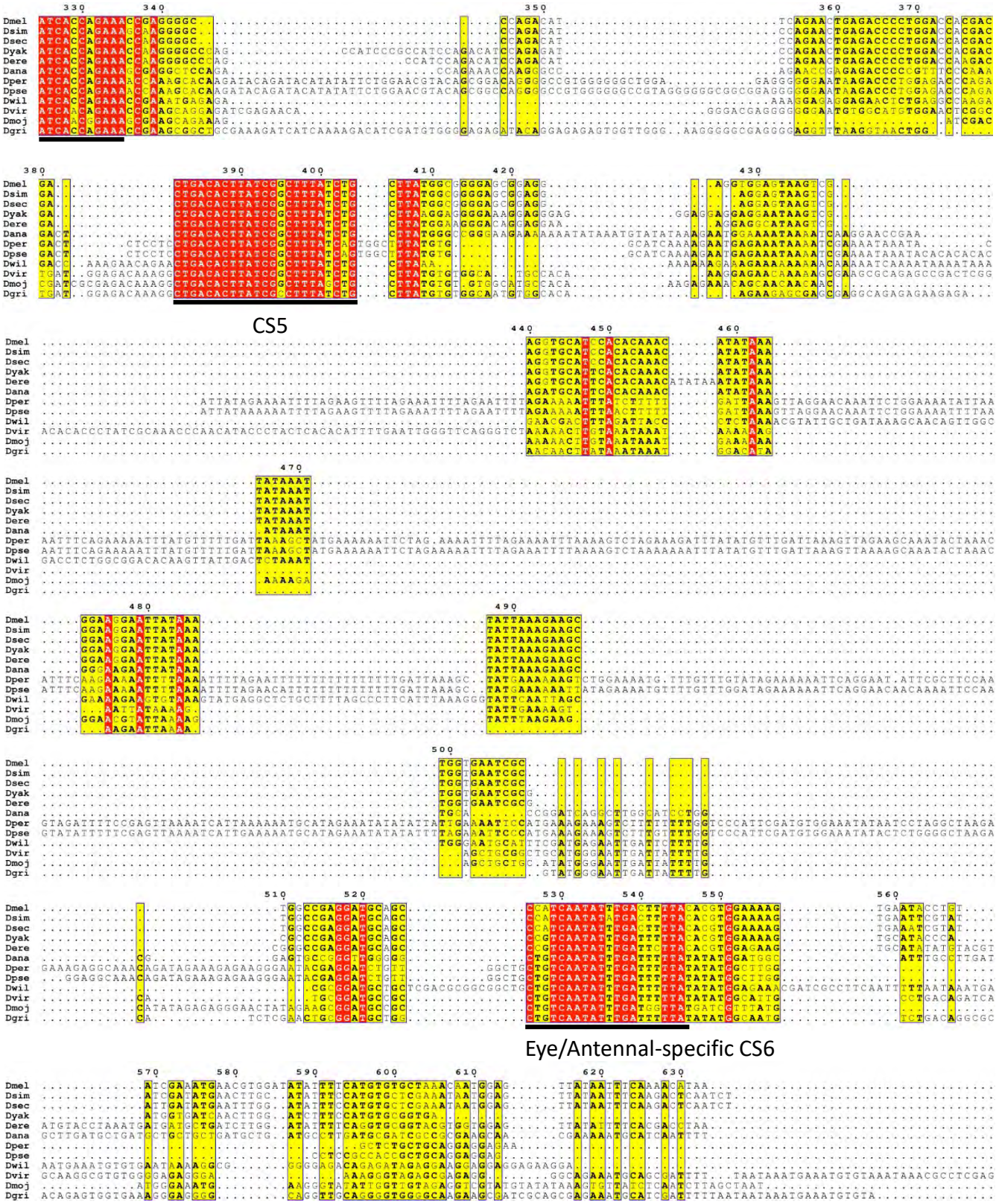

BER^{OCS8} sequence conservation among Drosophilidae (Part1)

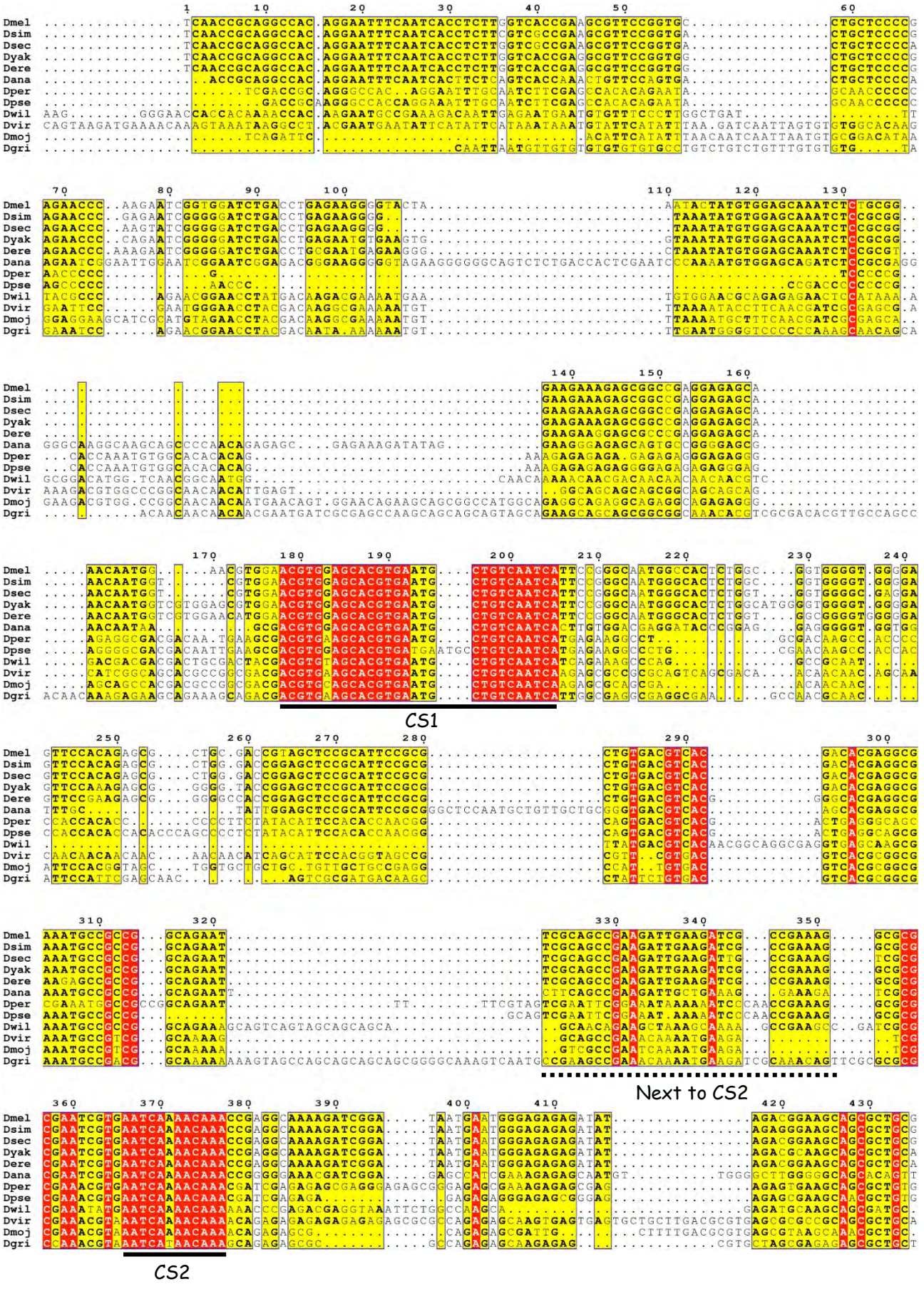

BER^{OCS8} sequence conservation among Drosophilidae (Part2)

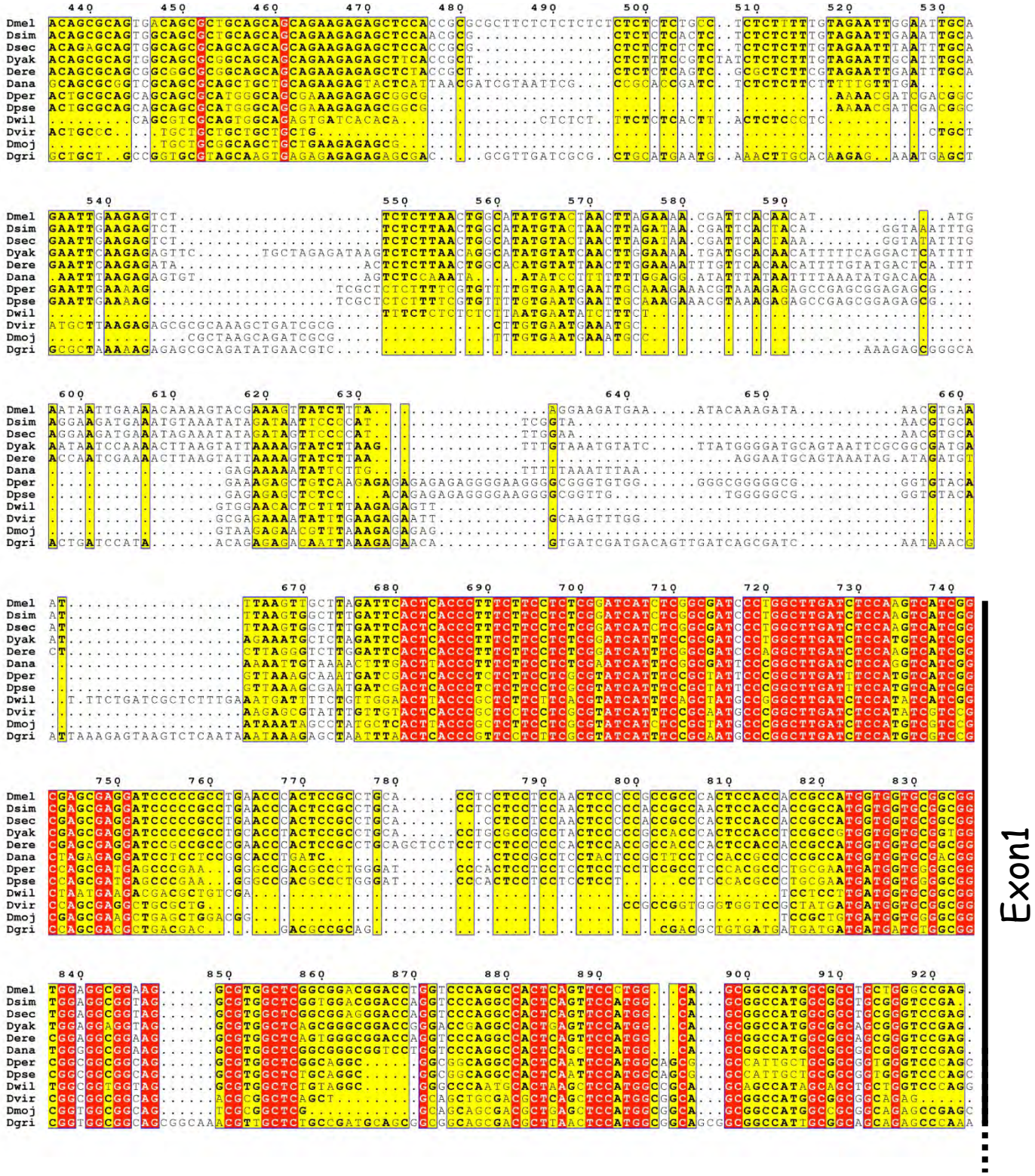

BER^{OCS9} sequence conservation among Drosophilidae (Part1)

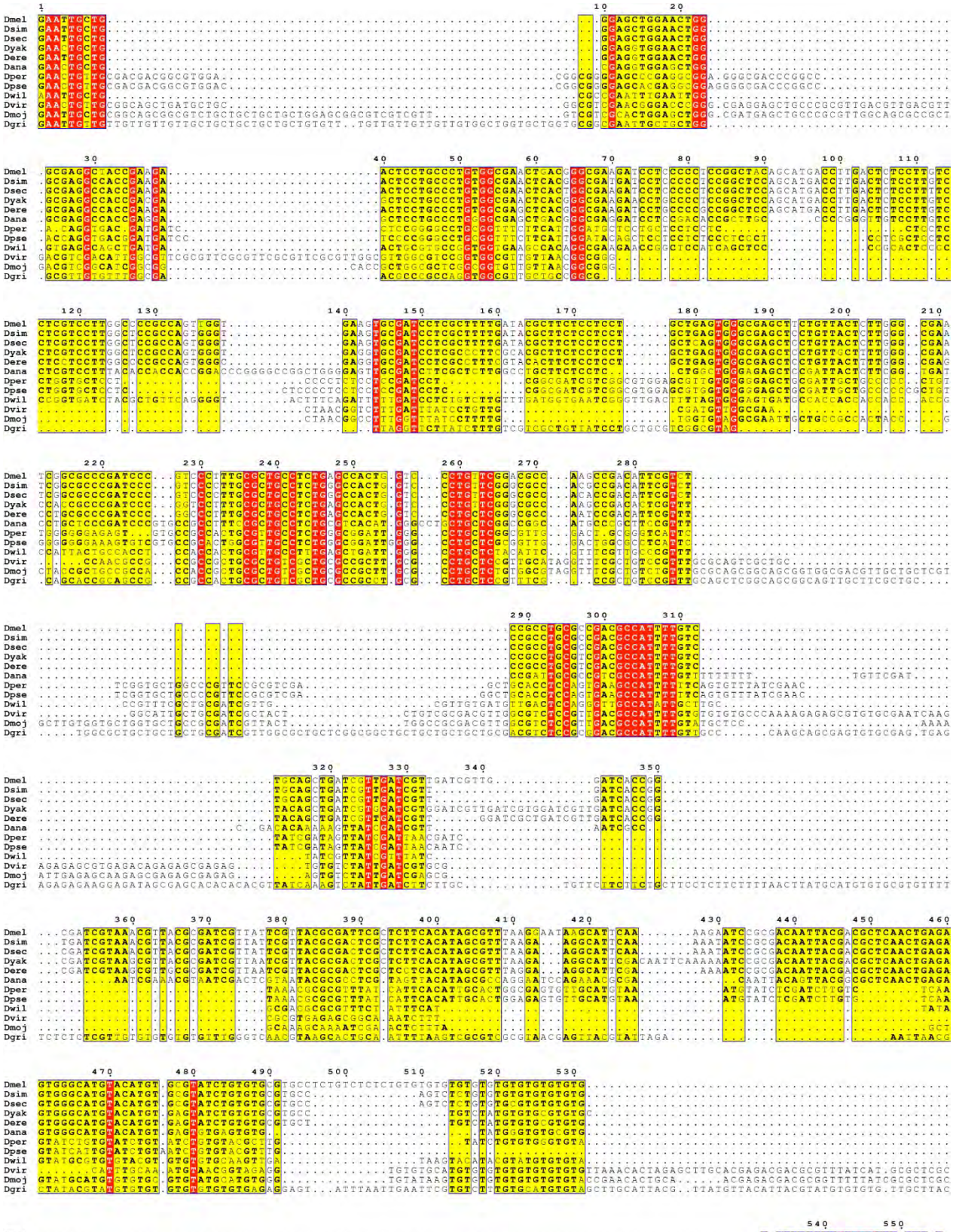

BER^{OCS9} sequence conservation among Drosophilidae (Part2)

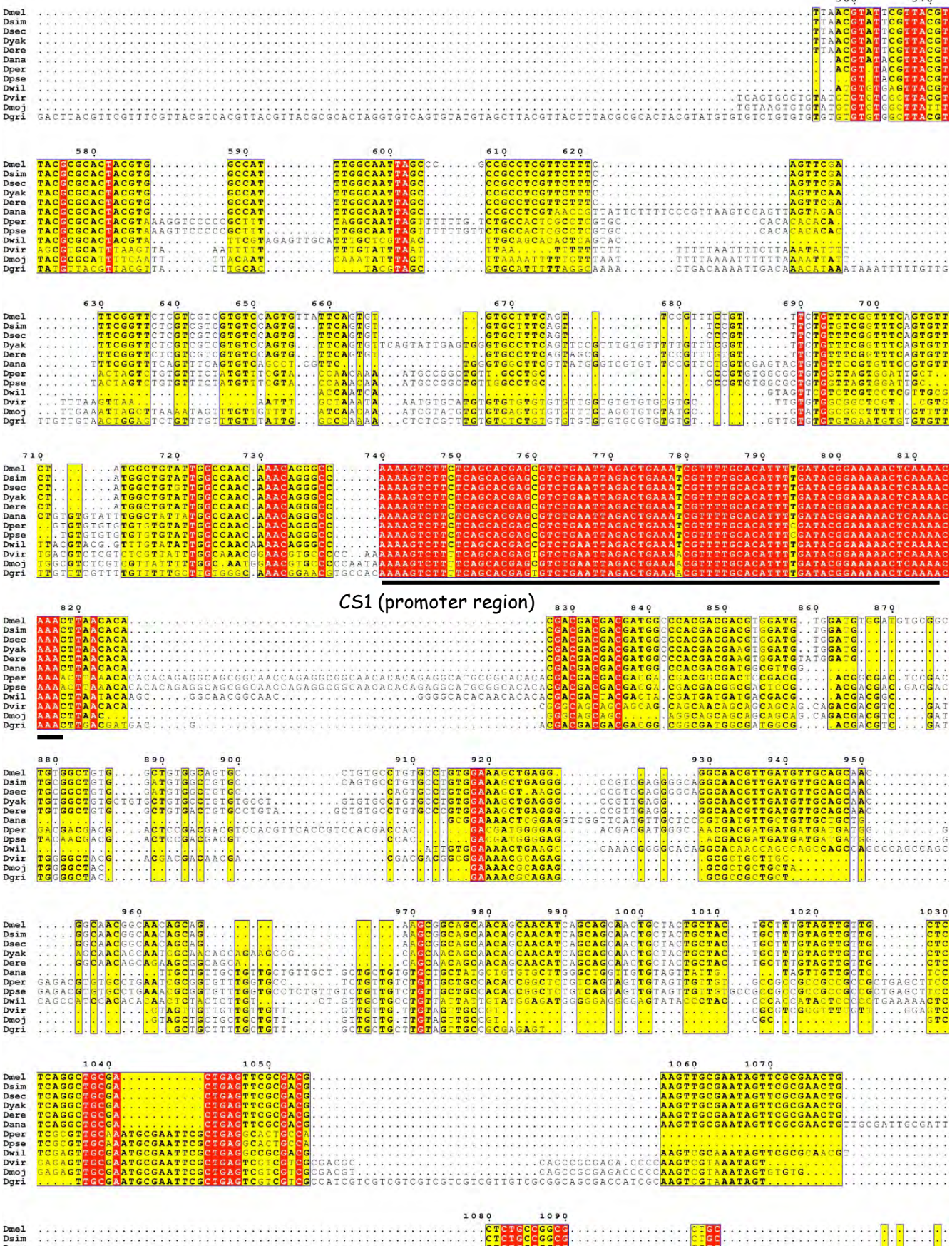

BER^{OCS9} sequence conservation among Drosophilidae (Part3)

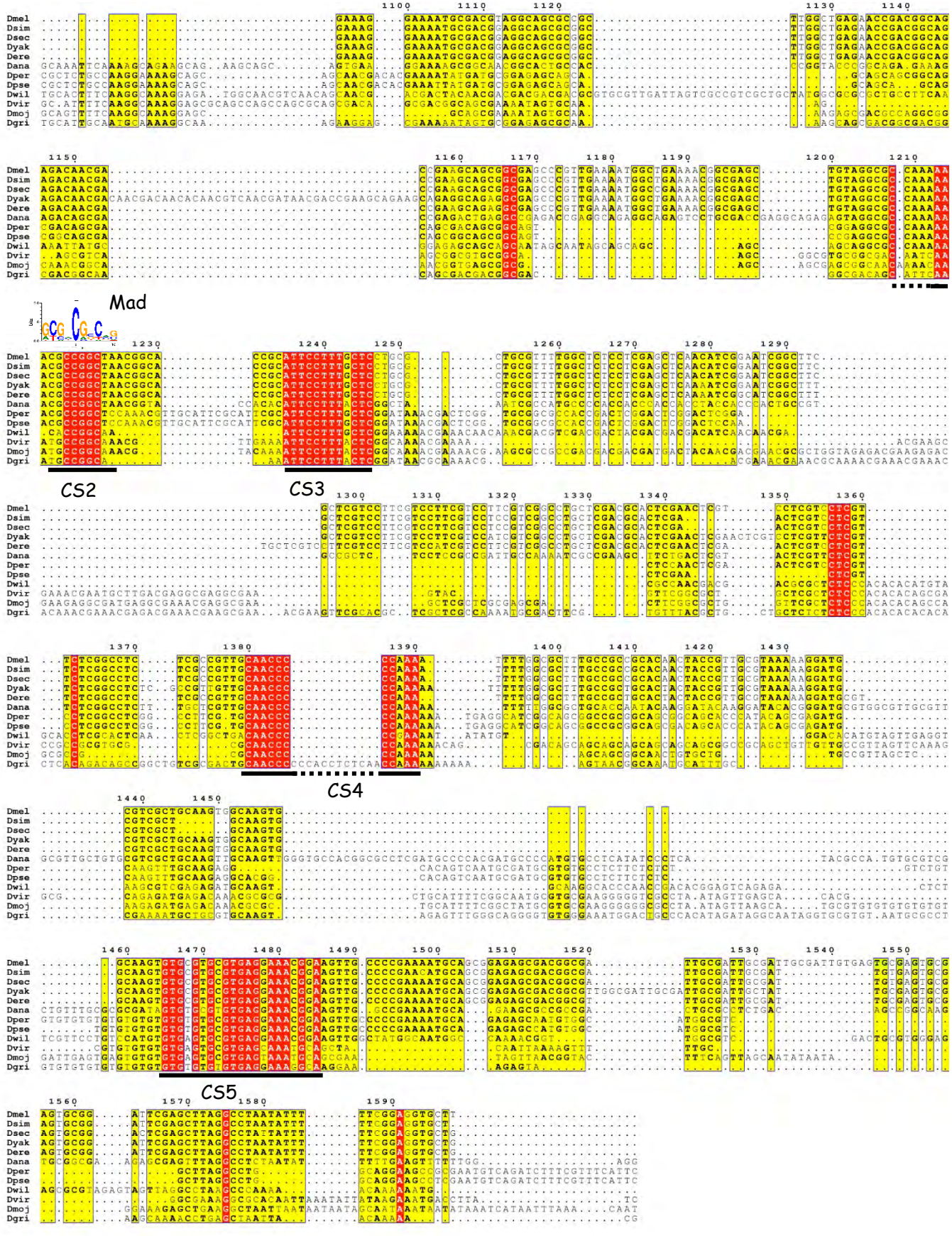

BER^{OCS10} sequence conservation among Drosophilidae (Part1)

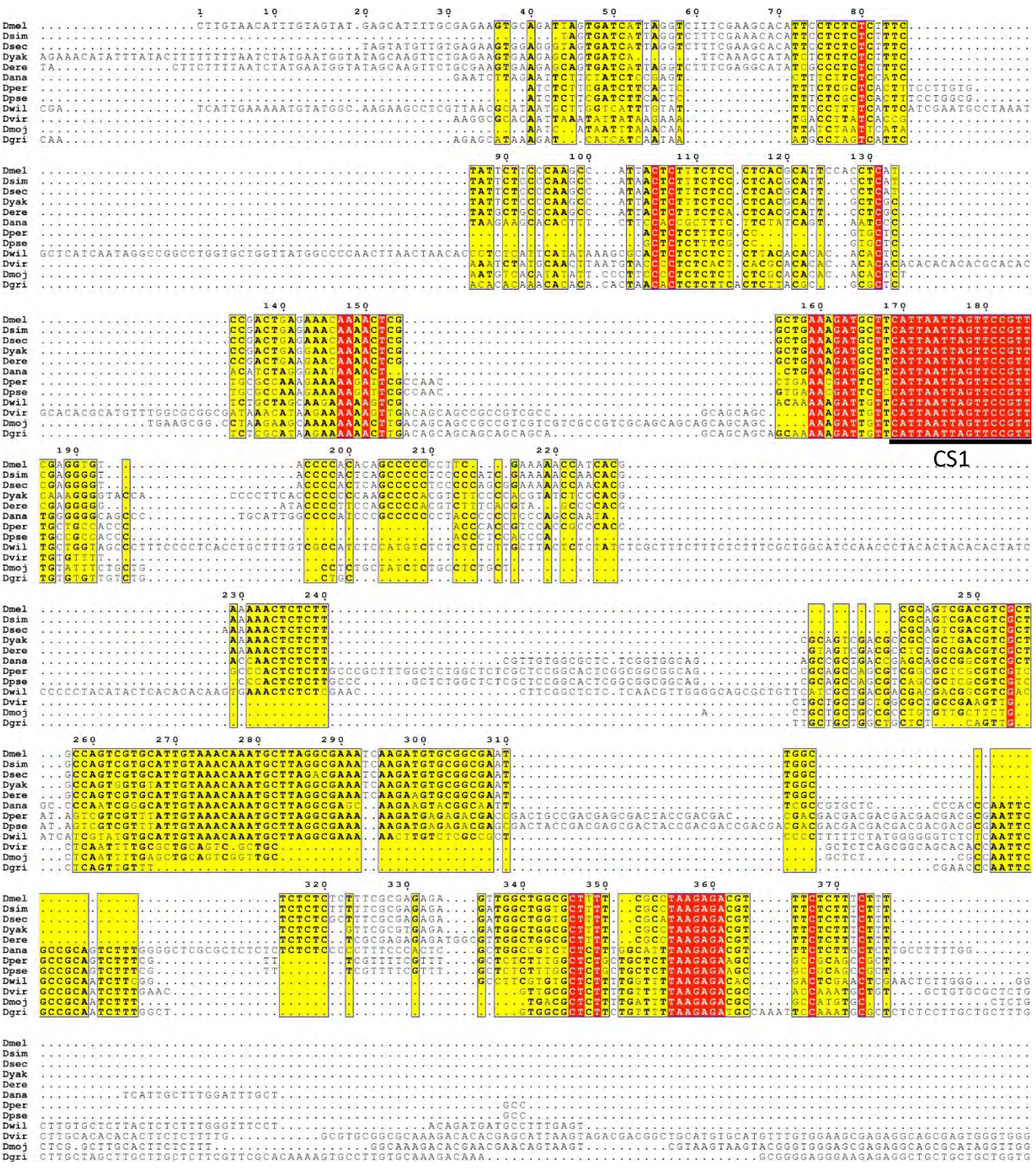

BER^{OCS10} sequence conservation among Drosophilidae (Part2)

LAE sequence conservation among Drosophilidae (Part1)

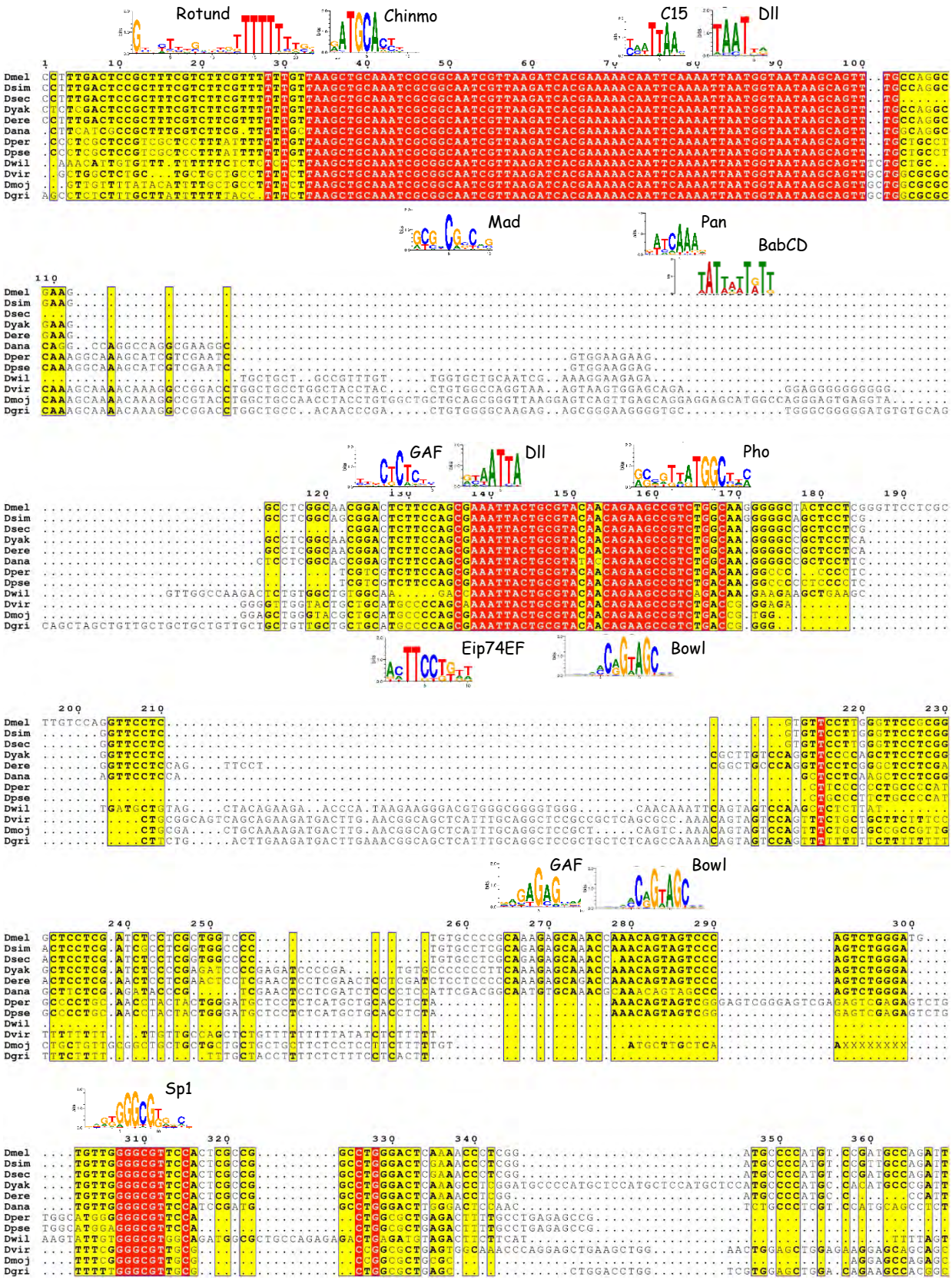

LAE sequence conservation among Drosophilidae (Part2)

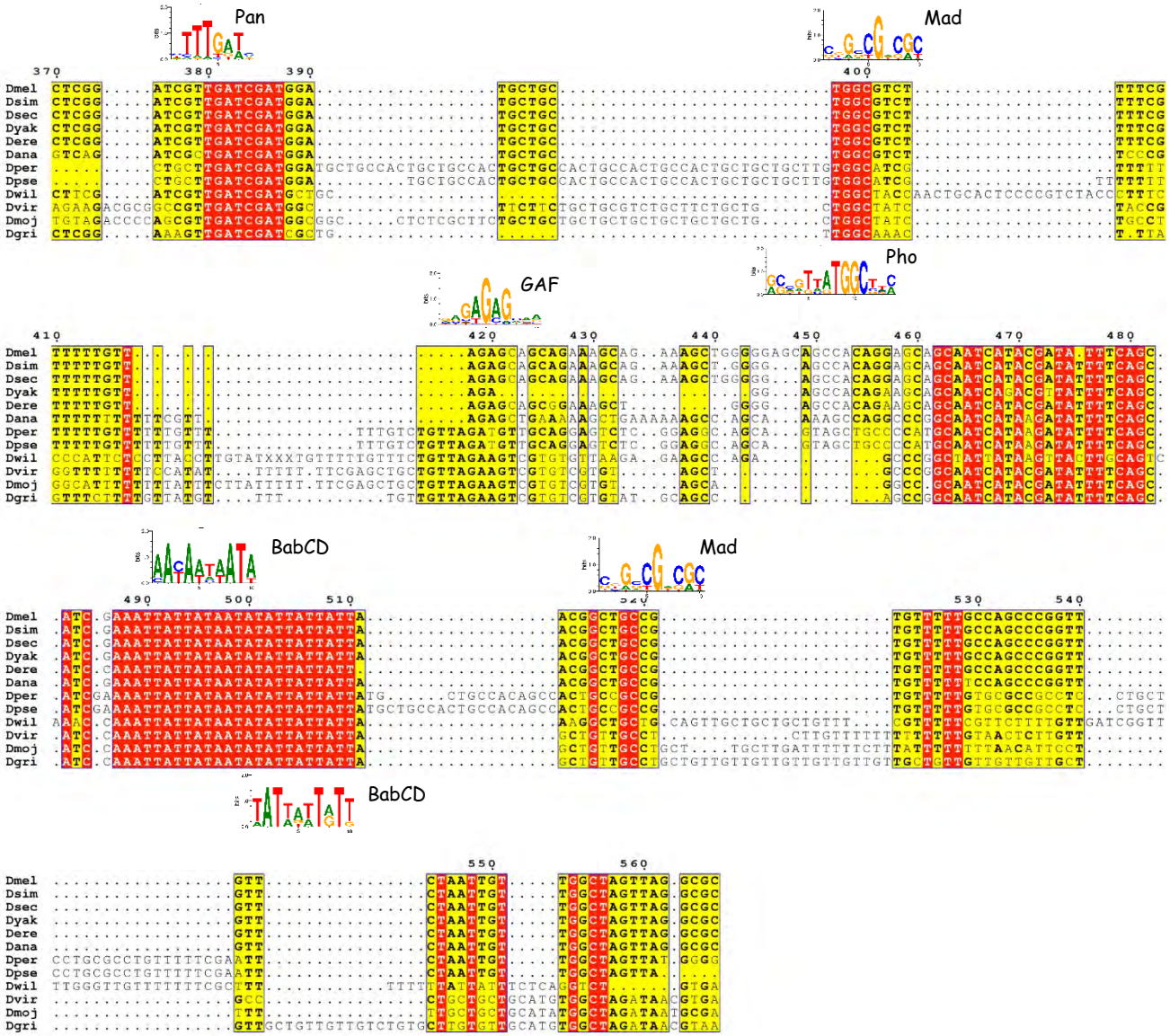

Cardiac CE sequence conservation among Drosophilidae (Part1)

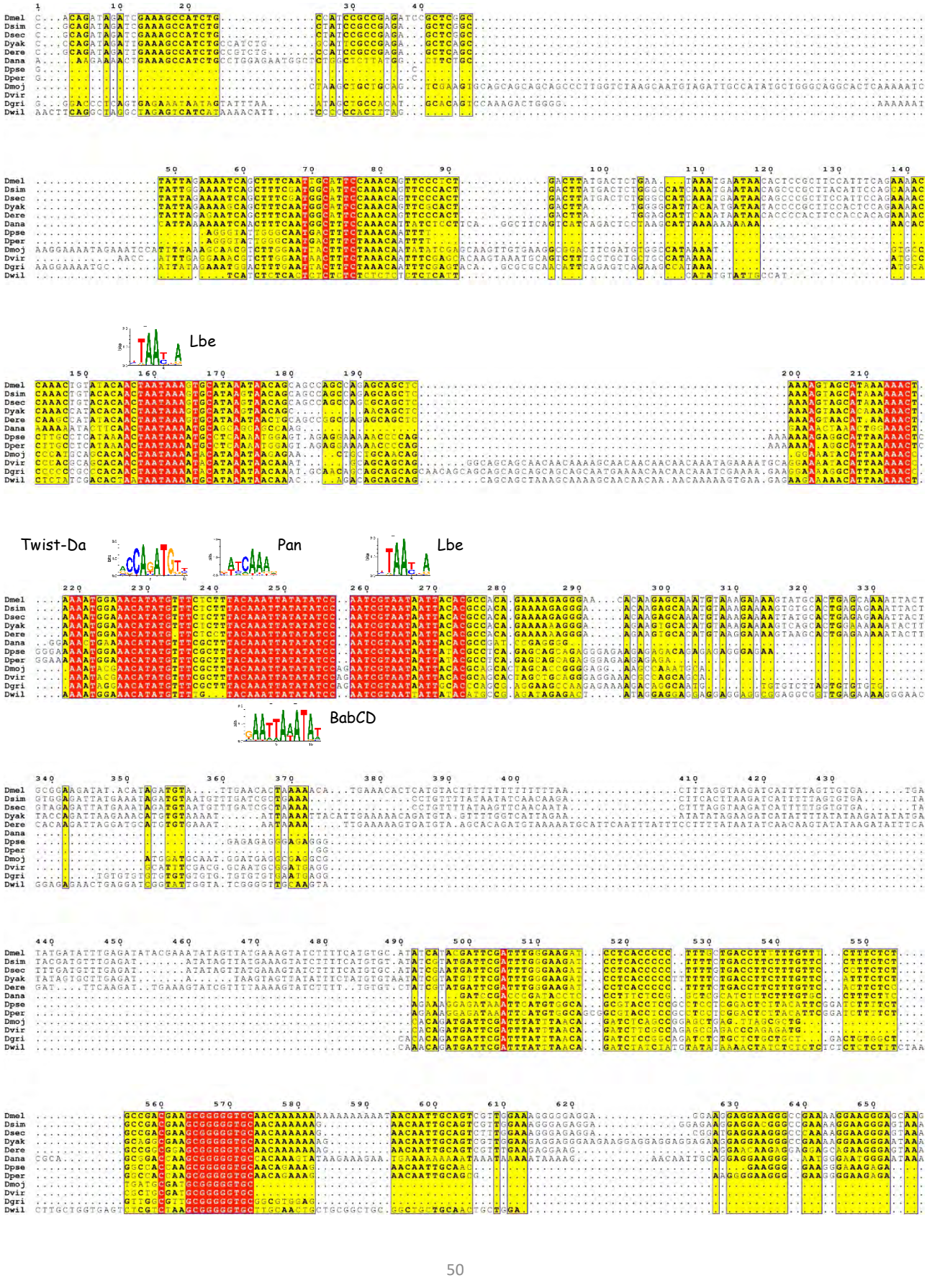

Cardiac CE sequence conservation among Drosophilidae (Part2)

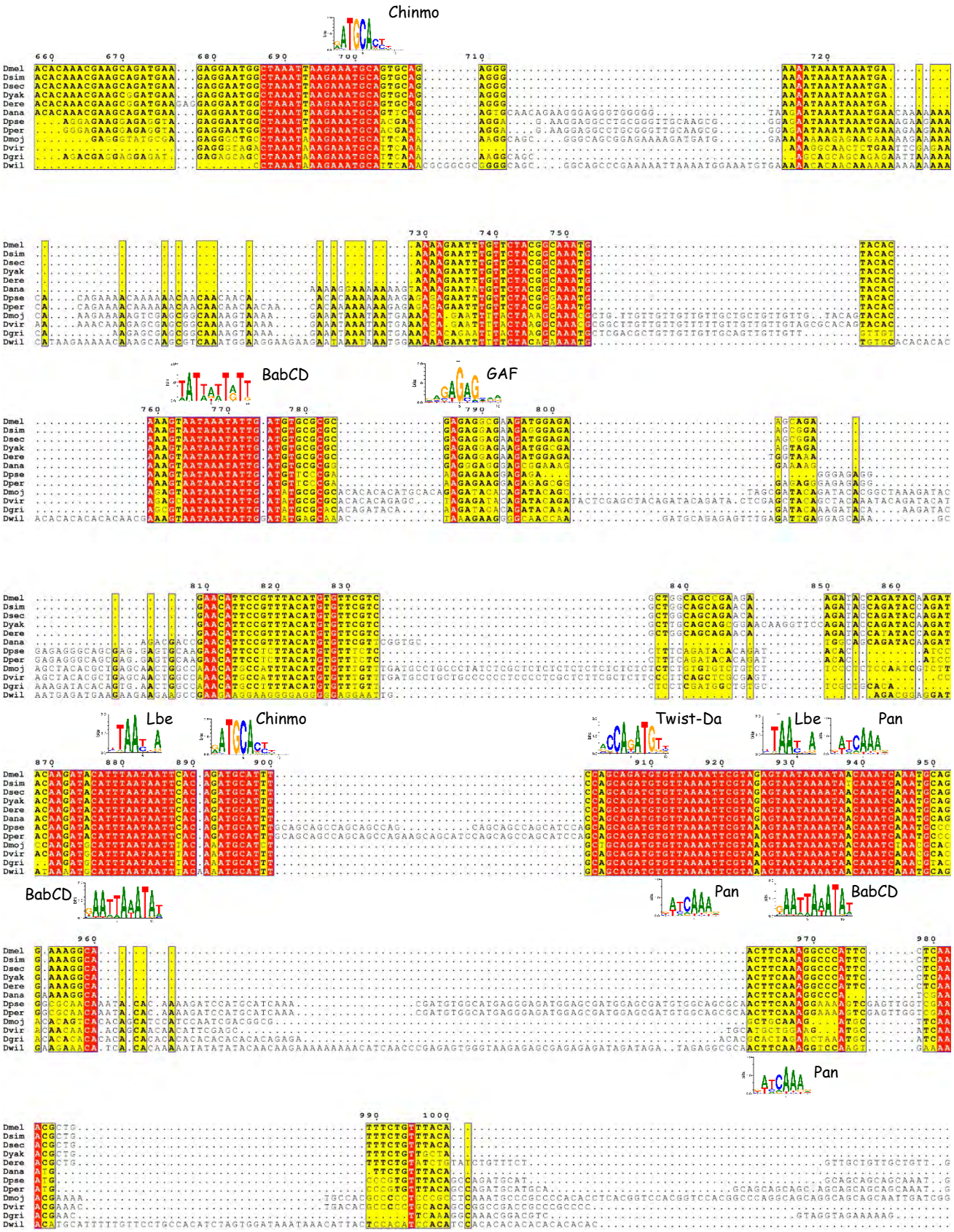

Abdominal AE sequence conservation among Drosophilidae (Part1)

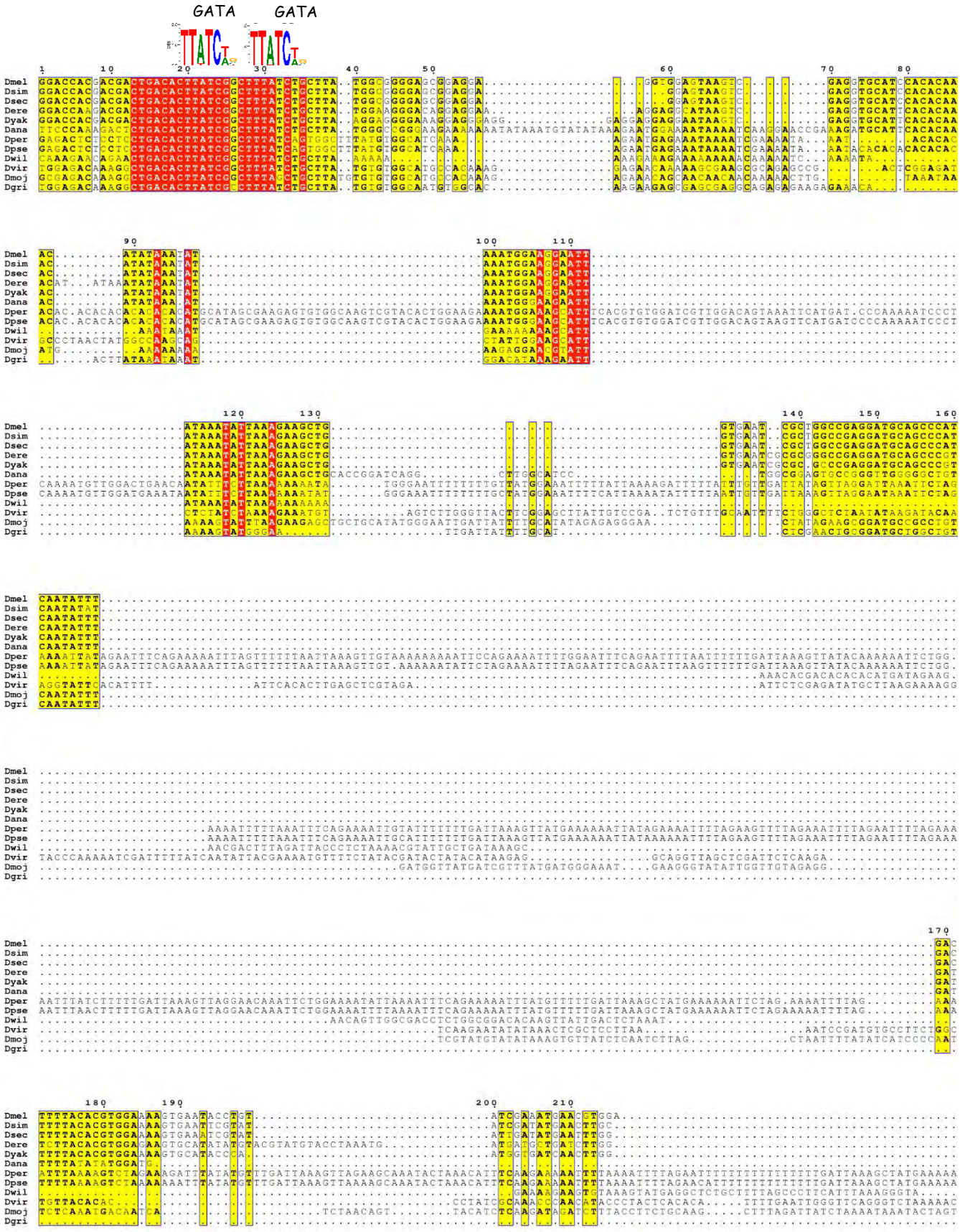

Abdominal AE sequence conservation among Drosophilidae (Part2)

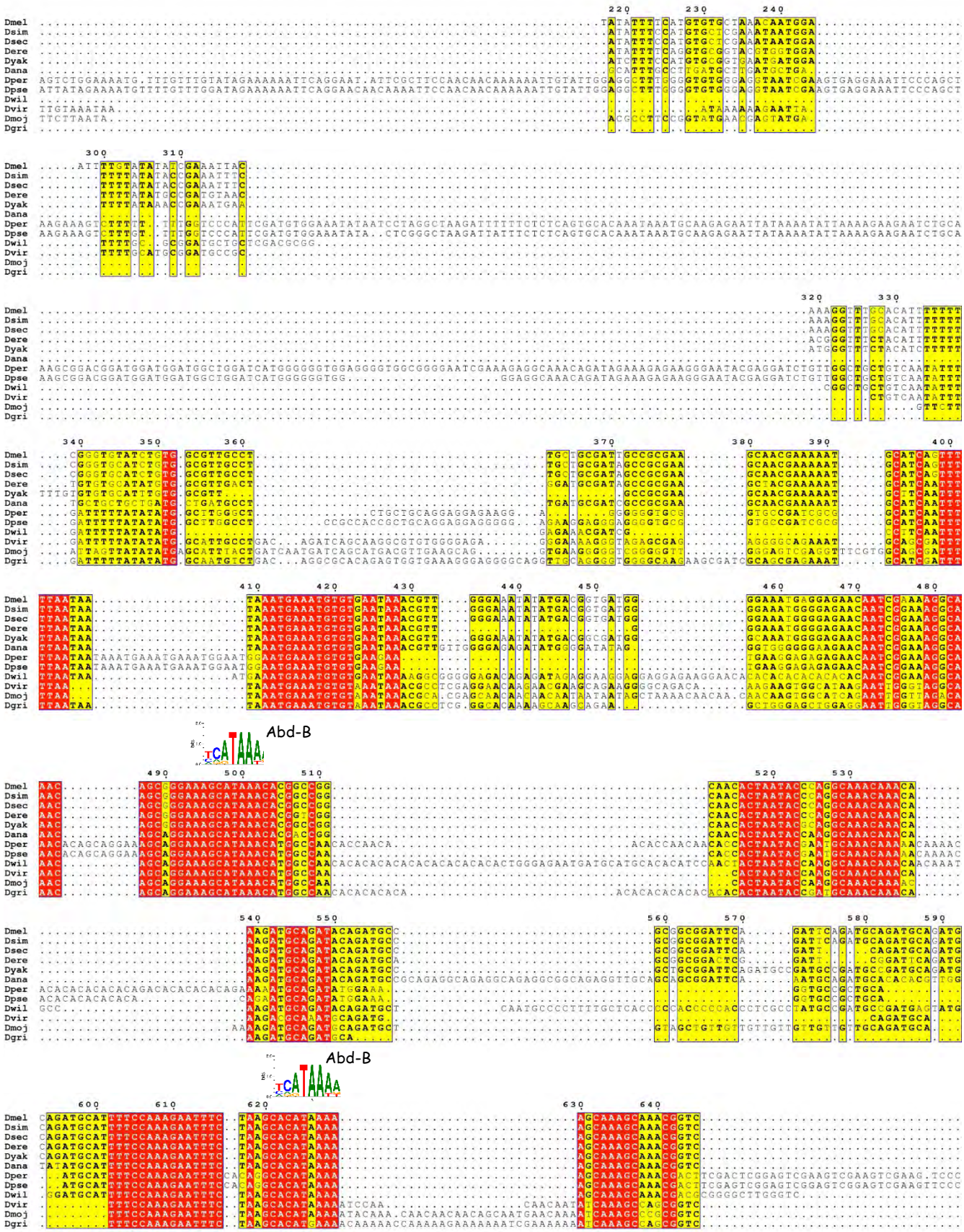

Abdominal AE sequence conservation among Drosophilidae (Part3)

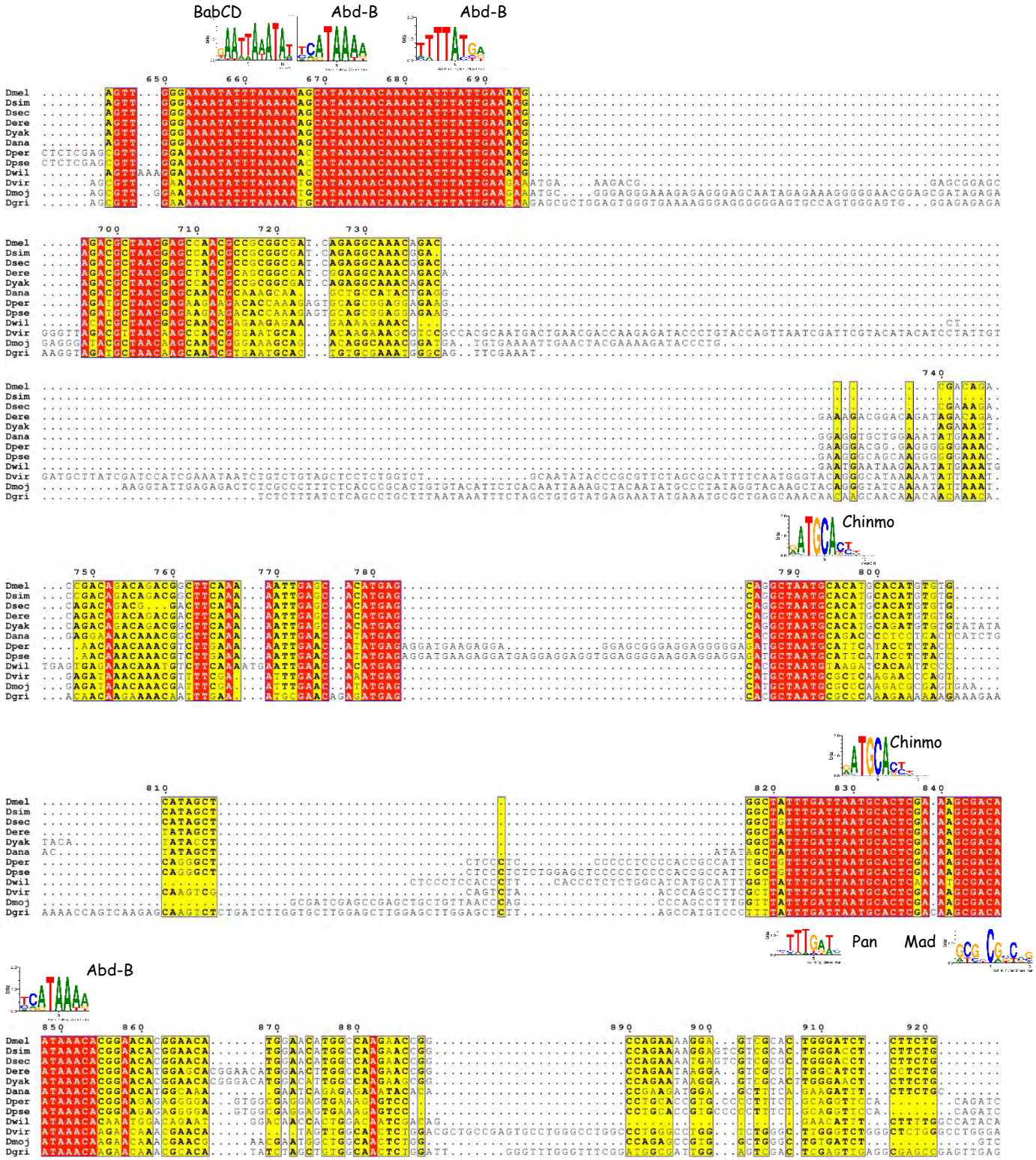

Abdominal AE sequence conservation among Drosophilidae (Part4)

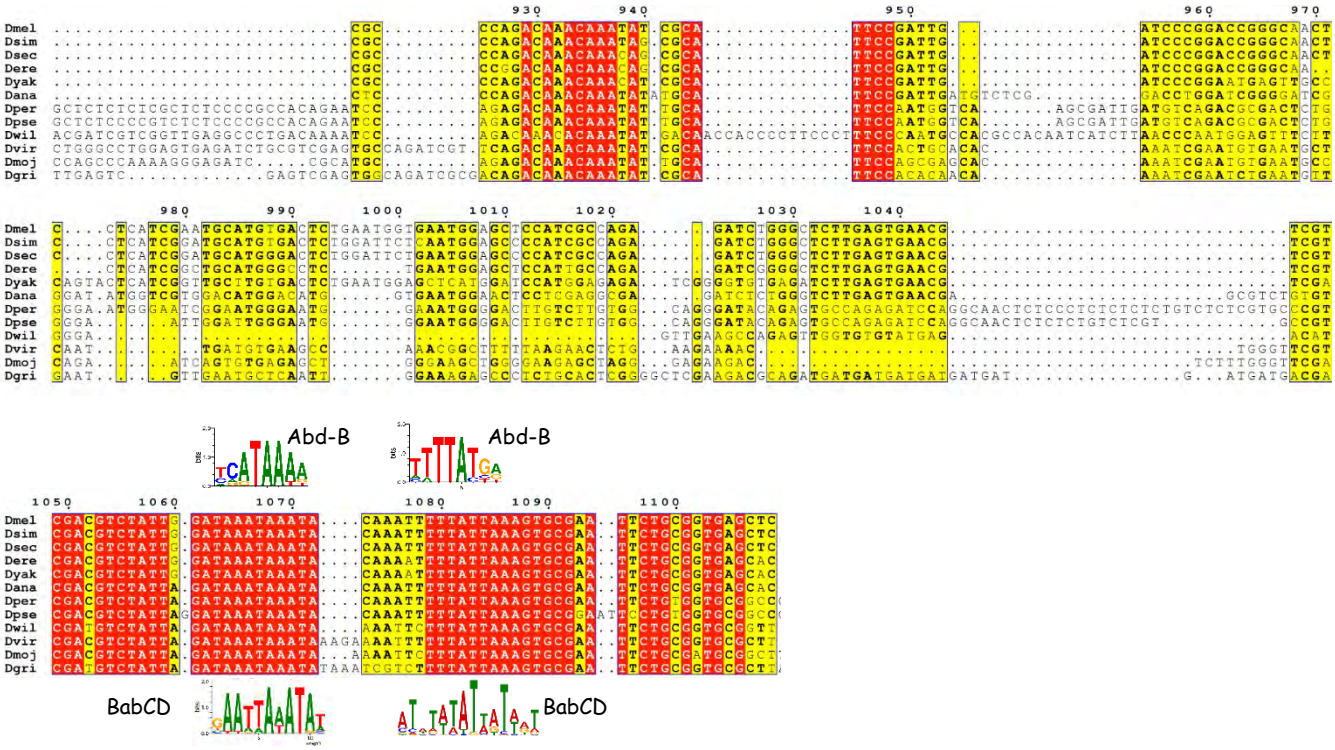

Abdominal DE sequence conservation among Drosophilidae (Part1)

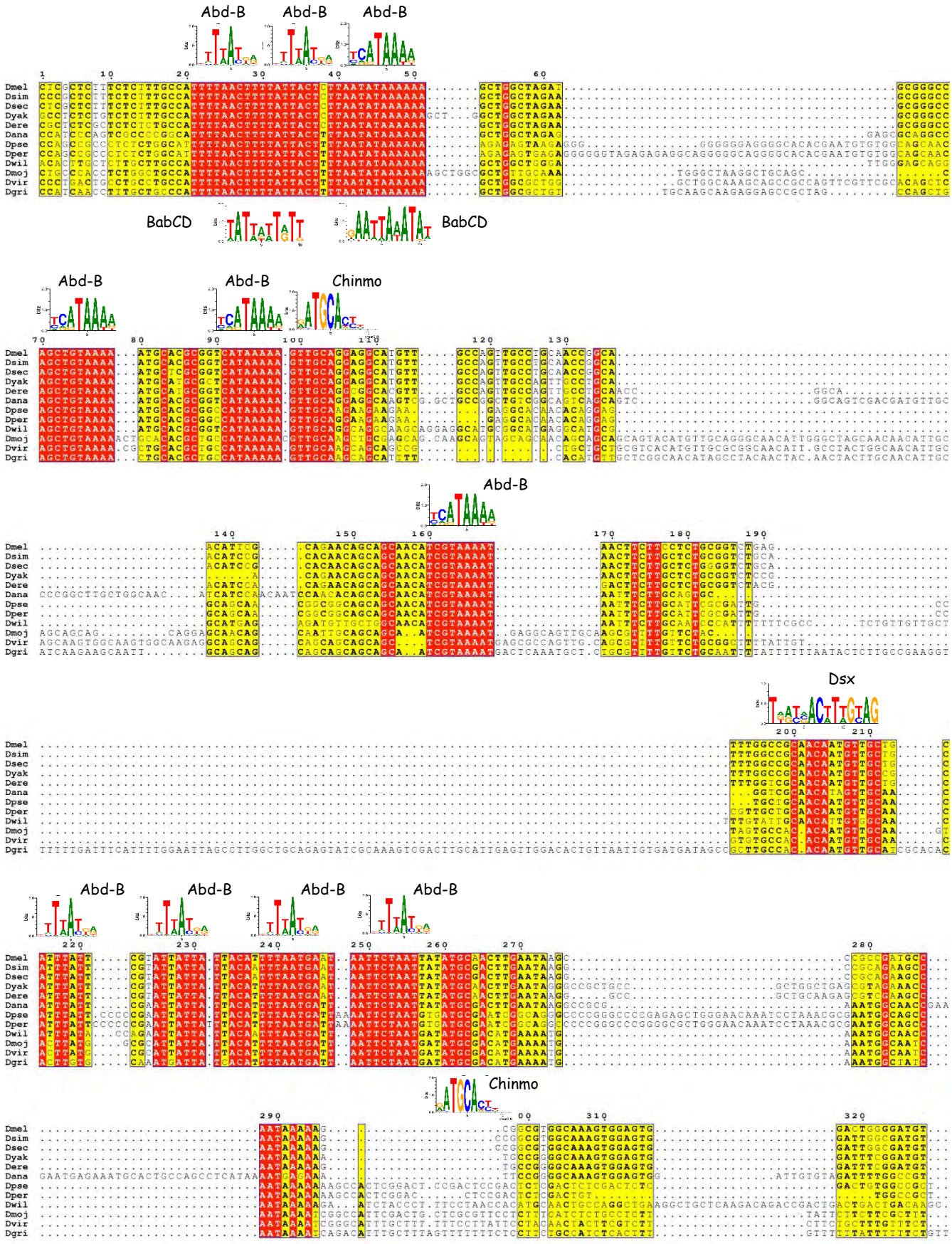

Abdominal DE sequence conservation among Drosophilidae (Part2)